Analysis of Electromechanical Phenomena in the Power-Angle Domain

Andrew J. Arana

Dissertation submitted to the faculty of the Virginia Polytechnic Institute and State University in partial fulfillment of the requirements for the degree of

Doctor of Philosophy
in
Electrical Engineering

Committee Members
Dr. Jaime De La Reelopez (Chair)
Dr. Virgilio A. Centeno
Dr. Jim S. Thorp
Dr. Arun G. Phadke
Dr. Yilu Liu
Dr. Kathleen Meehan
Dr. Carl L. Prather

December 4th, 2009
Blacksburg, VA

Keywords: event identification, modal analysis, state-space analysis,

FNET, wide-area monitoring, traveling waves, adaptive protection

ANALYSIS OF ELECTOMECHANICAL PHENOMENA IN THE POWER-ANGLE DOMAIN

by

Andrew J. Arana

Dr. Jaime De La Reelopez, Chairman

(ABSTRACT)

The idea of performing power systems dynamic analysis in the power-angle domain has been hinted at by previous researchers, but this may be the first published document to develop detailed techniques by which entire power systems can be represented and solved in the power-angle domain. With the widespread deployment of phasor measurement units and frequency data recorders the industry is looking for more real-time analytical tools to turn real-time wide-area measurements into useful information. Applications based on power-angle domain analysis are simple enough that they may be used online.

Power-angle domain analysis is similar to DC load-flow techniques in that a flat voltage profile is used and it is assumed that real power and voltage angle are completely decoupled from reactive power and voltage magnitude. The linearized equations for the dynamics of generators and loads are included in the model, which allows the electromechanical response to be solved using conventional circuit analysis techniques. The effect of generation trips, load switching, and line switching can be quickly approximated with nodal analysis or mesh analysis in the power-angle domain.

The analysis techniques developed here are not intended to be as accurate as time-domain simulation, but they are simpler and fast enough to be put online, and they also provide a better analytical insight into the system. Power-angle domain analysis enables applications that are not

readily available with conventional techniques, such as the estimation of electromechanical propagation delays based on system parameters, the formulation of electromechanical equivalents, modal analysis, stability analysis, and event location and identification based on a small number of angle or frequency measurements. Fault studies and contingency analysis are typically performed with detailed time-domain simulations, where the electromechanical response of the system is a function of every machine in the interconnection and the lines connecting them. All of this information is rarely known for the entire system for each operating condition; as a result, for many applications it may be more suitable to compute an approximation of the system response based on the current operating state of only the major lines and generators. Power-angle domain analysis is adept at performing such approximations.

ACKNOWLEDGEMENT

First and foremost, I would like to thank my academic advisor, Dr. Jaime De La Reelopez, for his guidance, support, and patience throughout my research. Dr. De La Reelopez is a great teacher who has been an invaluable resource when I've needed to discuss a new idea or clarify an old concept. It has truly been a pleasure to conduct research under his guidance. Special thanks go to Dr. Virgilio Centeno who has served as an advisor and friend to me throughout my tenure at Virginia Tech. I must also express my appreciation to Professors Jim Thorp and Arun Phadke who also worked on my research group. I consider myself extremely fortunate to have been able to work closely with such distinguished researchers and teachers. My appreciation also goes out to the remaining members of my advisory committee, Professors Yilu Liu, Kathleen Meehan, and Carl Prather for their genuine interest and continuous support for this research.

The financial support for my research that was provided by California ISO and the utilities that it incorporates is greatly appreciated. Vahid Madani of Pacific Gas & Electric (PG&E) was particularly active in working with our research group and addressing many of the practical issues that arose. It is difficult to imagine our research being successfully completed without his assistance. Additionally, during my two internships at PG&E, Vahid's mentorship significantly increased my knowledge and appreciation of operations engineering and transmission protection.

I also wish to thank the power systems students that I have worked with in both my own research group and others. I have thoroughly enjoyed discussing ideas with them and gaining a variety of different perspectives. Their assistance and friendship made the many difficulties of graduate school much easier.

Most importantly, I thank my parents, Winsome and Belito Arana, for their countless sacrifices in raising me and supporting me in all my endeavors. They have always believed in me and encouraged me to shoot for the stars. My thanks also go out to my sisters, Anelly and Alicia, whose continuous love and support help me to persevere through the most arduous situations. Lastly, I thank all my friends at Virginia Tech who have filled the last five years with pleasant memories that will last a lifetime.

TABLE OF CONTENTS

List of Figures

List of Tables

Chapter 1 Introduction

The function of the electric power system is to generate electricity at one location and transport it to loads at another location. Excluding the few storage devices that are installed for reliability or economic reasons, the power system is not intended to store energy. However, electric and magnetic energy is stored in transmission lines, transformers and shunt devices; mechanical energy is stored in the rotating energy of machines; and thermal energy is stored in boilers. Events that cause a change in the energy stored in the power system result in oscillations and transients. These transients generally occur on the same time scale as the length of time it takes to convert the stored energy into electrical energy and vice-versa (1). The thermodynamics of a power system occur in the boilers of large thermal power plants. These transients occur on a far longer time scale than is relevant for most protection or stability studies. This document will not consider thermodynamic transients; instead it will focus on electromechanical transients and to a smaller extent, electromagnetic transients.

The remainder of this chapter defines electromagnetic and electromechanical phenomena in power systems and briefly lists a few of their applications. Chapter 2 gives an overview of the existing techniques for analyzing electromechanical phenomena by describing the continuum model and state-space analysis. In chapter 3 the models for power-angle domain analysis are derived and used to calculate disturbance propagation delays, electromechanical equivalents, and the system response to contingencies. Chapter 4 considers how power-angle domain analysis could be used from a system operator's perspective. Contingency screening, power system restoration, modal analysis, and stability analysis can all be performed online in the power-angle domain. In chapter 5, power-angle domain analysis is used for protection applications such as

the supervision of relay trip characteristics and the development of adaptive out-of-step tripping relays. Possibly the most widely used application of wide-area synchronized measurements is for post-disturbance analysis. In chapter 5, an event location and identification algorithm that requires unsynchronized measurements of angle or frequency at a small number of buses is developed. The report concludes with a discussion of the ongoing and future work in this area. With the rapid deployment of PMUs and digital relays it is likely that the applications developed in this research are merely scratching the surface of the real-time protection and control systems that will be crucial to safe and efficient operation of the future power system

1.1 Electromagnetic Traveling Waves

Electromagnetic dynamics are governed by the circuit elements of the system. Electromagnetic transients arise due to changes in the energy stored in inductors and capacitors in the form of magnetic and electric fields respectively. Faults, switching events, lightning, winding resonances (transformer, generator, and reactor windings), network resonances, and harmonics from power electronic devices cause changes in voltages and currents. Because inductors and capacitors store energy they can temporarily support the voltage or current effectively maintaining the pre-disturbance levels as the stored energy is discharged. These transients occur on a time scale of 10^{-6} to 10^{-3}s (1). Figure 1-1 shows a transmission line modeled as an RLC network. For an RLC network, each node supports the voltage and current for a short time causing a propagation delay as a disturbance moves along the line.

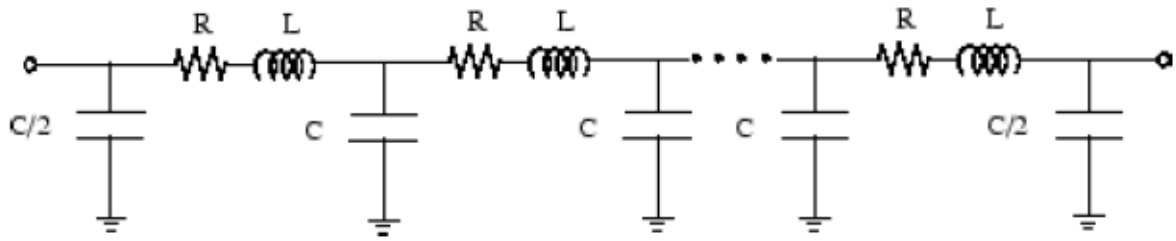

Figure 1-1: Transmission Line with Distribution Parameters

For long transmission lines, typically longer than 150 miles, the fact that the line parameters are distributed and not lumped must be accounted for by using the distributed π-model. Consider the expression for the voltage difference across an infinitesimally small element of the line given by the expressions below:

$$V(x+\Delta x) - V(x) = z\Delta x I(x) \tag{1.1}$$

$$\frac{V(x+\Delta x) - V(x)}{\Delta x} = zI(x) \tag{1.2}$$

As Δx→0,

$$\frac{dV(x)}{dx} = zI(x) \tag{1.3}$$

Similarly, the current flowing into the shunt admittance of the line may be considered.

$$I(x+\Delta x) - I(x) = y\Delta x V(x) \tag{1.4}$$

$$\frac{dI(x)}{dx} = yV(x) \tag{1.5}$$

Differentiating (1.3) and substituting into (1.5) yields:

$$\frac{d^2V(x)}{dx^2} = z\frac{dI(x)}{dx} = zyV(x) \tag{1.6}$$

Let, $\gamma = \sqrt{zy}$, $\frac{d^2V(x)}{dx^2} - \gamma^2 V(x) = 0$

Solving:

$$V(x) = A_1 e^{\gamma x} + A_2 e^{-\gamma x} \tag{1.7}$$

Where,

$$A_1 = \frac{V_R + Z_C I_R}{2}, \quad A_1 = \frac{V_R - Z_C I_R}{2}$$

$$Z_C = \sqrt{\frac{z}{y}},$$

$$\gamma = \sqrt{zy} = \sqrt{(r + jwL)(g + jwC)} = \alpha + j\beta$$

γ is the propagation constant

α is the attenuation constant

β is the phase constant

(1.7) is the rms expression for the phasor value of voltage at any point along a long transmission line. The first term represents the incident wave and the second term represents the reflected wave. Both the incident and reflected waves are traveling waves in that they vary sinusoidally with both distance, x, and time, since V_R and I_R are phasors representing time-varying quantities. It is important to note that the summation of both the incident and reflected waves, the total instantaneous voltage, is a standing wave(2).

(1.8) shows the instantaneous value of voltage instead of the phasor value.

$$\begin{aligned} V(t,x) &= \sqrt{2}\Re e\{A_1 e^{\gamma x} e^{j\omega t\}} + \sqrt{2}\Re e\{A_2 e^{-\gamma x} e^{j\omega t}\} \\ &= \sqrt{2}\Re e\{A_1 e^{\alpha x} e^{j(\omega t + \beta x)}\} + \sqrt{2}\Re e\{A_2 e^{-\alpha x} e^{j(\omega t - \beta x)}\} \end{aligned} \tag{1.8}$$

The first term in (1.8) is the incident wave and the second term is the reflected wave.

The peak amplitude occurs at $\omega t - \beta x = 2k\pi$ or $x = \frac{\omega}{\beta} t - \frac{2k\pi}{\beta}$

The wave speed is $v = \frac{dx}{dt} = \frac{\omega}{\beta} = \frac{2\pi f}{\beta}$

When line losses are neglected (g=0, r=0): α=0, $\beta = \omega\sqrt{LC}$, $Z_C = \sqrt{\frac{L}{C}}$, and $v = \frac{1}{\sqrt{LC}}$

For a lossless line when the internal flux linkage of the conductor is neglected $v = \frac{1}{\sqrt{\mu_0 \varepsilon_0}} = 3 \times 10^8 m/s$. Typical extra high voltage lines will have propagation speeds from 250,000 – 291,000 km/s (3).

Transient overvoltages on a power system are created by lightening discharges or switching operations. Lightning is always a potential hazard to electrical equipment, but at voltages over 230kV surges due to switching operations become potentially damaging as well. An understanding of electromagnetic traveling waves is needed to properly design the system to withstand these transients. Insulation levels must be appropriately set and reactors are often placed close to large electrical equipment. Often an electromagnetic transient program (EMTP) is used to determine the maximum voltage or current surge and choose appropriate locations and ratings for reactors. ETMP studies are becoming more important as the operating times of relays decrease and systems become more non-linear. Electromagnetic transient analysis is also needed to properly analyze harmonics and non-linearities that play a significant role in the short time frames used in protective relaying. (1).

Electromagnetic traveling waves have also been used successfully for fault location and identification. High frequency synchronized current measurements are taken at both ends of a transmission line. Upon fault inception there will be large deviations in current on the faulted phases. The disturbance will also appear in the unfaulted phases due to mutual coupling, but to a far lesser extent. For phase faults the size of the current deviation will be approximately the same in each faulted phase; therefore, the type of fault is easily distinguishable. Because the current measurements are synchronized, the exact time at which a current deviation is measured at either end of the transmission line can be noted. For a fault in the middle of the line the transient will reach both ends at the same time. If the fault is closer to one end it will reach that

end faster. By knowing the difference in arrival time, the speed of the wave, and the length of the line the fault location can be calculated within 300m (3).

1.2 Electromechanical Traveling Waves

Electromechanical traveling waves were not directly observed until the advent of synchronized phasor measurement units. In July, 1993 a load rejection test in Texas with PMUs deployed at 4 sites revealed the presence of a propagating disturbance in frequency (4)(5)(6). There was a delay of 0.5s between the PMU at the location of the event and the PMU furthest away. Engineers determined that the disturbance was not electrical in nature due to low speed of propagation and low oscillation frequency. It was inferred that the dynamics were related to local inertia. In July 1995 similar tests in the Eastern Interconnection revealed a time delay of one second between detection of the disturbance in Florida and in New York (4).

Electromechanical dynamics are governed by the swing equation of synchronous machines. Electromechanical transients arise from changes in the mechanical energy stored in the rotating mass of machines. These transients occur on a time scale of 10^{-1} to 10s (1). Figure 1-2 shows a power system model with several synchronous machines in tandem. Generation trips, load trips, and some switching events cause changes in the power demand on synchronous machines and hence deviations in the machine's rotor angle. Because each machine stores mechanical energy, a power mismatch is compensated for by a discharge of the mechanical energy due to the rotating mass slowing down. The result of this is that the entire power mismatch is not immediately transferred to the adjacent machine, causing a propagation delay from one machine to the next.

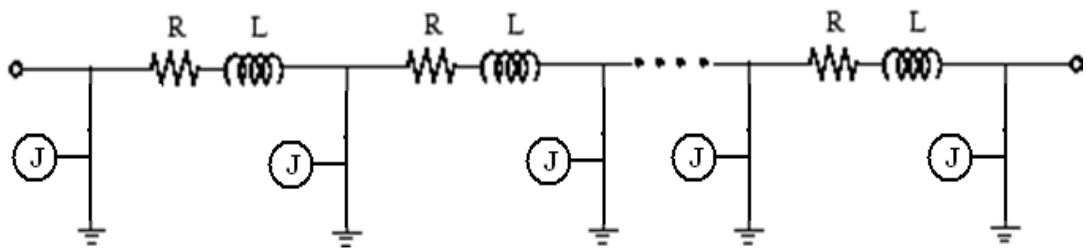

Figure 1-2: Synchronous Machines in Tandem

Figure 1-3 shows synchronous machines modeled as a constant voltage source behind a direct axis transient reactance. If X_G is very small compared to X_L then $\theta \approx \delta$.

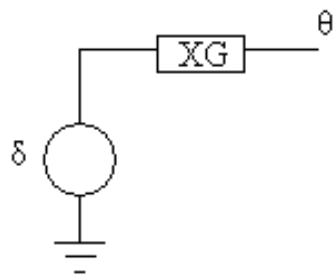

Figure 1-3: The Classical Model of a Generator

Figure 1-4 shows 5 synchronous machines in tandem with each machine modeled as a classical generator. For a step change in angle at the infinite bus, all of the bus angles will undergo a change within the same time required by an electromagnetic wave to travel from the location of the event to all other buses. Closer machines change more and electrically distant machines changing less. This time is significantly below the time frame of interest for electromechanical dynamics so these changes are considered to be instantaneous. The rotor's dynamics are governed by the swing equation below.

$$\frac{2H}{\omega}\frac{d^2\delta}{dt^2} = P_m - P_e - D\frac{d\delta}{dt} \tag{1.9}$$

D is the mechanical damping constant, H is the machine's inertia constant, and ω is the rotational speed of the rotor.

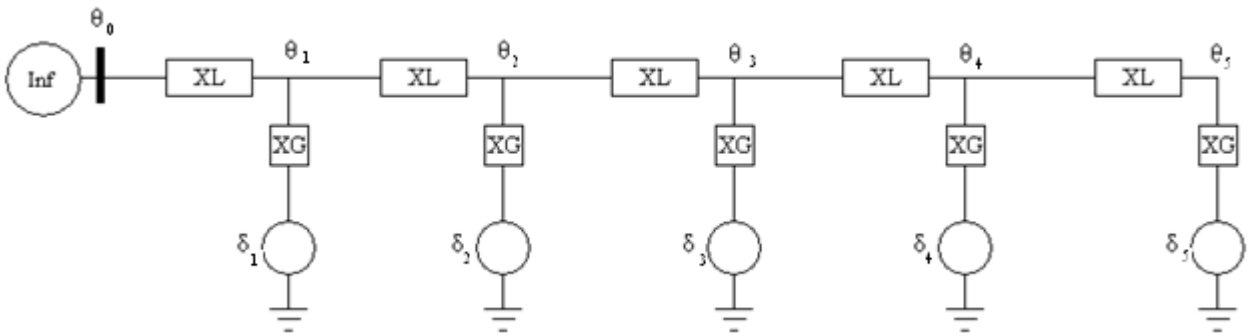

Figure 1-4: 5-Machine System

As the bus angle changes, a mismatch in electrical power is created at the machines which causes acceleration or deceleration of the rotor angles. As the rotor angle increases the bus angle increases further and the change in bus angle creates a change in power flow to the next bus causing that bus angle to increase as well. The disturbance is propagated from one bus to another in this way. It is important to note that X_G must be significantly less than X_L or else the bus angles will not closely approximate the rotor angles and the electromechanical propagation will be difficult to observe. A fundamental difference between the analysis of electromechanical and electromagnetic disturbance propagation is that a transmission line has distributed parameters; whereas, an electromechanical network is obviously lumped. Chapter 2 analyzes electromechanical propagation in detail.

Although the study of electromechanical traveling waves is fairly young, it already forms the basis for several applications. Virginia Tech's FNET (frequency network) system uses wide area frequency measurements to triangulate and identify power system events that cause load-generation mismatches. This is useful in an interconnected system when a utility needs to know

in real-time of events occurring in a neighboring system. The triangulation algorithms are based on the fact that machines closest to the power mismatch respond faster than machines further away. The speed at which these disturbances move through the power system is determined by the system topology, line parameters, and machine parameters. Several similar triangulation algorithms are under development at other institutions.

It should be noted that due to the relatively slow nature of electromechanical phenomena, they can be adequately observed with the FNET system and phasor measurement units. Anti-aliasing filters within the phasor measurement unit will severely attenuate the high-frequency transients of electromagnetic phenomena. Step changes in voltages and currents caused by faults and other switching events can be more or less observed by PMUs although there will be a time lag introduced (7). For applications based on observing electromagnetic traveling waves specialized high frequency, time-synchronized measurement devices are used. Usually these devices transmit and record data only when triggered by an event.

1.3 Manifestation in Power System Variables

Voltage angle and frequency are wide area parameters in that they yield information on the health of the entire interconnected system; whereas, voltage magnitude is a localized parameter and is not necessarily influenced by distant events (8). Unlike deviations in frequency, voltage deviations (even those of significant magnitude) are usually present only in a localized area and not the whole interconnection. Furthermore, steady-state voltage magnitude measurements are not necessarily an indication of global voltage stability throughout the interconnection, but by definition time-averaged frequency must be equal throughout a synchronized interconnection (8).

In this study electromechanical traveling waves are always observed in angle and frequency and electromagnetic traveling waves are observed in voltage magnitude and current magnitude.

In section 1.1 it was stated *that electromagnetic transients arise due to changes in energy conversions between electrical energy and the energy stored in inductors and capacitors in the form of magnetic and electric fields respectively*. The energy stored in inductors and capacitors is referred to as reactive power. Reactive power is not useful in the sense that the energy is stored in the circuit itself instead of being used to do work, and over a full cycle the change in reactive power is zero. The aforementioned statement from section 1.1 can be rephrased simply as: *electromagnetic transients arise from changes in reactive power*. Similarly, in section 1.2 *it was stated that electromechanical transients arise from changes in energy conversions between electrical energy and the mechanical energy stored in the rotating mass of machines*. This can be restated simply as: *electromechanical transients arise from mismatches in real power*.

The decoupled power flow theory states that voltage angle and frequency are strongly coupled to real power and voltage magnitude is strongly coupled to reactive power. Coupling between angle and frequency with reactive power and voltage magnitude with real power exist but it is a second order relationship and usually insignificant. Based on the initiating events for electromechanical and electromagnetic disturbances, the decoupled power flow theory indicates that electromagnetic disturbances are best observed in voltage and current magnitude and electromechanical disturbances are best observed in angle and frequency.

Chapter 2 Analysis of Electromechanical Phenomena

In section 1 electromechanical disturbance propagation was described conceptually. In this chapter electromechanical propagation will be analyzed mathematically for simplified power system models. The power system is represented in a continuum model by assuming that generator and load parameters can be spatially distributed. For both state-space analysis and analysis in the power-angle domain the equations must be linearized around a quiescent operating point and all the assumptions of DC power flow analysis must be used for the system can be solved. The assumptions of DC power flow analysis will be discussed in detail in section 2.2.

2.1 Introduction

In power system analysis significant effort is devoted to studying and controlling power system oscillations. Large oscillations may reduce the transfer capacity of transmission systems below their thermal limits, lead to instability, and also wear down the rotating parts of electric machines. These oscillations are stationary waves that result from the superposition of 2 or more traveling waves. The same phenomenon is occurs with electromagnetic waves. Equation (1.8) shows the expression for an electromagnetic standing wave created by the superposition of the incident and reflected waves along a transmission line. These standing waves are less obvious than their electromechanical counterpart since their wavelengths are much longer, as shown below, so an entire wavelength is rarely ever observed.

$$\lambda = \frac{v}{f} \approx \frac{3 \times 10^8}{60} \approx 5000km \tag{2.1}$$

An event that causes a mismatch in real power will first create traveling waves that propagate away from the disturbance and then at the boundaries of the system they reflect back and the

superposition of the incident and reflected waves causes a standing wave or oscillation. Interarea oscillations may seem to occur in the absence of any event; however, these are the results of undamped or very lightly damped modes in the system. For such cases small variations in loads and generation are sufficient to excite the mode. The study of such phenomena is referred to as small-signal stability analysis. In this chapter the analytical tools for studying both traveling and stationary electromechanical waves are described.

One of the principal objectives of this research is to calculate electromechanical propagation delays between different locations of the transmission network. This is done by finding the difference in the arrival time of the disturbance at the different buses. The onset of a traveling wave can be determined with the use of various discriminant functions. This is particularly useful for cases where dispersion and reflection causes the onset of the traveling wave to become distorted. For applications in which only the initial arrival of the wave is of concern a very simple discriminant function is formulated by identifying one of three points: the first peak, the threshold crossing, or the bifurcation point. Figure 2-1 shows the angle on one generator in the 5-machine system of Figure 1-4 in response to a step change in bus angle several buses away. The system was simulated in Matlab by simultaneously solving the equations for power flow along a transmission line and the swing equations for each generator.

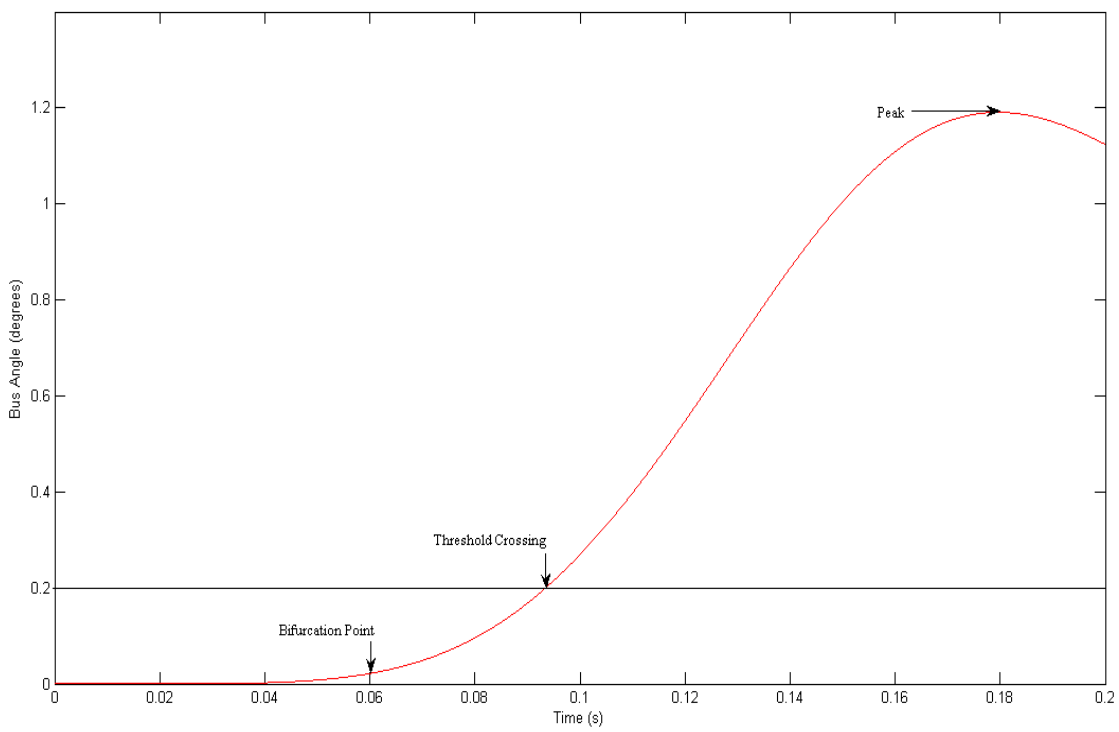

Figure 2-1: An Electromechanical Wavefront

Delays in traveling waves must be computed by comparing points in different locations that are at exactly the same point in the same periodic cycle. The peaks of a sinusoidal wave tend to be the easiest points to identify in the cycle; hence, the time of arrival can be noted at the time of the first peak. This method becomes inaccurate when buses exhibit significantly different frequencies of oscillation.

In Figure 2-1 the bus angle starts increasing from the time of the disturbance, but the angle deviation is insignificant until the point of maximum acceleration, $max\left(\frac{d^2\delta}{dt^2}\right)$, at 0.055s. In this research the point of maximum acceleration is called the bifurcation point since this is the point at which the angle splits apart from the rest of the angles in the synchronized power system. For a tightly coupled system the onset of a traveling wave is preceded by an increase in angle deviation, referred to as the *precursor toe*. The precursor toe may make it quite difficult to

visually determine the actual onset of the electromechanical traveling wave at the bus. In these cases identifying the bifurcation point is helpful.

The threshold crossing method is not theoretically sound if different buses have deviations of differing sizes since they may cross the threshold at different points on their cycle. However, due to noise and inaccuracies in real wide area time-synchronized measurements, most PMU and FNET applications use a static threshold to determine the times of arrival. In section 2.3.1 other advantages of this method will be presented. Throughout this paper all three methods will be discussed, but most emphasis will be placed on the threshold method.

2.2 The Continuum Model

Following deregulation in North America and Europe, the size of the interconnected system has increased significantly. Now there are systems spanning almost entire continents. It has been suggested that the global stability behavior of such systems cannot be properly understood with conventional power system models. From a wide-area perspective the generators, lines, and loads appear to form continuum instead of a discrete system. With the continuum model the wave-like properties of electromechanical phenomena that have been observed through actual measurements, can be better understood. Figure 2-2 shows one node in the continuum model of a power system (4). The rotor's angular rotation in is described by the swing equation in Equation (1.9).

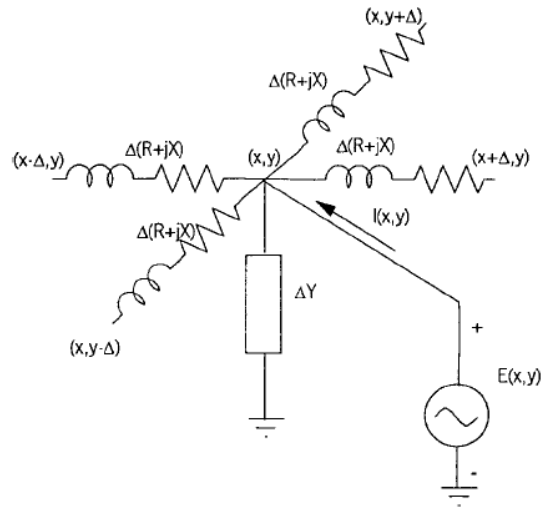

Figure 2-2: The Continuum Model (4)

The generator supplied current, I_{ij}, divides into the four branch currents labeled $I_{i+1/2,j}$, $I_{i-1/2,j}$, $I_{i,j+1/2}$, and $I_{i,j-1/2}$:

$$I_{i+1/2,j} = \frac{E_{ij}-E_{i+1,j}}{Z} \qquad I_{i-1/2,j} = -\frac{E_{ij}-E_{i-1,j}}{Z}$$

$$I_{i,j+1/2} = \frac{E_{ij}-E_{i,j+1}}{Z} \qquad I_{i,j-1/2} = -\frac{E_{ij}-E_{i,j-1}}{Z}$$

If E is the line voltage and $Z = R + j\omega L = R + jX$ Kirchoff's current law at node (i,j) yields:

$$I_{ij} = I_{i+1/2,j} - I_{i-1/2,j} + I_{i,j+1/2} - I_{i,j-1/2} + \Delta Y E_{i_\tau j} \tag{2.2}$$

$$I_{ij} = \frac{1}{Z}(4E_{ij} - E_{i+1,j} - E_{i-1,j} - E_{i,j+1} - E_{i,j-1}) + \Delta Y E_{i_\tau j} \tag{2.3}$$

To get to the continuum limit each (i, j) node is associated with a Cartesian coordinate (x,y). The separation between adjacent nodes is an infinitely small increment, Δ. Substituting the Taylor series expansions of E(x+Δ,y), E(x-Δ,y), E(x,y+Δ), E(x,y-Δ), and E(x,y) up to fourth order into (2.3) yields:

$$I(x,y) = -\frac{\Delta^2}{Z}\left[\Delta^2 E(x,y) + \frac{\Delta^2}{12}\Delta^4 E(x,y)\right] + \Delta Y E(x,y) \tag{2.4}$$

If Δ is infinitely small the fourth-order term may be neglected.

$$P_e(x,y) = Re\{\hat{E}(x,y)\hat{I} * (x,y)\} \tag{2.5}$$

If $E(x,y) = Ve^{j\delta(x,y)}$ then the real power is:

$$P_e(x,y) = -\frac{\Delta^2 V^2}{|Z|^2}[X\nabla^2\delta - \mathrm{R}(\nabla\delta)^2] + \Delta V^2 G \tag{2.6}$$

Where G=Re{Y}

In taking the continuum limit of the swing equation, the inertia constant, mechanical damping, and line impedance become distributed parameters which are functions of the spatial coordinates x and y. Upon substituting (2.6) into (1.9) we obtain:

$$\frac{2h}{\omega}\frac{\partial^2\delta}{\partial t^2} + \omega d\frac{\partial\delta}{\partial t} - \frac{V^2}{|z|}[sin\theta\nabla^2\delta - \cos\theta(\nabla\delta)^2] = p_m - GV^2 \tag{2.7}$$

Where, $z(x,y) = |z|(cos\theta + js2sin\theta)$

Equation (2.7) can be rewritten in the form of a second-order hyperbolic wave equation.

$$\frac{\partial^2\delta}{\partial t^2} + \upsilon\frac{\partial\delta}{\partial t} - v^2\nabla^2\delta + \mathrm{u}^2(\nabla\delta)^2 = P \tag{2.8}$$

Where, $v^2 = \frac{\omega V^2 sin\theta}{2h|z|}$

$u^2 = \frac{\omega V^2 cos\theta}{2h|z|}$

$P = \frac{\omega(p_m - GV^2)}{2h}$

$\upsilon^2 = \frac{\omega^2 d}{2h}$

In (9) Parashar develops the equations describing the dynamics of the continuum model with many of the simplifying assumptions removed; however, the results are very similar to the simpler version. The continuum model is used to analyze the global dynamic characteristics of large scale power systems. If the system and load flow parameters are known the rates of growth

or attenuation of an electromechanical wave can be calculated. Results have shown that waves propagating in the same direction as the power flow tend to grow; whereas, waves propagating opposite to the direction of power flow shrink. The equations above show how the speed of propagation can be calculated from line and machine parameters. The speed, as observed through simulation, has been found to be very close to the calculated value from the continuum model. For typical power system parameters, calculated electromechanical propagation speeds are approximately 500km/s. This matches observed values from PMU and FNET systems (4).

The continuum model is particularly adept at analyzing the wave properties of electromechanical phenomena. Reflection, interference, and dispersion are all readily observed and analyzed. The dispersion is frequency dependent, so by perturbing the system with a smooth function instead of a non-continuous disturbance, such as an impulse or step function, the dispersion is heavily limited. Traveling waves propagate through the system and then reflect back and forth creating the standing waves, or inter-area oscillations. In (10) the continuum model technique was used to design a zero-reflection controller for generators at the ends of a power system.

In an interconnected power system changes in the power output of any generator will cause changes in power output of every other generator in the system. These induced changes will be largest in neighboring machines and insignificant in very distant machines. At the continuum limit the coupling matrix would approach an infinite dimension if the effect of each generator on every other generator in the system was accounted for. This problem is addressed by using simplifications such that the electrical power of each machine is affected by a relatively small number of neighboring machines regardless of the size of the network. For example, in the 64-machine ring system a perturbation on one machine immediately affects only the 8 nearest

machines. This effectively reduces the number of machines that experience precursor toes to only the 8 nearest machines. An error of 0.34% was introduced(10).

2.4 State-Space Analysis

State-space analysis of the electromechanical dynamics of a power system is not a new concept (11); it has been used in stability studies to examine the eigenvalues of the plant matrix, as well as in disturbance analysis to study the frequency signatures of large generators (12). State-space techniques can also be used to calculate expressions for angles and frequencies as a function of time. This chapter will also illustrate how state-space analysis could be used to determine delays in the propagation of an electromechanical disturbance.

Throughout this research and other papers on similar topics, the terms *bus angle* and *rotor angle*, are used somewhat interchangeably since in most cases they are approximately equal. Before delving into the state-space representation of power systems it is important to define these terms and how they are derived.

Faraday's law of electromagnetic induction shows that the induced voltage is equal to the rate of change of magnetic flux through the circuit.

$$v = -\frac{d\lambda}{dt} \tag{2.9}$$

For a synchronous machine the flux linkage, λ, is a function of the flux density, B, the area of the armature coil, S, and the armature's angular position, θ.

$$\lambda = SBcos\theta \tag{2.10}$$

When the coil is rotated at a speed equal to ω, with θ=ωt, the voltage of the coil is given by

$$v(t) = \frac{d\lambda}{dt} = \frac{d}{dt}sBcos(\omega t) = -SB\omega sin(\omega t) \tag{2.11}$$

Equation (2.11) shows that the frequency of the voltage is directly related to the speed of the generators. If δ(t) is the angular position of the rotor with respect to a synchronously rotating frame of reference then it can be expressed as:

$$\delta(t) = \int_{t_0}^{t} \omega_r(\tau)\, d\tau - \omega_s t + \delta_0 \tag{2.12}$$

Where, $\omega_r(\tau)$ is the angular velocity of the rotor,

ω_s is the synchronous speed

δ_0 is the initial value of the rotor angle.

It is important to realize that the electrical angle of the generator's internal voltage is directly related to this angle since the poles of the machine, and thus the rotor's flux, cut the armature conductors at the rate prescribed by the rotor's speed. This cutting action is what produces the internal voltage and hence the internal voltage angle. For a machine with more than two poles a proportionality constant needs to be included in the equation. These relationships are derived in more detail in various texts (13)(2).

In previous papers, small-signal state models were used to study system stability and generator frequency signatures (12). Governor response is often neglected since it occurs on a longer time frame than the dynamic activity being studied. The plant matrix, A, is a matrix whose elements are all purely real and constant. The states are usually the machine speed differences and the machine internal voltage angle differences with respect to a reference machine. There are two reasons using differences in speeds and angles as the states instead of absolute speeds and angles. Firstly, an n - machine system will have 2n-2 states when differences are used instead of 2n states when absolute values are used. For a 3 – machine system this results in a 4 x 4 matrix versus a 6 x 6 matrix, cutting the number of elements that must be calculated from 36 to 16. The

second, and more important reason, is that the primary objective in stability studies is to determine how well the synchronous machines maintain coherency or "stick" together following a disturbance. Differences in speed and internal voltage angle better indicates this than the absolute values. Rigid-body modes occur when all system states drift together away from a quiescent operating point. This is not revealed in the "differences" state model. For systems with swing buses (or machines with very high inertias), the voltage angle at the swing bus is held constant so rigid-body modes are not possible.

For the state-space representation to be accurate the model must be linearized and only used for *small* deviations around a quiescent point. *Small* in this context is qualified as follows – as the state moves through the state space, there must be an approximately linear relationship between the first derivative of each state variable and the state variables themselves. The change in state position as the state moves through the state space does not necessarily need to be *small* compared to some reference quantity, such as the magnitude of the quiescent point that the system is linearized about. The term *small* is not at all relative to the size of the deviation, but whether or not the deviation remains in a linear region.

For an n-machine system, the state-space representation takes on the form:

$$\frac{d}{dt}\begin{bmatrix}\Delta\delta(t)\\ \Delta\omega(t)\end{bmatrix} = A\begin{bmatrix}\Delta\delta(t)\\ \Delta\omega(t)\end{bmatrix} \tag{2.13}$$

Where Δδ(t) is an n x 1 column vector of machine internal voltage angle deviations and Δω(t) is an n x 1 column vector of machine speed deviations. Hence, the state vector, $x = \begin{bmatrix}\Delta\delta(t)\\ \Delta\omega(t)\end{bmatrix}$ resides in $\Re^{2n}$ and the plant matrix A is a 2n x 2n matrix with all real non-time varying elements.

The plant matrix is developed by writing the governing differential equation for each machine and decomposing each governing equation into a pair of first order equations. To get the

elements of the plant matrix the first derivative of each state must be expressed as a linear combination of all of the other states. (2.14) shows the first derivative of the *i* th state, $x_i(t)$ expressed in this form:

$$\frac{dx_i(t)}{dt} = \sum_{j=1}^{n} a_{ij} \cdot x_j(t) \tag{2.14}$$

Writing the swing equation for each machine in an n – machine system yields:

$$\frac{2H_i}{\omega_s}\frac{d^2\delta_i(t)}{dt^2} = P_{mi} - P_{ei} = P_{mi} - \sum_{j=1}^{n} E_i E_j B_{ij} \sin\left(\delta_i - \delta_j\right) \tag{2.15}$$

There are a few features of this equation that need to be discussed. First, the equation describes the motion of the *i* th machine connected to a lossless system. There is no line resistance or damping on synchronized machines in the system. Second, this is a non-linear differential equation with constant coefficients. (2.15) may be linearized around a quiescent operating point, which should be the post-disturbance quiescent point. After a disturbance the system will be oscillating around the post-disturbance quiescent point. Third, the terms B_{ij} are the elements of the post-fault short circuit admittance matrix. The short circuit admittance matrix is an (n-1) x (n-1) matrix and differs from the load flow admittance matrix since it takes into account generator internal reactances. It must be noted that this admittance matrix is a reduced form of the standard short circuit matrix which relates injected currents to applied voltages only at each generator internal voltage. The other buses are eliminated from the matrix via some reduction technique such as a Kron reduction (14). For a Kron reduction all loads must be approximated as constant impedances. For dynamic studies this is unacceptable due to the frequency stability of most loads; however, for small signal disturbances the changes in bus frequency should be small enough for the approximation to suffice. For disturbances that result in large angle and frequency deviations, a non-linear analysis needs to be performed. The

quiescent point around which (2.15) is to be linearized may be expressed as $x_0 = [\delta_{10} \cdots \delta_{n0} \quad \omega_{10} \cdots \omega_{n0}]^t$ so the linearization of (2.15) results in the following expression:

$$\frac{2H_i}{\omega_s}\frac{d^2\Delta\delta_i(t)}{dt^2} = -\sum_{j=1}^{n} E_i E_j B_{ij} \cos\left(\delta_{i0} - \delta_{j0}\right)\left[\Delta\delta_i(t) - \Delta\delta_j(t)\right] \tag{2.16}$$

Since,

$$\frac{d\Delta\delta_i(t)}{dt} = \Delta\omega(t) \tag{2.17}$$

Equation (2.16) can be expressed in the state-space formulation of (2.13). The state vector may be solved for in closed loop form if the initial condition is known.

$$x(t) = e^{At} \cdot x_0 \tag{2.18}$$

Where e^{At} is the transition matrix defined by the power series representation of the exponential function. If all of the eigenvalues of A are distinct, as they will be for a practical system, then A may be diagonalized as follow (12) :

$$A = P\Lambda P^{-1} = \phi \begin{bmatrix} \lambda_1 & 0 & 0 \\ 0 & \ddots & 0 \\ 0 & 0 & \lambda_n \end{bmatrix} \psi \tag{2.19}$$

Where $\phi = [\phi_1 \quad \cdots \quad \phi_n]$ and $\psi = [\psi_1 \quad \cdots \quad \psi_n]$ where ϕ is an n x n matrix who's columns, ϕ_i, are the normalized right eigenvectors of A; ψ is an n x n matrix who's rows, ψ_i, are left eigenvectors (not necessarily normalized) of A; and the λ_i's in the diagonal matrix, Λ, are the n distinct eigenvalues of A. The solution, x(t), may be expressed as

$$x(t) = \langle \psi_1, x(t_0) \rangle \cdot \phi_1 \cdot e^{\lambda_1 t} + \cdots + \langle \psi_n, x(t_0) \rangle \cdot \phi_n \cdot e^{\lambda_n t} \tag{2.20}$$

Each term in the summation corresponds to a mode of the system's natural response. Each eigenvalue, $e^{\lambda_i t}$, in the summation indicates whether or not the *i*th mode is oscillatory or non-oscillatory, damped or undamped. Each inner product term, $\langle \psi_i, x(t_0) \rangle$, in the summation is the excitation magnitude of the *i*th mode. (2.20) indicates that the states will be a linear combination

of sinusoidal terms.

To use this model to calculate the response of bus angles to an event, a relationship between the states and the outputs (measureable variables) needs to be developed. The method developed in (12) is based on DC power flow relationships. DC power relationships are suitable for applications utilizing time-synchronized wide area phasor measurements because of its simplicity and its use of bus phasor angles. The simplifications of the DC power flow model are as follows:

1. Transmission lines are purely reactive. For EHV lines the reactance is so much larger than the resistance that this is a reasonable assumption.
2. The line model does not include shunt reactances. This feature may render the DC power flow model useless for widespread systems.
3. All of the bus voltage magnitudes have a value of 1.0 pu.
4. The voltage angle difference across transmission lines is low enough for the power flow on the line to be modeled with a linear equation instead of with a trigonometric relation.

For the full AC load flow solution, the power flow on a transmission line is given by:

$$P_{ij} = V_i V_j b_{ij} sin(\delta_i - \delta_j) \tag{2.21}$$

With the 4 simplifications of the DC power flow, the expression reduces to:

$$P_{ij} = b_{ij} \cdot (\delta_i - \delta_j) \tag{2.22}$$

If (2.22) is written for each line at a given node in the system, the total power injected at the node takes the form below.

$$P_{ij} = \sum_{j=1}^{n} b_{ij} \cdot (\delta_i - \delta_j) \quad \text{for i=1, 2,…n} \tag{2.23}$$

This can be written in matrix form as:

$$P = B\delta \tag{2.24}$$

Where P is an n x 1 column vector of the power injections at each bus, δ is an n x 1 column

vector of the voltage angles at each bus in the system, and B is an n x n susceptance matrix whose entries are the negative of the transfer admittance between the *i* and *j*th buses. n is the total number of buses in the system. Considering small changes in the bus angle vector, Δδ, (2.24) can be written as

$$\Delta P = B \cdot \Delta\delta \tag{2.25}$$

The next step is to partition the matrices in (2.25) to divide the states from the measurement quantities.

$$\begin{bmatrix} \Delta P_1 \\ \vdots \\ \Delta P_n \\ \hline \Delta P_{n+1} \\ \vdots \\ \Delta P_p \end{bmatrix} = \left[\begin{array}{ccc|ccc} b_{11} & \cdots & b_{1n} & b_{1(n+1)} & \cdots & b_{1p} \\ \vdots & \ddots & \vdots & \vdots & \ddots & \vdots \\ b_{n1} & \cdots & b_{nn} & b_{n(n+1)} & \cdots & b_{np} \\ \hline b_{(n+1)1} & \cdots & b_{(n+1)n} & b_{(n+1)(n+1)} & \cdots & b_{(n+1)p} \\ \vdots & \ddots & \vdots & \vdots & \ddots & \vdots \\ b_{p1} & \cdots & b_{pn} & b_{p(n+1)} & \cdots & b_{pp} \end{array}\right] \cdot \begin{bmatrix} \Delta\delta_1 \\ \vdots \\ \Delta\delta_n \\ \hline \Delta\delta_{n+1} \\ \vdots \\ \Delta\delta_p \end{bmatrix} \tag{2.26}$$

Here the number of buses that have measurement is equal to p-n. The lower partition of the column vectors is associated with the outputs and the upper partition of the Δδ vector is part of the system state. (2.26) can be written in compact form:

$$\begin{bmatrix} \Delta P_{states} \\ \Delta P_{output} \end{bmatrix} = \begin{bmatrix} B_{11} & B_{12} \\ B_{21} & B_{22} \end{bmatrix} \cdot \begin{bmatrix} \Delta\delta_{states} \\ \Delta\delta_{output} \end{bmatrix} \tag{2.27}$$

To use the equation above to explicitly relate the outputs to the states, the ΔP_{output}, must be approximated as zero. This approximation is reasonable in the small signal model especially for lightly loaded systems in which the voltage magnitude does not vary significantly for small angle swings if the load is not highly frequency-dependent and if the frequency deviations are very small compared to rated frequency. With this approximation (2.27) becomes:

$$\begin{bmatrix} \Delta P_{states} \\ 0 \end{bmatrix} = \begin{bmatrix} B_{11} & B_{12} \\ B_{21} & B_{22} \end{bmatrix} \cdot \begin{bmatrix} \Delta\delta_{states} \\ \Delta\delta_{output} \end{bmatrix} \tag{2.28}$$

And the following relationship can be derived:

$$-B_{21}\Delta\delta_{states}=B_{22}\Delta\delta_{output} \tag{2.29}$$

If B_{22} is invertible the equation can be rearranged to give:

$$\Delta\delta_{output}=-B_{22}^{-1}B_{21}\Delta\delta_{states} \tag{2.30}$$

(2.30) gives a linear relationship between the states and the outputs. This is the output equation in the standard state space representation, $y(t) = Cx(t)$. After developing expressions for machine rotor angles and bus voltage angles we can use a non-linear solving technique such as Newton's method to find the point at which a certain threshold is crossed, the point at which the first stationary point occurs (peak), or the point at which the second derivative is maximized (bifurcation point). Obviously, this is an indirect means of calculating propagation delays and the wave properties of the electromechanical propagating disturbance are difficult to analyze. However, state-space analysis is one of the most common methods of performing modal analysis on large power systems.

Chapter 3 Analysis in the Power Angle Domain

In the previous chapter, two methods of analyzing electromechanical phenomena were described. The continuum model is suitable for studying global system characteristics such as stability and electromechanical wave propagation, but in assuming the system to be a continuum much of the details associated with the dynamics of individual machines are lost (7). For more accurate analysis of the swings in the immediate vicinity of the disturbance this method may not be accurate. Applications of state-space analysis and other modal analysis techniques have been developed and tested by various researchers and have proven to be useful in analyzing measured oscillations in the post-disturbance system. It is also possible to use them to predict swings for a given contingency and operating condition; however, it involves solving the state equation and using an output equation to calculate the changes in angle and rotor speed; which can be quite tedious. Various other tools have been proposed and developed to predict swings and analyze stability; such as, the transient energy function, the extended equal area criterion, and various pattern recognition techniques. This chapter contains a brief overview of other methods for analyzing electromechanical phenomena in power systems and assessing the system stability and then it focuses on developing techniques for analysis in the power-angle domain.

3.1 Introduction

For most situations the stability of a system can be analyzed with detailed time-domain simulations. For a time-domain simulation to be comprehensive it must be executed many times to account for all possible operating conditions. Time-domain simulations use non-linear integration to solve a set of linear and non-linear differential equations describing the dynamics of the power system. For a sophisticated model the results are more accurate than those obtained

by any other technique; however, this method is unable to provide an analytical insight into the qualitative behavior of the dynamic system. Therefore, it is difficult to design screening and stability tools based on analysis with only dynamic simulations (15). Additionally, dynamic simulation is computationally intensive and requires a large amount of data on every component in the system, making it difficult to update and execute in real-time.

The transient energy function is based on Lyapunov's second method and it determines the stability of the system without explicitly solving the system's differential equations. The energy added to a system by some disturbance is computed by summing the change in rotor kinetic energy, rotor potential energy, the energy dissipated in branches, and the energy stored in branches. If the critical energy, the maximum amount of transient energy that the system can absorb, is exceeded then the system will go unstable. Although this technique is academically appealing, it has been difficult to apply for several reasons: (i) the critical energy is dependent on the trajectory of the disturbance and difficult to predict in real-time, (ii) it is computationally intensive for a large system, (iii) only highly simplified power system models are acceptable, (iv) it fails to predict second swing instability in some cases (15)(16).

The extended equal area criterion assesses the stability of the system by aggregating the multi-machine system into a 2 machine equivalent and then into a one machine infinite bus equivalent. The equal area criterion can then be used to determine stability and calculate the critical clearing time. Sources of errors in this method arise from the representation of a large number of machines by one equivalent machine. This results in the rotor angles of many individual machines being replaced by their corresponding center of angle. This technique has been successfully used to determine the stability of a system after a major disturbance; however,

because of the simplification to a 2- machine system it is unsuitable for any oscillation analysis, angle predictions or detailed analysis of power flows (15).

The decision tree transient stability method uses a set of measurements or indicators to make a number of decisions leading to a final assessment of whether the system is stable or not. The decision tree is built by running a large number of simulations and recording a set of measurements for each simulation and an assessment of whether the system was stable or unstable. This set of simulations along with their assessment of stability is called the training set. To ensure that the decision tree is accurate for a wide range of conditions the training set must contain a large number of cases from different operating conditions. Statistical methods are then used to build the optimum decision tree based on the data from the training set. Online applications are created by inputting measurements from PMUs into the system and the decision tree determines whether the system is stable or not. Essentially, the current operating state is compared to simulated operating states that are known to be stable or unstable. This technique provides a very quick assessment of stability and if the training set was properly created and spanned all feasible operating conditions the decision tree will produce accurate results (17) (15). However, this method suffers from the same drawbacks of time-domain simulation in that it doesn't provide an analytical understanding of the system and it is difficult to use in stability analysis. It is essentially a useful tool for analyzing the results of time-domain simulations.

The remainder of this chapter will describe the analysis of electromechanical phenomena in the power-angle domain. A technique for creating electromechanical equivalents in the power-angle domain will be developed and demonstrated on some sample systems.

It is important to emphasize that the P-δ domain model assumes that the system can be linearized around a quiescent operating point. Because of this assumption, P-δ domain analysis

is unsuitable for events that cause large deviations in angle since the system's response becomes largely non-linear. The study of a power system's response to large events is known as *transient stability analysis*. Transient events include faults on the EHV network, large generation trips, large load trips, or even switching of heavily loaded lines. P-δ domain analysis may only be used for *small-signal stability analysis*, which assumes that change in angle due to an event is small enough that the system's response can be considered linear.

3.2 Derivation of Equations

The generator model in the P-δ domain is based on the classical generator model which is a constant voltage source behind the direct axis transient reactance. To describe this model let's re-look at the 5-machine system of Figure 1-4. The diagram below shows the 5-machine system again with the changes in bus angle, Δθ, and the changes in rotor angle, Δδ, as the variables of concern. The changes in bus angles instead of the absolute angles are used to avoid considering the steady-state angles. In this section, the power-angle model will be developed without regard to the quiescent operating point.

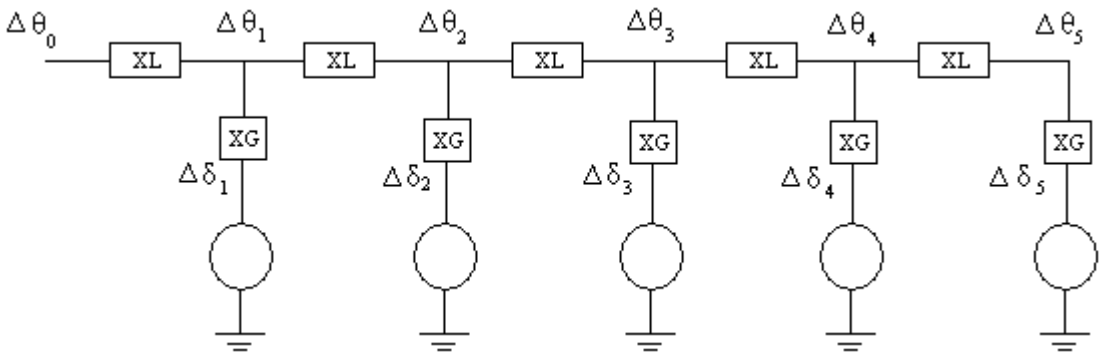

Figure 3-1: 5-Machine System

The rotor angle will be a time-integral of the difference in mechanical and electrical power at the generator; therefore, it cannot change within the time frame of electromagnetic phenomena. If the system in Figure 3-1 was being analyzed only within the time frame of electromagnetic phenomena the electromechanical variables, which are the generator rotor angles, would not change significantly so the generators could be short-circuited leaving a purely electrical system. Figure 3-2 shows the equivalent circuit during the electromagnetic time frame.

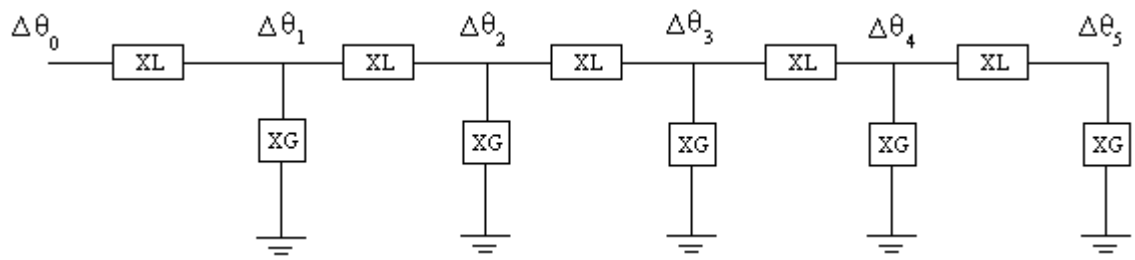

Figure 3-2: 5-Machine System within an Electromagnetic Time Frame

The change in rotor angle will be zero within the electromagnetic time frame so in the P-δ domain it is grounded. Note that the machine's electrical power will change as the angle of the terminal voltage changes. The system's response will be a function of only the generator and network impedances. Short-circuit analysis programs treat generators in a similar way; however, the line impedances and the internal impedances of the generators would be modeled in far more detail. This system could be analyzed as a conventional electrical ladder circuit with $\Delta\theta$ being analogous to voltage and power flow being analogous to current. It could easily be shown that for a step change in $\Delta\theta_0$ the buses that are closer to Bus 0 have a higher change than the buses that are further away.

Referring to Figure 3-1, while maintaining the analogy of the angle-power relationships and the voltage-current relationships, it can be seen that every bus voltage angle in the system is a linear combination of all of the machine angles. If the assumptions of the DC load flow are acceptable then we may perform the equivalent of nodal analysis at each node in the system in the power-angle domain. For bus 1 this yields:

$$\frac{\theta_1 - \theta_0}{X_L} + \frac{\theta_1 - \delta_1}{X_G} + \frac{\theta_1 - \theta_2}{X_L} = 0 \tag{3.1}$$

Or

$$\theta_1 = \theta_0 \frac{X_G}{2X_G + X_L} + \delta_1 \frac{X_L}{2X_G + X_L} + \theta_2 \frac{X_G}{2X_G + X_L} \tag{3.2}$$

If it is assumed that X_G is small enough that it is approximately zero then the preceding equation yields $\theta_1 \approx \delta_1$. An implicit assumption in most PMU and FNET applications is that a PMU at a transmission bus that is very close to a generator has the same dynamics as the generator's rotor angle. This is based on the assumption that the generator's internal impedance is insignificant compared to the system's driving impedance at that location.

Now let us analyze the small-signal stability case for which $\Delta\delta$ is oscillating. The swing equation, (1.9), is stated again below for convenience.

$$\frac{2H}{\omega}\frac{d^2\delta}{dt^2} = P_m - P_e - D\frac{d\delta}{dt} \tag{1.9}$$

Let us consider a small deviation $\Delta\delta$ from the initial operating point δ_0:

$$\delta = \delta_0 + \Delta\delta \tag{3.3}$$

This expression can be inserted into the swing equation.

$$M\frac{d^2(\delta_0 + \Delta\delta)}{dt^2} = P_m - P_e - D\frac{d(\delta_0 + \Delta\delta)}{dt} \tag{3.4}$$

For simplification it is assumed that there is no damping (D=0):

$$M\frac{d^2(\delta_0 + \Delta\delta)}{dt^2} = P_m - P_e \tag{3.5}$$

P_e is the electrical power flowing through the line connecting the generator to the system:

$$M\frac{d^2(\delta_0 + \Delta\delta)}{dt^2} = P_m - \frac{|V_1||V_2|}{X}\sin(\delta_0 + \Delta\delta) \tag{3.6}$$

Or

$$M\frac{d^2\delta_0}{dt^2} + M\frac{d^2\Delta\delta}{dt^2} = P_m - \frac{|V_1||V_2|}{X}(\sin\delta_0\cos\Delta\delta + \cos\delta_0\sin\Delta\delta) \tag{3.7}$$

If $\Delta\delta$ is small, $\cos\Delta\delta \approx 1$ and $\sin\Delta\delta \approx \Delta\delta$:

$$M\frac{d^2\delta_0}{dt^2} + M\frac{d^2\Delta\delta}{dt^2} = P_m - \frac{|V_1||V_2|}{X}\sin\delta_0 - \frac{|V_1||V_2|}{X}\cos\delta_0\Delta\delta \tag{3.8}$$

Since at the initial operating point:

$$M\frac{d^2\delta_0}{dt^2} = P_m - \frac{|V_1||V_2|}{X}\sin\delta_0 \tag{3.9}$$

Subtracting (3.9) from (3.8) gives the linearized swing equation:

$$M\frac{d^2\Delta\delta}{dt^2} = -\frac{|V_1||V_2|}{X}\cos\delta_0\Delta\delta \tag{3.10}$$

If it assumed that the bus voltages are approximately 1.0 pu this becomes:

$$M\frac{d^2\Delta\delta}{dt^2} = -\frac{\cos\delta_0}{X}\Delta\delta \tag{3.11}$$

Converting to the Laplacian domain gives:

$$Ms^2\Delta\delta = -\frac{\cos\delta_0}{X}\Delta\delta \tag{3.12}$$

Or

$$Ms^2\Delta\delta = -\Delta P_e \tag{3.13}$$

In power systems analysis the convention is to define the power leaving the generator as positive; however, in the P-δ domain model it is easier to define the power entering the generator as positive so as to avoid the negative sign in the expression for the change in machine angle. We will call the power entering the generator P instead of P_e.

$$\Delta P = -\Delta P_e \tag{3.14}$$

Hence,

$$\Delta\delta = \frac{\Delta P}{Ms^2} \tag{3.15}$$

(2.22) showed the expression for the power flow through a transmission line under the assumptions of DC load flows. Rearranging this equation and using the reactance instead of the susceptance yields:

$$X = \frac{\delta_1 - \delta_2}{\Delta P} \quad \text{or} \quad X = \frac{\Delta\delta}{\Delta P} \tag{3.16}$$

Rearranging (3.16) yields:

$$\frac{1}{Ms^2} = \frac{\Delta\delta}{\Delta P} \tag{3.17}$$

Based on (3.16) and (3.17), X and $\frac{\mathbf{1}}{\boldsymbol{Ms^2}}$ have the same effect. They are both functioning as a *resistance to power flow* across an angle difference. This is analogous to impedance being a resistance to current flow across a voltage difference. Based on this we establish models for power systems analysis in the P-δ domain. The model for a single generator in the P-δ domain is shown below.

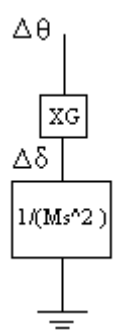

Figure 3-3: Generator Model in the P-δ Domain

Using the linearized angles, the power flowing into the generator, P, is given by:

$$\Delta P = -\Delta P_e = \frac{cos(\theta_0 - \delta_0)}{X_G}(\Delta\theta - \Delta\delta) \tag{3.18}$$

Neglecting the initial difference in angles yields:

$$Ms^2\Delta\delta = -\Delta P_e = \frac{1}{X_G}(\Delta\theta - \Delta\delta) \tag{3.19}$$

The Laplacian operator, s, is equal to jΔω, where Δω is the difference between the rotor's speed and synchronous speed. For the system in steady-state Δω is zero resulting in the model of Figure 3-2. Immediately following an event, electromechanical variables will not have changed significantly so Δω can be considered to be zero. Otherwise Δω is not zero and should be solved for. Figure 3-4 shows a schematic of the 5-machine system in the P-δ domain.

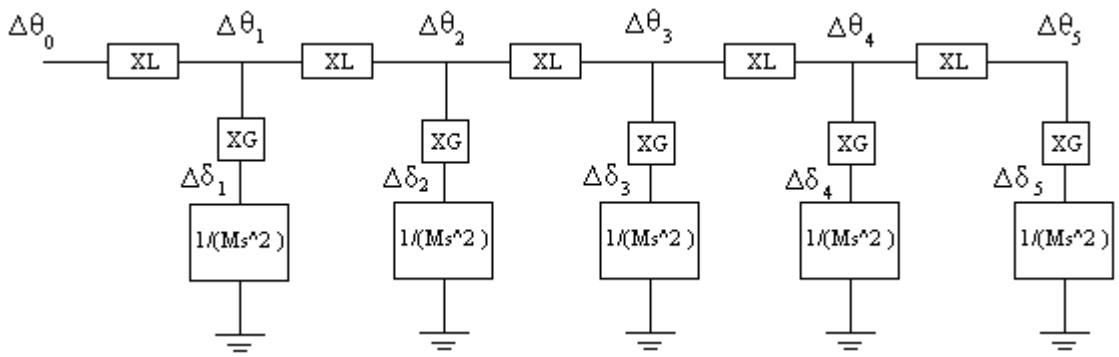

Figure 3-4: Model for a 5-Machine System in the P-δ Domain

For a step change in angle of 10^0 at the first bus, $\Delta\theta_0 = 10u(t)$, expressions for each of the bus angles or rotor angles can be developed in the Laplace domain.

Let:

H=5 pu on a 1000MVA base

X_L=0.05pu on a 100MVA base

X_G=0.00005 on a 100MVA base

To find the expression for θ_1 we must replace everything behind the first node with an equivalent.

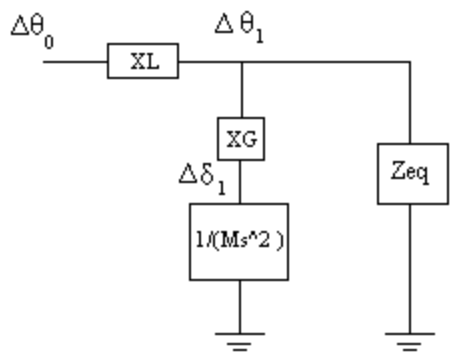

Figure 3-5: Computing $\Delta\theta_1$ in the P-δ Domain

The equivalent is created by adding in series and parallel each "*resistance to power flow*" the same way that resistors in a ladder circuit are combined. The Laplace domain expression for a 5-machine system is too large to be shown here; however, the time-domain expressions consist of only 5 sinusoidal components.

$$\theta_1(t) = 10 - 3.6\cos(2.5t) - 3.0\cos(7.2t) - 2.1\cos(11.4t) - 1.1\cos(14.6t) - 0.3\cos(16.6t) \quad (3.20)$$

Referring to Figure 3-3 the rotor angle can easily also be solved for if the bus angle is known using the equivalent of voltage division.

$$\delta_1(s) = \frac{\frac{1}{Ms^2}}{\frac{1}{Ms^2} + X_G}\theta_1(s) \quad (3.21)$$

$$\delta_1(t) = 10 - 3.6\cos(2.5t) - 3.0\cos(7.2t) - 2.1\cos(11.4t) - 1.1\cos(14.6t) - 0.3\cos(16.6t \quad (3.22)$$

With X_G so small relative to X_L, the machine's rotor angle is approximately equal to the voltage angle at its terminals. If an expression for $\theta_1(s)$ is known then Figure 3-6 shows how the adjacent bus angle can be solved for.

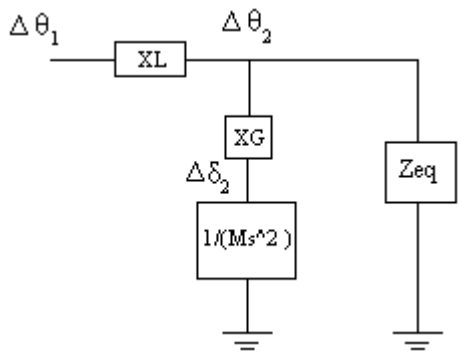

Figure 3-6: Computing $\Delta\theta_2$ in the P-δ Domain

All 5 bus voltage angles and rotor angles can be solved for in this manner. The expressions for the 5 bus angles are shown below:

$$\theta_1(t) = 10 - 3.6\cos(2.5t) - 3.0\cos(7.2t) - 2.1\cos(11.4t) - 1.1\cos(14.6t) - 0.3\cos(16.6t)$$

$$\theta_2(t) = 10 - 6.8\cos(2.5t) - 3.9\cos(7.2t) - 0.59\cos(11.4t) + 0.9\cos(14.6t) + 0.48\cos(16.6t)$$

$$\theta_3(t) = 10 - 9.6\cos(2.5t) - 2.2\cos(7.2t) + 1.9\cos(11.4t) + 0.3\cos(14.6t) - 0.526\cos(16.6t)$$

$$\theta_4(t) = 10 - 11.5\cos(2.5t) + 1.1\cos(7.2t) + 1.1\cos(11.4t) - 1.2\cos(14.6t) + 0.4\cos(16.6t)$$

$$\theta_5(t) = 10 - 12.5\cos(2.5t) + 3.6\cos(7.2t) - 1.6\cos(11.4t) + 0.6\cos(14.6t) - 0.15\cos(16.6t)$$

A more efficient method of computing all five angles would be to solve the nodal equation in matrix form. For an electrical circuit the nodal equations are:

$$[\mathrm{I}] = [\mathrm{Y}][\mathrm{V}] \tag{3.23}$$

For analysis in the P-δ domain the equivalent equations are:

$$[\Delta\mathrm{P}] = [\mathrm{Y}][\Delta\theta] \tag{3.24}$$

Where ΔP is the change in injected power at a bus and Y is the *admittance to power flow* (Y=1/X).

Since there are no constant power loads in the system the power injection at all buses is zero, except at Bus 1 where the power flow from Bus 0 is treated as an injection. To do this Bus 0 is represented as a Norton equivalent.

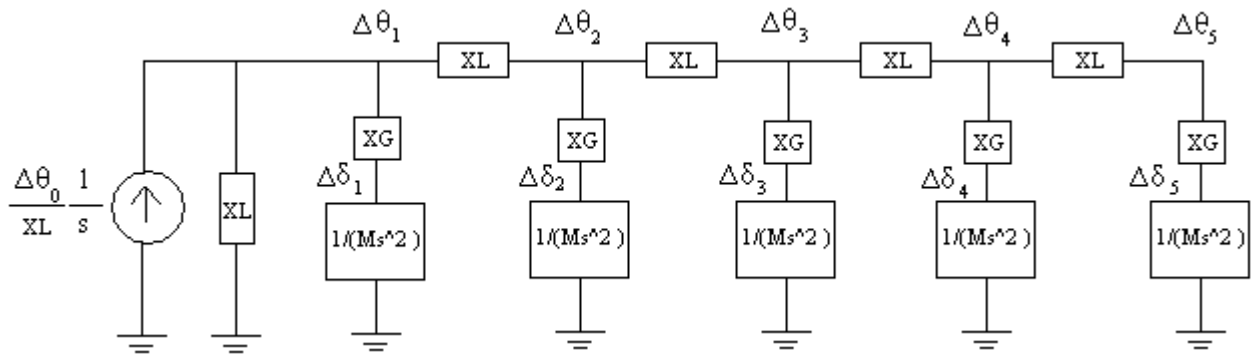

Figure 3-7: Load Trip in the P-δ Domain

Note that Bus 0 could also be represented as a voltage source that undergoes a step change, but by representing it as a Norton equivalent Bus 0 is removed from the circuit and its connecting impedance and power injection are attached to Bus 1. The matrix equations for this network are shown below:

$$\begin{bmatrix} \frac{\Delta\theta_0}{X_L}\frac{1}{s} \\ 0 \\ 0 \\ 0 \\ 0 \end{bmatrix} = \begin{bmatrix} \frac{1}{x_G+\frac{1}{Ms^2}}+2y_L & -y_L & 0 & 0 & 0 \\ -y_L & \frac{1}{x_G+\frac{1}{Ms^2}}+2y_L & -y_L & 0 & 0 \\ 0 & -y_L & \frac{1}{x_G+\frac{1}{Ms^2}}+2y_L & -y_L & 0 \\ 0 & 0 & -y_L & \frac{1}{x_G+\frac{1}{Ms^2}}+2y_L & -y_L \\ 0 & 0 & 0 & -y_L & \frac{1}{x_G+\frac{1}{Ms^2}}+y_L \end{bmatrix} \begin{bmatrix} \Delta\theta_1 \\ \Delta\theta_2 \\ \Delta\theta_3 \\ \Delta\theta_4 \\ \Delta\theta_5 \end{bmatrix} \tag{3.25}$$

$$\begin{bmatrix} \Delta\theta_1 \\ \Delta\theta_2 \\ \Delta\theta_3 \\ \Delta\theta_4 \\ \Delta\theta_5 \end{bmatrix} = \begin{bmatrix} \frac{1}{x_G+\frac{1}{Ms^2}}+2y_L & -y_L & 0 & 0 & 0 \\ -y_L & \frac{1}{x_G+\frac{1}{Ms^2}}+2y_L & -y_L & 0 & 0 \\ 0 & -y_L & \frac{1}{x_G+\frac{1}{Ms^2}}+2y_L & -y_L & 0 \\ 0 & 0 & -y_L & \frac{1}{x_G+\frac{1}{Ms^2}}+2y_L & -y_L \\ 0 & 0 & 0 & -y_L & \frac{1}{x_G+\frac{1}{Ms^2}}+y_L \end{bmatrix}^{-1} \begin{bmatrix} \frac{\Delta\theta_0}{X_L}\frac{1}{s} \\ 0 \\ 0 \\ 0 \\ 0 \end{bmatrix} \tag{3.26}$$

Using Matlab to perform the matrix multiplication and find the inverse laplace transform yields exactly the same equations for the bus angles as the previous method. The results are plotted in the figure below.

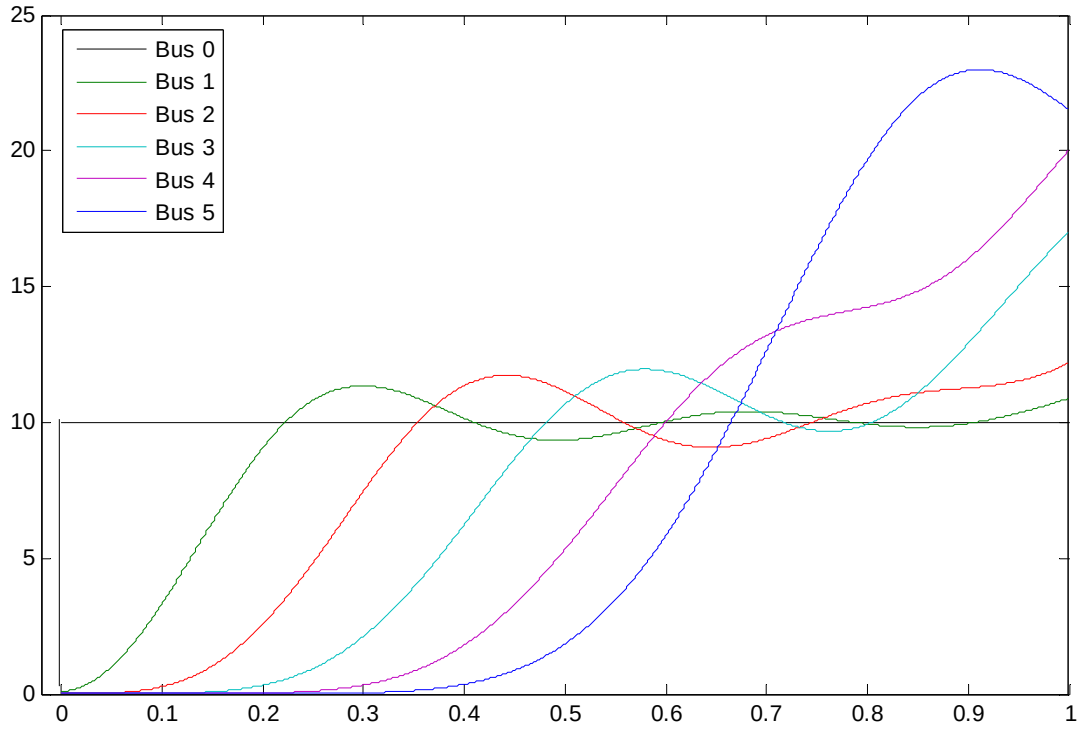

Figure 3-8: Step Change in Angle in the 5-Machine System

These results are verified through simulation and also through state-space analysis. This analysis can be fully programmed in mathematica or matlab. Figure 3-8 clearly shows a disturbance propagating from the bus that is closest to the disturbance to more distant buses. In the following section P-δ domain analysis will be used to approximate electromechanical delays. The threshold or bifurcation method that was discussed in chapter 2 will be used.

3.3 Calculation of propagation delays

An expression for the velocity of an electromagnetic traveling wave and hence, the propagation delay across a transmission line of known parameters can be found fairly simply since electromagnetic propagation is governed by the parameters of the local lines and loads.

Additionally, a transmission line has continuous parameters so calculus can be used to analyze electromagnetic phenomena without any simplifications. Electromechanical traveling waves are affected by every machine in the system and the transmission lines between them. Therefore, an expression for the velocity of an electromechanical traveling wave would have to include properties from every line and generator in the system. The non-uniformity of the system would make this expression very large. Since the status and parameters of all the generators and motors in the system cannot be known, an exact expression governing electromechanical traveling waves is of no value. Instead, this section will develop a method to quickly estimate the angle response at every machine in the system using only the properties of the major generators and lines. It should also help to develop a better understanding of the properties that affect electromechanical propagation.

3.3.1 The threshold method of detecting a wavefront

As mentioned in section 2.1, delays can be calculated using either the stationary point, bifurcation, or threshold crossing methods by explicitly determining the entire trajectory of the bus angles. Having described the process of calculating bus angles in the P-δ domain in the preceding chapter, the method of calculating arrival times using the first peak and bifurcation method will be only described on a high level. The first peak is calculated by finding the derivative of each bus angle and solving for the value of time at which it is zero. For a sinusoidal response there will be more than one stationary point in the system, but a non-linear solver can be set to find the first stationary point after the event. To find the bifurcation point either the maximum value of the second derivative of the bus angles can be found, or the first

stationary point in the third derivative if the non-linear solver cannot easily be set up to find maximum points.

The threshold method, as well as the bifurcation method, determines times of arrival at the beginning of the disturbance as opposed to the first stationary point, which is the maximum deviation for stable cases. The analysis can be greatly simplified by assuming that all machines behind the buses at which delays are being calculated have not been significantly affected before or at the time of the threshold crossing. A similar assumption is required for analysis of electromechanical phenomena with the continuum model. It was assumed that only the 8 closest machines were affected throughout the entire trajectory of the disturbance. Figure 3-9 shows the response of all bus angles in a 5-machine system.

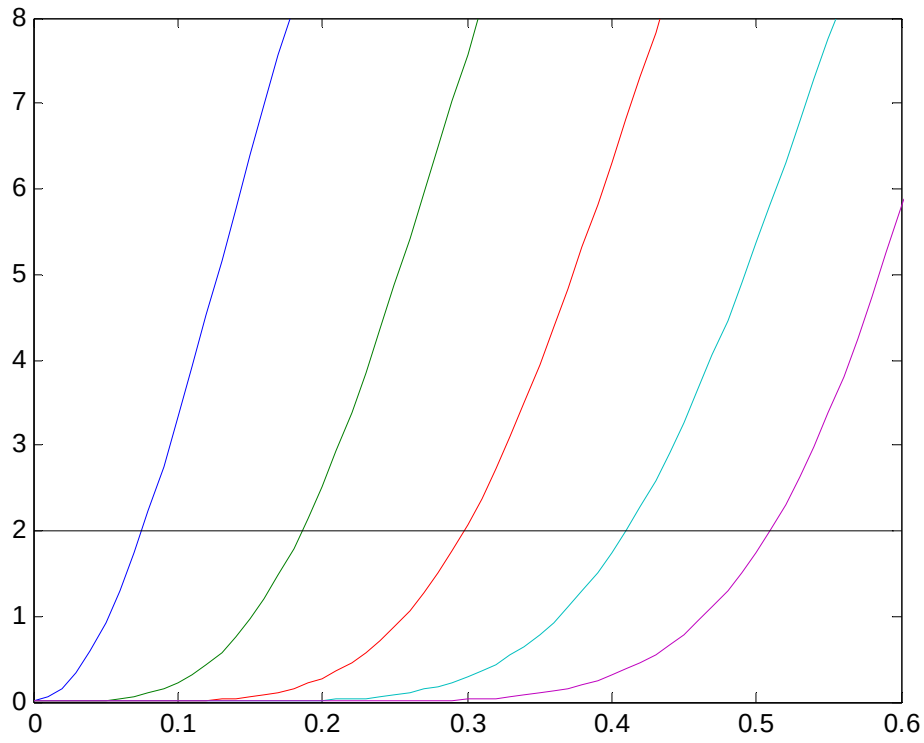

Figure 3-9: Electromechanical Disturbance Threshold Crossings

Referring to the figure above it can be seen that the threshold must be appropriately placed in order for the assumption that more distant buses have not been affected to be valid. If the threshold was too high, say above 5 degrees then when θ_1 crosses the threshold, θ_2 and possibly even θ_3 may be too high to be considered zero without significantly detracting from the accuracy of the model. For analyzing the voltage angle at bus 1 before the threshold crossing is exceeded the model below can be used instead of the complete system in Figure 3-4. This model neglects more distant machines by assuming that their change in power injection, ΔP, is zero, and hence they are open-circuits.

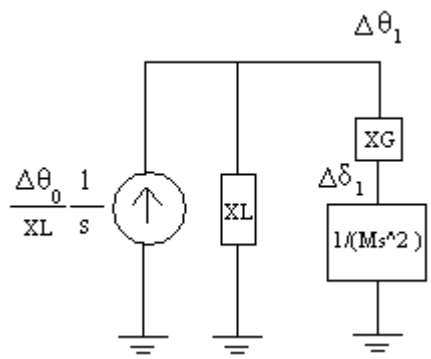

Figure 3-10: Time of Arrival at Bus 1 with the Threshold Method

For simplification let's assume that $X_G \approx 0$ and Figure 3-11 shows the *admittances to power flow* instead of the *resistances to power flow*.

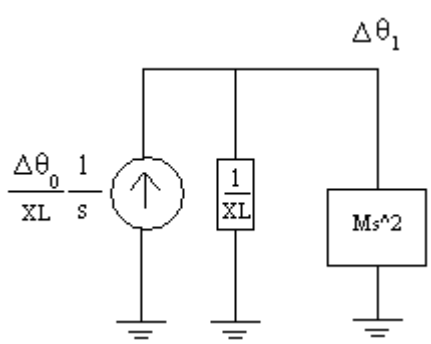

Figure 3-11: Diagram with Admittances to Power Flow

Referring to the diagram above, for $\Delta\theta_0 = 10$:

$$\frac{10}{X_L s} = \left(\frac{1}{X_L} + Ms^2\right)\Delta\theta_1(s) \tag{3.27}$$

$$\Delta\theta_1(s) = \frac{10}{s(1 + MX_L s^2)} \tag{3.28}$$

$$\Delta\theta_1(t) = 10\left[1 - cos\left(\frac{t}{\sqrt{MX_L}}\right)\right]u(t) \tag{3.29}$$

$$\Delta\theta_1(t) = 10[1 - cos(8.683t)]u(t) \tag{3.30}$$

Figure 3-12 shows the system model in the P-δ domain that is used to calculate the time of arrival at Bus 2 with the threshold method.

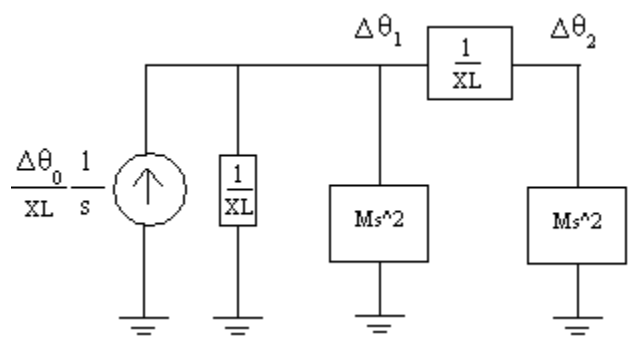

Figure 3-12: Time of Arrival at Bus 2 with the Threshold Method

Matrix analysis techniques will be used here to calculate the angle responses.

$$\begin{bmatrix} \frac{10}{X_L s} \\ 0 \end{bmatrix} = \begin{bmatrix} \frac{2}{X_L} + Ms^2 & -\frac{1}{X_L} \\ -\frac{1}{X_L} & \frac{1}{X_L} + Ms^2 \end{bmatrix} \begin{bmatrix} \Delta\theta_1(s) \\ \Delta\theta_2(s) \end{bmatrix} \tag{3.31}$$

$$\begin{bmatrix} \Delta\theta_1(s) \\ \Delta\theta_2(s) \end{bmatrix} = \begin{bmatrix} \frac{10(1 + MX_L s^2)}{s(1 + 3MX_L s^2 + M^2 {X_L}^2 s^4} \\ \frac{10}{s(1 + 3MX_L s^2 + M^2 {X_L}^2 s^4} \end{bmatrix} \tag{3.32}$$

$$\Delta\theta_1(t) = 10[1 - 0.724cos(5.367t) - 0.276\cos(14.05 * t)]u(t) \quad (3.33)$$

$$\Delta\theta_2(t) = 10[1 - 1.17cos(5.367t) + 0.176\cos(14.05 * t)]u(t) \quad (3.34)$$

Figure 3-13 shows the voltage angles at Bus 1 and Bus 2. It is important to emphasize again that this estimate is valid only for the part of the trajectory that occurs before bus angles further down the system start increasing.

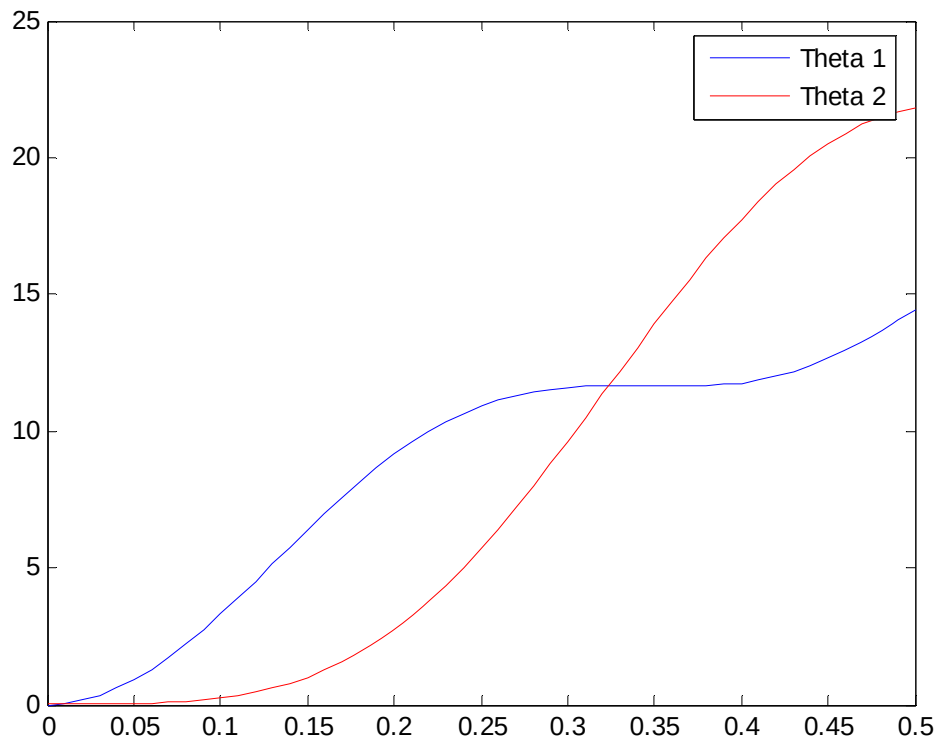

Figure 3-13: Estimates of Voltage Angles at Bus 1 and 2

The diagram below shows the three terms in $\Delta\theta_2$ plotted separately. It is apparent that the summation of the changes in the first two cosines for the first 0.05 seconds is very close to zero. This is where the apparent delay in the electromechanical propagating wave comes from. As more machines are considered there will be more components to each bus angle and it will become even more difficult to assess the delays.

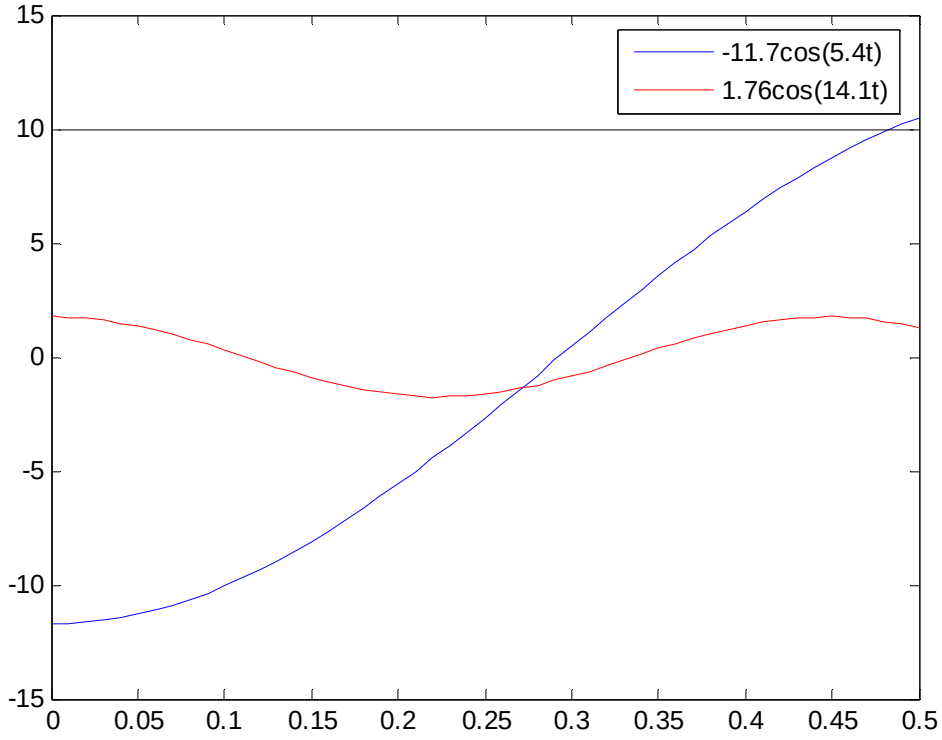

Figure 3-14: Components of the Voltage Angle at Bus 2

From (3.30) and (3.33) it should be expected that the expression for $\Delta\theta_1$ is slightly different when the machine behind it is considered. Figure 3-15 compares the angle at Bus 1 when all other machines are ignored, with only the machine at Bus 2 being considered, and with all other machines being considered.

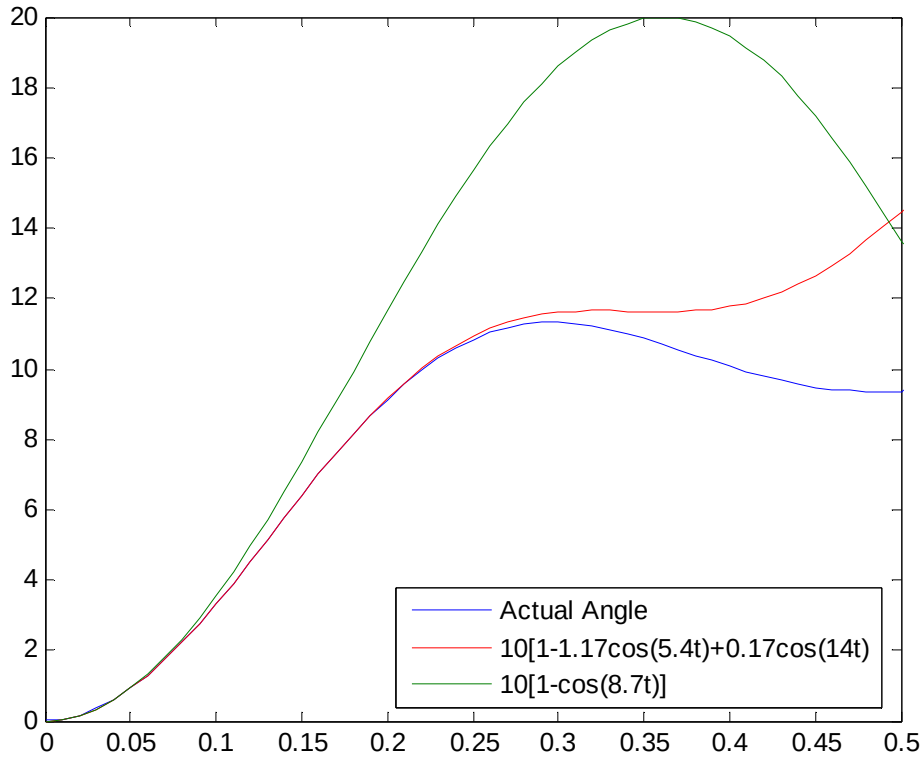

Figure 3-15: Comparison of Estimates of the Voltage Angle at Bus 1

It is apparent that the first part of the trajectory, before $\Delta\theta_2$ has significantly increased, that the two estimates for $\Delta\theta_1$ are very close. As the event progresses, the estimate that was made with all other machines neglected shows a much higher deviation than the other estimate and the actual response. The reason for this is that the step change in angle at Bus 0 caused a mismatch in real power that was initially present entirely at the first machine. When the angle at the first bus started to increase a portion of the power mismatch was presented to the next machine. As a result, when the next machine is considered the deviation in angle at Bus 1 is lower and its dynamics are affected by the properties of the machine at Bus 2. These results illustrate how the threshold method of detecting a wavefront can be used to simplify the calculation of the angle responses, but the accuracy of the results quickly degrade as the angle deviation increases.

3.3.2 Deriving an expression for electromechanical propagation

The preceding section shows that a reasonable estimate of the first part of the trajectory of a bus voltage angle can be achieved using the simplifications of the threshold detection method. In this section an expression for the bus voltage angles in a uniform radial system will be made with the following assumptions and simplifications:

i. Machines further away do not affect the initial bus angle trajectory and can be ignored.

ii. The first few terms of the Taylor series expansion are sufficient to represent the first part of a cosine function.

Referring to the 5-machine system of Figure 3-4, for $\Delta\theta_0(t) = \Delta\theta_0 u(t)$:

$$\Delta\theta_1(s) = \frac{1 + MX_G s^2}{1 + M(X_L + X_G)s^2}\frac{\Delta\theta_0(s)}{s} \tag{3.35}$$

$$\Delta\theta_1(t) = \Delta\theta_0\left[1 - \frac{X_L}{X_L + X_G}cos\left(\frac{t}{\sqrt{M(X_L + X_G)}}\right)\right]u(t) \tag{3.36}$$

The Taylor series is used to approximate the cosine function:

$$\Delta\theta_1(t) = \Delta\theta_0\left[\frac{X_G}{X_L + X_G} + \frac{X_L}{2!\,M(X_L + X_G)^2}t^2 - \frac{X_L}{4!\,M^2(X_L + X_G)^3}t^4 + \frac{X_L}{6!\,M^3(X_L + X_G)^4}t^6 - \cdots\right] \tag{3.37}$$

For small values of time the terms with higher powers of t are insignificant:

$$\Delta\theta_1(t) \approx \Delta\theta_0\left[\frac{X_G}{X_L + X_G} + \frac{X_L}{2!\,M(X_L + X_G)^2}t^2\right] \tag{3.38}$$

If $\Delta\theta_1(t)$ is of the form $A_1u(t) + A_2t^2u(t)$:

$$\Delta\theta_2(s) = \frac{1 + MX_G s^2}{1 + M((X_L + X_G)s^2}\left(\frac{A_1}{s} + \frac{2!\,A_2}{s^3}\right) \tag{3.39}$$

Finding the inverse Laplace transform and using the first 4 terms of the Taylor series yields:

$$\Delta\theta_2(t) \approx \Delta\theta_0 \left[\left(\frac{X_G}{X_L + X_G} \right)^2 + \frac{2X_L X_G}{2!\, M(X_L + X_G)^3} t^2 + \frac{{X_L}^2}{4!\, M^2 (X_L + X_G)^4} t^4 \right] \tag{3.40}$$

If $\Delta\theta_2(t)$ is of the form $A_1u(t) + A_2t^2u(t) + A_3t^4u(t)$ the same procedure yields:

$$\Delta\theta_3(t) \approx \Delta\theta_0 \left[\left(\frac{X_G}{X_L + X_G} \right)^3 + \frac{3X_L {X_G}^2}{2!\, M(X_L + X_G)^4} t^2 + \frac{3{X_L}^2 X_G}{4!\, M^2 (X_L + X_G)^5} t^4 + \frac{{X_L}^3}{6!\, M^3 (X_L + X_G)^6} t^6 \right] \tag{3.41}$$

Considering the first 3 bus angles, an expression can be found for any bus angle in a uniform radial system:

$$\Delta\theta_n(t) \approx \Delta\theta_0 \left[\left(\frac{X_G}{X_L + X_G} \right)^n + \sum_{j=1}^{n-1} \frac{{X_L}^j {X_G}^{n-j}}{(2j)!\, M^j (X_L + X_G)^{n+j}} t^{2j} + \frac{{X_L}^n}{(2n)!\, M^n (X_L + X_G)^{2n}} t^{2n} \right] \tag{3.42}$$

This expression shows that the angle perturbation at any bus in the system is affected by the line impedance, generator internal impedance, generator inertia, and the distance that the generator is from the event. The first term shows that a step change in angle anywhere within the system will result in a step change in angle at all buses in the system, which decreases as the distance from the event increases. If the generator's internal impedance is insignificant compared to line impedances, then this step change will also be insignificant. The expression also shows that as the machine's inertia increases the size of the angle perturbation will decrease, effectively causing the propagation speed to decrease, especially if the threshold method of detection is used.

The figure below shows the response of the 5-machine system to a step input at Bus 0. The continuous lines are simulation results and the dotted lines are results from analysis in the P-δ domain. Only the beginning of the trajectory is shown since this is the relevant part for finding threshold crossings and beyond this part many of the simplifications used to create (3.42) become invalid. The diagram below shows that angles on buses closer to the location of the disturbance are calculated more accurately than angles on distant buses and that as time

progresses the accuracy decreases further. This is expected according to the assumptions (i) and (ii). In fact, for a system such as this, perhaps only the first part of the trajectory of the first 2 buses could be reasonably predicted.

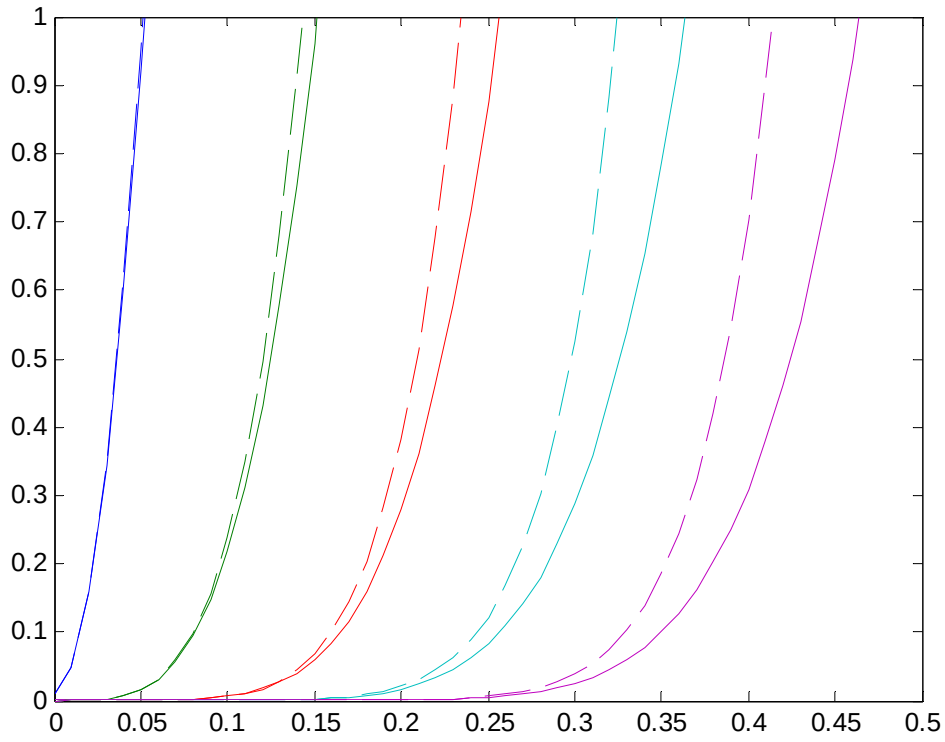

Figure 3-16: Estimating Initial Angle Trajectories

The errors in the calculated delays are a result of ignoring more distant machines in the system and using the Taylor series to simplify the resulting expressions. If the effect of every machine in the system on each individual machine was considered and the Taylor series approximation was not used, then the exact solution could be found. However, that solution would be too difficult to express in a closed-loop expression. A better solution could be obtained by considering the effects of nearby machines on the dynamics of each generator, similar to what was done in the continuum model. Figure 3-16 shows that the accuracy decreases for more distant buses but for calculating delays the difference between threshold crossing points of

adjacent buses is of principle concern and this will have a much smaller error. Table 3-1 compares calculated and simulated values for electromechanical delays in the 5-machine system when the threshold is set at 0.005s.

Table 3-1: Delays in a 5-machine system

Line	Simulated Delay (s)	Calculated Delay (s)
Bus 1-2	0.09	0.09
Bus 2-3	0.10	0.09
Bus 3-4	0.10	0.09
Bus 4-5	0.11	0.09

3.4 Formation of Equivalents

For many power systems studies it is necessary to reduce the system size by replacing the parts of the system outside the area of interest with an equivalent. This equivalent should represent the aggregate response of all the machines that it represents. For load flow analysis this equivalent is fairly easy to compute. The equivalent should be adjusted such that the real power output, reactive power output, and scheduled voltage at the lines connecting the equivalent to the rest of the system match the original case. For a dynamic simulation the electromechanical properties of the equivalent must be set so that the inertia and damping of the equivalent match total of all the machines being replaced. Additionally, the electrical properties of the equivalent machine and the line/s connecting it to the rest of the system should be set so that the equivalent machine is at the center of inertia of the areas being replaced. Typically equivalents are created based on the application that they are needed for (load flow studies, stability studies, or fault studies). This section will describe how an equivalent can be created for stability studies in the P-δ domain.

Let's start with a situation where there are two identical synchronous machines at a bus. The equivalent in this case can be created by combining the *resistances to power flow* for each machine in parallel. Figure 3-17 shows that the electromechanical equivalent machine is simply double the machine reactance and inertia.

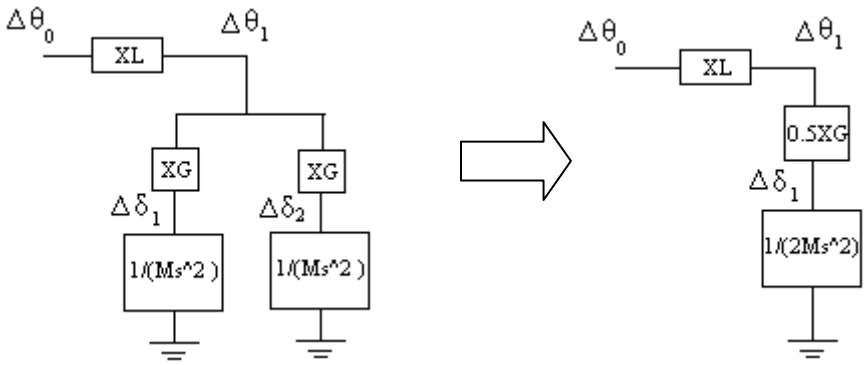

Figure 3-17: Equivalencing 2 machines at The Same Node

If multiple machines are separated by impedances, a mathematical expression can be created by combining the *resistances to power flow* in series and parallel. This expression will be in the Laplace domain and for a large system it may become quite complicated. Equation (3.43) shows the expression for the 5 machine system of Figure 3-1. If the angle or power is known at Bus 0 this expression could be incorporated into a simulation program to represent the electromechanical dynamics of the 5 machines. However, this technique does not reduce the computational complexity of the system; it just presents the system mathematically instead of graphically.

$$\frac{(3.934\text{x}10^{-8})(9.093+s^2)(75.32+s^2)(176.57+s^2)(265.376+s^2)(75.398+s^2)}{s^2(126242+.6704\,s^2+93.53\,s^4+.4737s^6+.000787s^8)} \qquad (3.43)$$

A more useful equivalent reduces the complexity of the system by representing a number of machines as a single machine. Information on the modes of the system will always be lost by doing this since a system with N machines has N-1 modes of oscillation; so if M machines are

replaced by a single equivalent machine there will now be N-M modes of oscillation. The objective is to maintain the overall dynamic characteristics of the system. The system will be replaced by a synchronous machine with the sum of the individual machine inertias, located at the center of inertia of the system.

Let's demonstrate this in the 5-machine system of Figure 3-1. In the previous example Bus 0 was acting as an infinite bus since its angle was held constant a 10^0 after an initial step change. The initiating event will now be a 20MW impulse in power at Bus 1, $\Delta P = -0.2\delta(t)$. For a practical system this corresponds to a 20MW generator's circuit breaker being momentarily tripped and then being reclosed immediately. Figure 3-18 show's how this event is modeled in the P-δ domain.

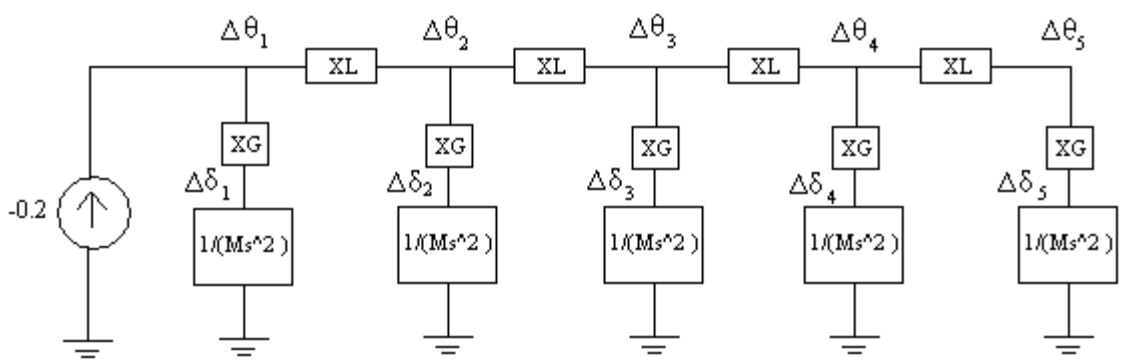

Figure 3-18: A Generator Circuit Trip in the P-δ Domain

The matrix equations for this network are:

$$\begin{bmatrix} -0.2 \\ 0 \\ 0 \\ 0 \\ 0 \end{bmatrix} = \begin{bmatrix} \frac{1}{x_G+\frac{1}{Ms^2}} + y_L & -y_L & 0 & 0 & 0 \\ -y_L & \frac{1}{x_G+\frac{1}{Ms^2}} + 2y_L & -y_L & 0 & 0 \\ 0 & -y_L & \frac{1}{x_G+\frac{1}{Ms^2}} + 2y_L & -y_L & 0 \\ 0 & 0 & -y_L & \frac{1}{x_G+\frac{1}{Ms^2}} + 2y_L & -y_L \\ 0 & 0 & 0 & -y_L & \frac{1}{x_G+\frac{1}{Ms^2}} + y_L \end{bmatrix} \begin{bmatrix} \Delta\theta_1 \\ \Delta\theta_2 \\ \Delta\theta_3 \\ \Delta\theta_4 \\ \Delta\theta_5 \end{bmatrix} \qquad (3.44)$$

The system response is shown below. For many PMU applications a reference angle is used, but Figure 3-19 the absolute angles are shown. Note that the entire system has a downward trend since the power balance (P_m-P_e) was temporarily negative and there was no infinite bus or load frequency control (LFC) to counteract it.

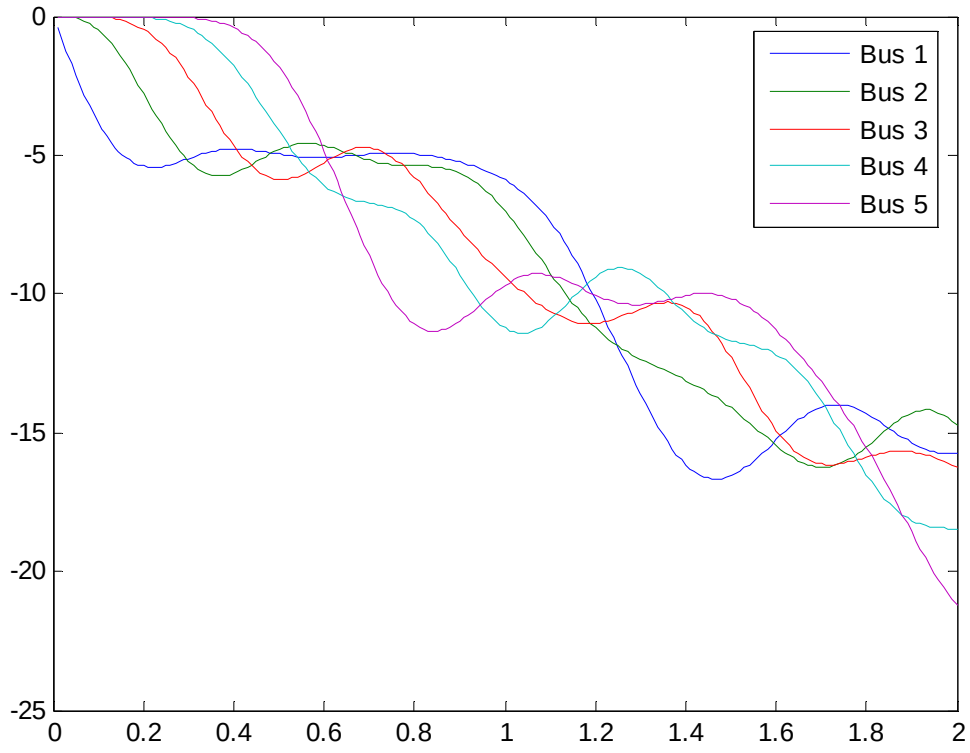

Figure 3-19: 5 Machine System's Response to a Power Impulse

For a homogenous system the center of inertia will be at the physical center of the system, Bus 3 in this case. The total inertia of the system will be the 5 times the inertia of the individual machines. In this system the generator's internal impedance does not significantly affect the center of inertia, since it is the same for every machine and it is small compared to the line impedance, so it can be neglected from the equivalent.

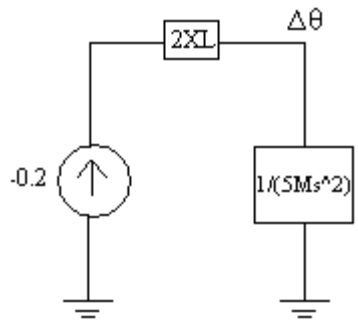

Figure 3-20: Equivalent Machine for the 5 Machine System

The angle response for this equivalent system can easily be computed.

$$\Delta\theta(s) = \frac{-0.2}{5Ms^2} \tag{3.45}$$

$$\Delta\theta(t) = \frac{-0.2}{5M}t$$

$$= -0.1508t \text{ rads}$$

$$= -8.64t \text{ degs}$$

Figure 3-21 compares the response of the equivalent generator with the response of all 5 machines. We can see that the equivalent machine accurately represents the overall trend of the system although none of the oscillatory characteristics are preserved. For a machine to exhibit oscillations it must experience a time-varying electrical torque from other machines in the system or from an infinite bus. In this system there is only one machine so there are no modes of oscillation and it exhibits a first order response.

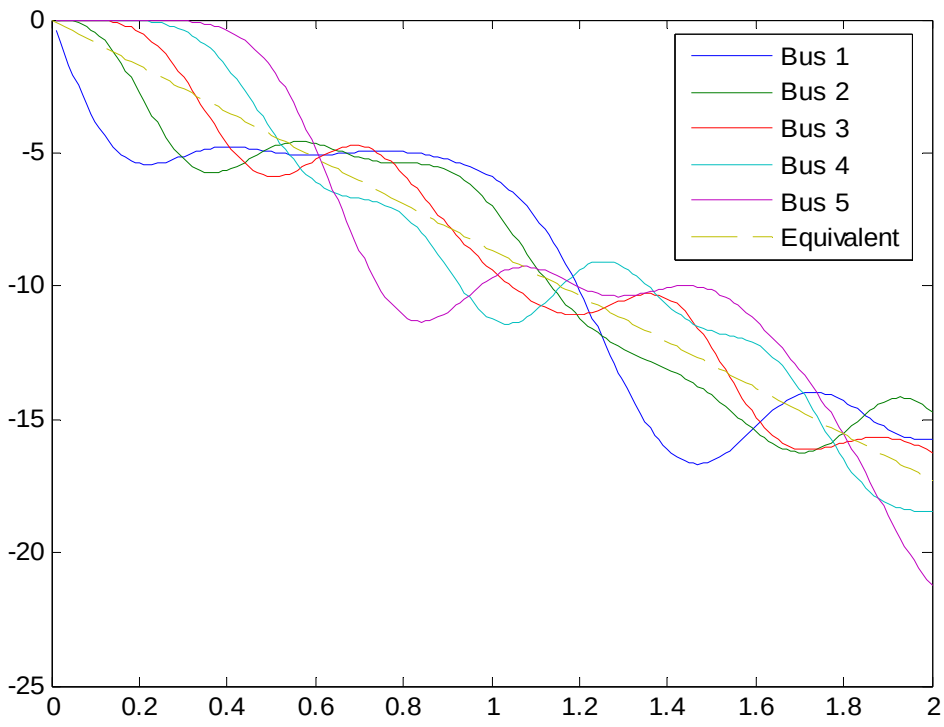

Figure 3-21: Comparison of the Full Model and the Equivalent Machine

Let's consider the case where only the last 3 machines are represented by an equivalent machine. The center of inertia of this system will be at Bus 4. The model of this system in the P-δ domain is shown below.

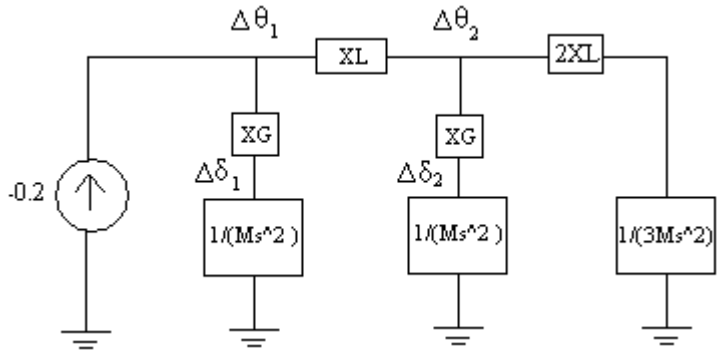

Figure 3-22: Equivalent Machine for the Last 3 Machines

Evaluating this system with the same technique that was used for the previous system yields the response below.

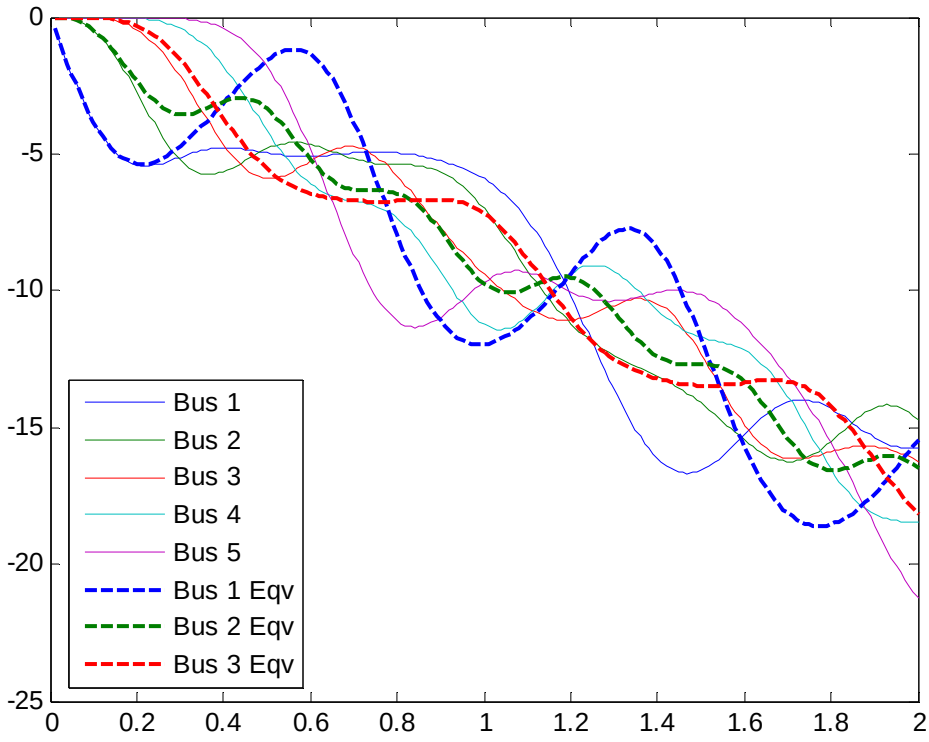

Figure 3-23: Comparison of the Full Model and the 3 Machine Equivalent

Notice that with the equivalent machine replacing the last 3 machines, the overall transient response of the machines at Bus 1 and Bus 2 is similar to the original response. If the equivalent machine was improperly calculated the dynamic response of the bus angles would be completely different. The small-signal behavior of the angles at Buses 1 and 2 has been altered although the parameters of the machines at these buses were not changed. This is expected since a synchronous machine's dynamics depends on the characteristics of every other machine in the system. As stated in Chapter 2, a power system will have N-1 modes of oscillation, where N is the number of synchronous machines. Therefore, in the 5-machine system each bus angle had 4 modes, but in the reduced system each bus angle had only 2 modes. As a result, the small-signal

behavior of a power system cannot be preserved exactly when one equivalent machine is used to represent multiple machines. To preserve the small-signal behavior a mathematical expression for the equivalent *resistance to power flow*, similar to (3.43) should be used; however, this does not correspond with a real power system component.

It is fairly simple to calculate the total inertia of the area to be replaced by an equivalent machine. The inertia of every generator and motor in the system should be summed.

$$M_{eq} = \sum_{i=1}^{N} M_i = \sum_{i=1}^{N} \frac{2H_i S_i}{\omega} \tag{3.46}$$

Where, N is the number of machines in the system

The center of inertia of the system is the unique point at which the system behaves as if all of its inertia is located there. For the homogenous one-line system of the previous examples, the center of inertia is at the geographical center of the system. For a non-homogenous system with multiple branches, calculating the center of inertia can be quite complicated. To illustrate the concept, the procedure for finding the center of mass for a one-dimensional body is first reviewed. Figure 3-24 shows a plank with two masses attached to it at distances x_1 and x_2 from the left end of the plank.

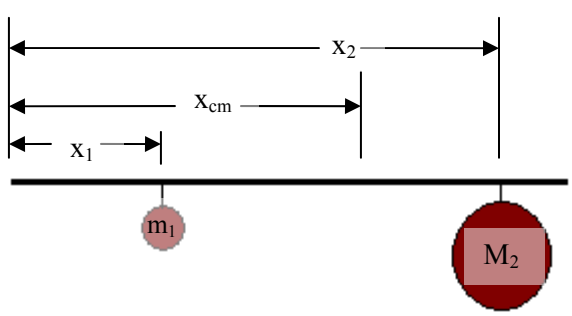

Figure 3-24: Calculating the Center of Mass

If the mass of the plank is insignificant then the center of mass, x_{cm}, can be calculated by summing the torques produced by the masses and dividing by the sum of the distances from the reference point that the individual torques are applied at.

$$x_{cm} = \frac{m_1 x_1 + m_2 x_2}{m_1 + m_2} \tag{3.47}$$

For the more generalized case of N masses:

$$x_{cm} = \frac{\sum_{i=1}^{N} m_i x_i}{\sum_{i=1}^{N} m_i} \tag{3.48}$$

The same technique can be used to calculate the center of inertia in a power system. The reactance of the lines connecting the generators, X, is analogous to distance and the inertia of the machines, M, is analogous to mass. It should be noted that Kundur and several other researchers define the position of the center of inertia as an inertia-weighted average of all the angles in the system (2). This is also referred to as the center of angle. In this application it is necessary to define the position of the center of inertia in units of reactance instead of angle. The expression for the distance to the center of inertia, x_{ci}, takes the same form as (3.48):

$$x_{ci} = \frac{\sum_{i=1}^{N} M_i X_L}{\sum_{i=1}^{N} M_i} \tag{3.49}$$

Let's reconsider the system of Figure 3-22 in which an equivalent is used to represent the last 3 machines of the system. For simplicity, the machine internal reactances are ignored.

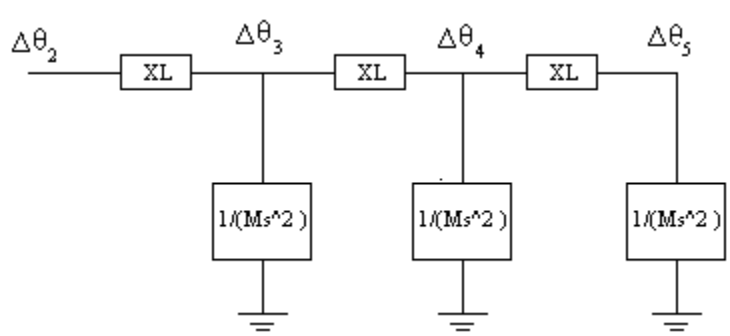

Figure 3-25: Calculating the Center of Inertia

Using (3.49) the distance to the center of inertia can be computed as follows:

$$x_{ci} = \frac{MX_L + 2MX_L + 3MX_L}{3M} = 2X_L \tag{3.50}$$

For a one-dimensional system calculating the reactance between any two points is quite straightforward. To be more accurate the reactance should be calculated up to machine's internal node instead of the machine's terminals. If this is done for the previous case the equations become:

$$x_{ci} = \frac{M(X_L + X_G) + M(2X_L + X_G) + M(3X_L + X_G)}{3M} = 2X_L + X_G \tag{3.51}$$

For a typical power system with multiple branches the equivalent reactance between non-adjacent nodes of the system can be calculated by a 3 step process:

(i) Form the matrix of *admittances to power flow*

(ii) Switch nodes so that Bus i becomes the second row and column in the matrix if the reactance to be calculated is between Bus 1 and Bus i

(iii) Perform matrix reduction so a new matrix of admittances to power flow is created to show only the equivalent admittance between at Bus 1 and Bus i.

The matrix of *admittances to power flow* was introduced in (3.24). The matrix must be modified to remove the all the generators. This leaves only the admittances of lines and transformers; in other words, the conventional admittance matrix with load admittances excluded. The Laplacian operator, s, in the expression for the machine's *resistance to power flow*, $\frac{1}{Ms^2}$, can be set to zero to do this. To find the reactance up to a machine's internal node instead of the machine's terminals the internal nodes could be used in the admittance matrix

instead of the external buses; however, it is simpler to calculate the reactance up to the bus and add the machine reactance. As shown in Figure 3-25, the distance of every machine to some reference point must be calculated. This reference point is outside of the area for which the equivalent is being calculated. It should be a boundary bus between the area being replaced and the rest of the system. This bus should be the first node in the matrix of admittances to power flow.

To perform matrix reduction the nodes to be retained must be separated from the nodes being eliminated. Bus 1 and the terminal bus at the machine for which the reactance from Bus 1 is being calculated, Bus i, are the only two nodes that should be retained. Therefore, the *matrix of admittances to power flow* must be rearranged so that Bus i is the second node in the system.

Matrix reduction is commonly used in power system analysis to eliminate nodes at which current does not enter or leave the network. These nodes are not necessary to solve the network equations and if their voltages are of no concern then removing them reduces the system complexity. Consider the matrix equation:

$$[I] = [Y][V] \tag{3.52}$$

If the matrices are partitioned so the nodes to be retained are separated from the nodes to be eliminated the equation becomes (14):

$$\begin{bmatrix} I_A \\ I_X \end{bmatrix} = \begin{bmatrix} K & L \\ L^T & M \end{bmatrix} \begin{bmatrix} V_A \\ V_X \end{bmatrix} \tag{3.53}$$

Where,

I_A is the submatrix composed of the currents entering the nodes to be retained.

I_X is the submatrix composed of the currents entering the nodes to be retained.

V_A is the submatrix composed of the voltages at the nodes to be retained.

V_X is the submatrix composed of the currents at the nodes to be retained.

The self- and mutual admittances composing K are those identified with nodes to be retained. The self- and mutual admittances composing M are those identified with nodes to be eliminated. The mutual admittances composing L and L^T are common to a node being retained and a node being eliminated.

Separating the partitions in (3.53) yields:

$$I_A = KV_A + LV_X \tag{3.54}$$

$$I_X = L^T V_A + MV_X \tag{3.55}$$

All elements of I_X are zero since otherwise these nodes cannot be removed. Rearranging (3.55) gives:

$$V_X = -M^{-1}L^T V_A \tag{3.56}$$

Substituting this into (3.54) yields:

$$I_A = KV_A - LM^{-1}L^T V_A \tag{3.57}$$

$$I_A = (K - LM^{-1}L^T)V_A \tag{3.58}$$

This is a new network equation with the admittance matrix:

$$Y = K - LM^{-1}L^T \tag{3.59}$$

This procedure can be used to perform matrix reduction on the *admittances to power flow* matrix so that a 2x2 matrix is created where the off-diagonal elements are the admittances between Bus 1 and Bus i. The matlab code, calculate_coi.m, in Appendix I is used to perform both the node switching and the matrix reduction and then compute the distance from the reference point to the center of inertia in terms of per unit impedance.

Let's revisit the system of Figure 3-22 and calculate the reactance between machine 5 and Bus 2 using this method. The original *admittances to power flow* matrix given in (3.44) is repeated here for convenience.

$$\begin{bmatrix} \frac{1}{x_G+\frac{1}{Ms^2}}+y_L & -y_L & 0 & 0 & 0 \\ -y_L & \frac{1}{x_G+\frac{1}{Ms^2}}+2y_L & -y_L & 0 & 0 \\ 0 & -y_L & \frac{1}{x_G+\frac{1}{Ms^2}}+2y_L & -y_L & 0 \\ 0 & 0 & -y_L & \frac{1}{x_G+\frac{1}{Ms^2}}+2y_L & -y_L \\ 0 & 0 & 0 & -y_L & \frac{1}{x_G+\frac{1}{Ms^2}}+y_L \end{bmatrix} \tag{3.44}$$

This matrix is edited by open-circuiting the generators and using the boundary bus, Bus 2, as the first node in the system.

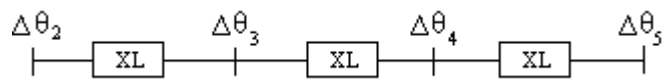

Figure 3-26: Open-circuiting Generators and Using the Boundary Bus

To create the *admittances to power flow* matrix the bus numbers are changed so they match the rows and columns of the matrix.

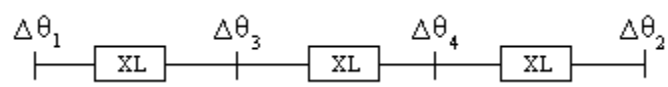

Figure 3-27: Switching Nodes

The network equation in the P-δ domain for this new system becomes:

$$\begin{bmatrix} P_1 \\ P_2 \\ P_3 \\ P_4 \end{bmatrix} = \begin{bmatrix} y_L & 0 & -y_L & 0 \\ 0 & y_L & 0 & -y_L \\ -y_L & 0 & 2y_L & -y_L \\ 0 & -y_L & -y_L & 2y_L \end{bmatrix} \begin{bmatrix} \theta_1 \\ \theta_2 \\ \theta_3 \\ \theta_4 \end{bmatrix} \tag{3.60}$$

Partitioning the *admittances to power flow* matrix yields:

$$K = \begin{bmatrix} y_L & 0 \\ 0 & y_L \end{bmatrix} \tag{3.61}$$

$$L = \begin{bmatrix} -y_L & 0 \\ 0 & -y_L \end{bmatrix} \tag{3.62}$$

$$M = \begin{bmatrix} 2y_L & -y_L \\ -y_L & 2y_L \end{bmatrix} \tag{3.63}$$

The new admittance matrix is:

$$Y = \begin{bmatrix} y_L & 0 \\ 0 & y_L \end{bmatrix} - \begin{bmatrix} -y_L & 0 \\ 0 & -y_L \end{bmatrix} \begin{bmatrix} 2y_L & -y_L \\ -y_L & 2y_L \end{bmatrix}^{-1} \begin{bmatrix} -y_L & 0 \\ 0 & -y_L \end{bmatrix} \tag{3.64}$$

$$Y = \begin{bmatrix} \frac{1}{3}y_L & -\frac{1}{3}y_L \\ -\frac{1}{3}y_L & \frac{1}{3}y_L \end{bmatrix} \tag{3.65}$$

The reactance between Bus 2 and Bus 5 is the negative of the reciprocal of the off-diagonal elements. If the machine's internal reactance is added to this, the final result is $3X_L + X_g$. To calculate the center of inertia this process would have to be repeated for the machine at Bus 4. Bus 3 is adjacent to Bus 2 so the reactance between them can be found by observation.

The voltage magnitude at the equivalent bus cannot be accurately solved with this technique since reactive power flows are not considered at all. An appropriate assumption is that the voltage magnitude at the reference bus and at the equivalent machine is equal. The angle difference between the reference point and the equivalent machine can be calculated if the power flowing from the reference point into the area being equivalenced is known using the equation below.

$$\delta_{ref} - \delta_{eq} = \sin^{-1}\left(\frac{x_{ci}}{|V_{ref}|^2}\right) \tag{3.66}$$

3.5 Analysis of the IEEE 14 Bus System

This chapter has developed the concept of power system analysis in the P-δ domain. In previous sections these concepts were illustrated with a simple one-dimensional power system.

In this section these techniques are applied to a sample system with a more realistic topology in order to address issues that will be faced in a real system. The IEEE 14 bus power system is used to illustrate the concepts described in this chapter. Figure 3-28 shows the topology of the system. The line, load, and generator data are available in Appendix II.

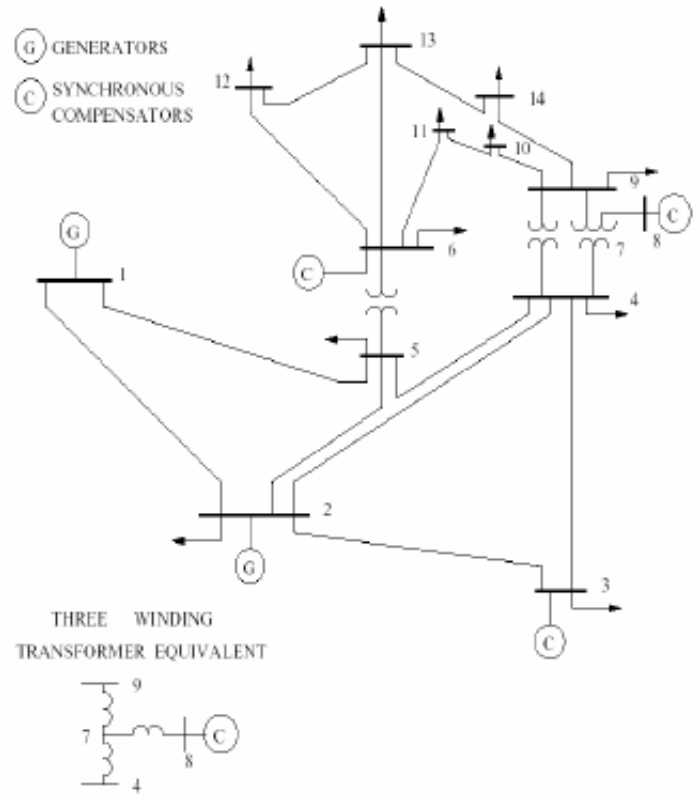

Figure 3-28: IEEE 14-Bus System

The system is highly interconnected, which means that a traveling wave will branch out along multiple paths and propagation delays will be more difficult to observe. The machines are dissimilar, with ratings varying from 615MVA at generator 1 to 25MVA at machines 6 and 8. Additionally, there are no machines above buses 6 and 8 so the inertia of the system will be non-uniformly distributed.

3.5.1 The quiescent point

In this section some of the simplifications that were previously used during the formulation of the P-δ domain model will be removed. (3.10) gave the linearized swing equation for power flow from a generator along a transmission line as:

$$M\frac{d^2\Delta\delta}{dt^2} = -\Delta P_e = -\frac{|V_1||V_2|}{X}\cos\delta_0\Delta\delta \tag{3.10}$$

In previous examples this expression was simplified by assuming that the voltage magnitudes were 1.0pu and that the initial angle difference across the line, δ_0, is zero. If those expressions are discarded the expression for *admittance to power flow* across a transmission line becomes:

$$\frac{\Delta P}{\Delta\delta} = \frac{|V_1||V_2|}{X}\cos\delta_0 \tag{3.67}$$

It is still assumed that bus voltage magnitudes are constant throughout the disturbance and that transmission lines are purely reactive. These assumptions are quite reasonable for small disturbances on high voltage lines, and to remove them would introduce a lot of complexity into the calculations. The preceding equation will be simplified by introducing a constant to represent the initial conditions called α.

$$\alpha = |V_1||V_2|\cos\delta_0 \tag{3.68}$$

Substituting α into (3.67) yields:

$$\frac{\Delta P}{\Delta\delta} = \alpha \cdot Y \tag{3.69}$$

In the preceding equation the dot multiplier indicates that an element-by-element multiplication is required instead of the matrix multiplication. Given that the admittance matrix is the inverse of the impedance matrix, the network equation in the P-δ domain becomes:

$$\Delta\delta = [\alpha \cdot Y]^{-1}\Delta P \tag{3.70}$$

The speed damping for a typical power system is negligible, but it is easy to include in the linearized swing equation.

$$\mathrm{M}\frac{\mathrm{d}^2\Delta\delta}{\mathrm{dt}^2} = \Delta P - \mathrm{D}\frac{\mathrm{d}\delta}{\mathrm{dt}} \tag{3.71}$$

Rearranging the preceding equation gives:

$$\frac{\Delta\delta}{\Delta P} = \frac{1}{\mathrm{Ms}^2 + \mathrm{Ds}} \tag{3.72}$$

The IEEE-14 Bus system will be analyzed in the power-angle domain with the pre-disturbance quiescent operating point accounted for through the constant, α. For more accurate computation of the electromechanical response following a disturbance, the post-disturbance quiescent operating point should be used; however, for many applications this may be unknown or there may not be sufficient time to calculate it. For a single disturbance in a large system the pre-disturbance quiescent point is often close enough to the post-disturbance quiescent point that it can be used to approximate it.

3.5.2 Comparison to simulation data

The IEEE-14 Bus system was simulated in GE-PSLF for a load trip at Bus 2. The load flow, dynamic data, and the EPCL code that was used to automate the simulation are in Appendix II. The generators are modeled as classical machines without any exciters, governors, stabilizers or any other control systems attached. Figure 3-29 shows the machine angle responses. Since the system is meshed and the generators are electrically closer to each other, it was expected that propagation delays would be more difficult to see than in the 5-machine system since the disturbance propagates from generator 2 to several other machines at once instead of sequentially from one machine to the next. Excluding the generator at Bus 1, the machines in this network

are relatively small so the energy that they can store and the electromechanical propagation delay they cause will also be small. It is also expected that generator 1 responds slowest since it has a significantly larger inertia than the other machines. Also the machines on buses 6 and 8 are electrically further away from Bus 2 than the machine on bus 3 so it is also expected that they respond slower.

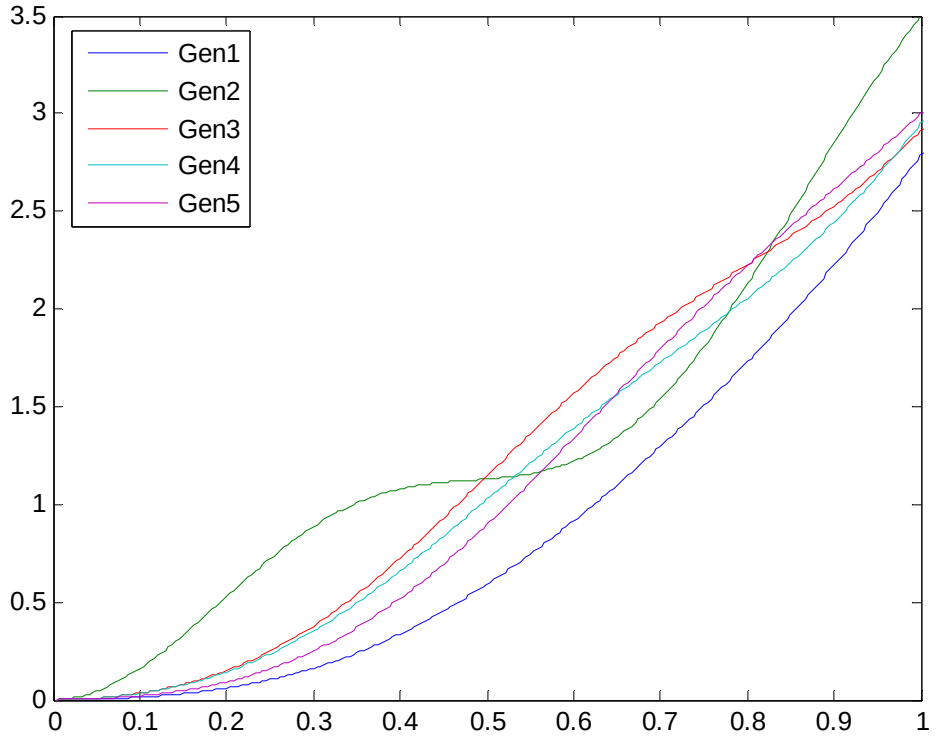

Figure 3-29: Simulation Results for Machine Angles in the IEEE-14 Bus System

Figure 3-30 shows the bus angles. Note that the change in angle is very small so the system can be accurately represented with a linearized model. The voltage angles for generator buses are shown in the dashed lines. It can be seen that the voltage angle at the generator terminals closely follow the generator rotor angles since the direct axis transient reactance is relatively small. It is interesting to note that the angles on buses 6, 9, 10, 11, 12, 13, and 14 are very close together. This is because there are no machines above buses 6 and 7 so there will be very little

electromechanical propagation delays. These angles follow the machine angle of generator 6 very closely. The angles on non-generator buses 4, 5, 7, 9, 10, 11, 12, 13, and 14 are algebraic functions of adjacent bus angles and the impedances between them. Buses 4 and 5 are directly connected to Bus 2, so when the angle on Bus 2 increases they experience a smaller, yet proportional increase.

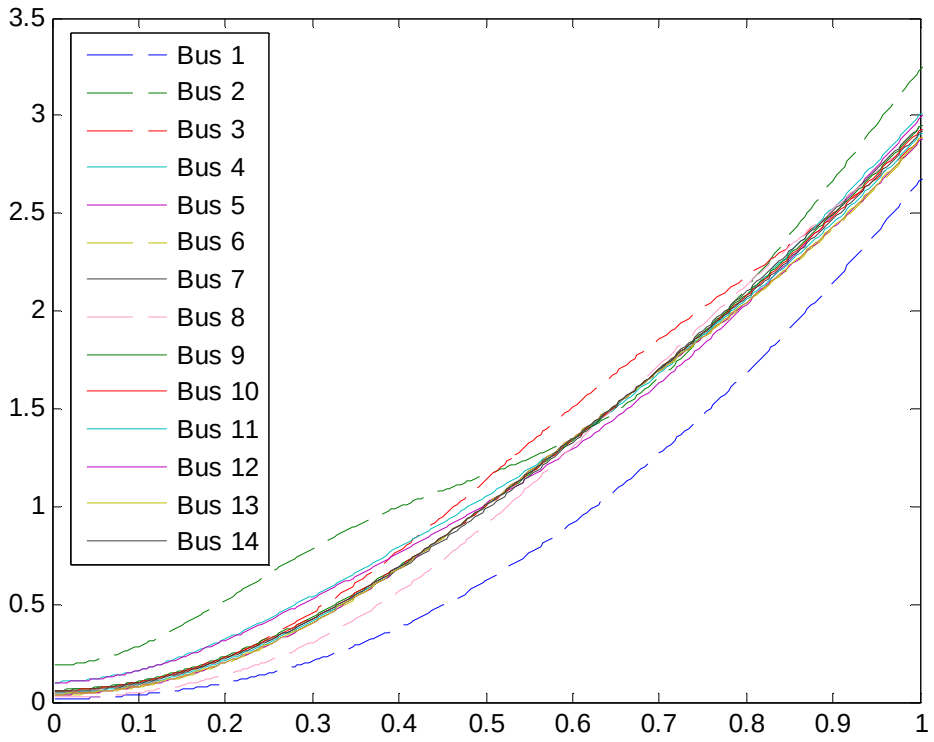

Figure 3-30: Simulation Results for Bus Angles in the IEEE-14 Bus System

The effect of initial power flows and off-nominal voltage magnitudes can be accounted for by using (3.24), but it must be assumed that the voltage magnitude remains constant throughout the disturbance. Figure 3-31 illustrates that following the load drop the variation in the bus voltage magnitudes is so small that it can reasonably be assumed to be constant.

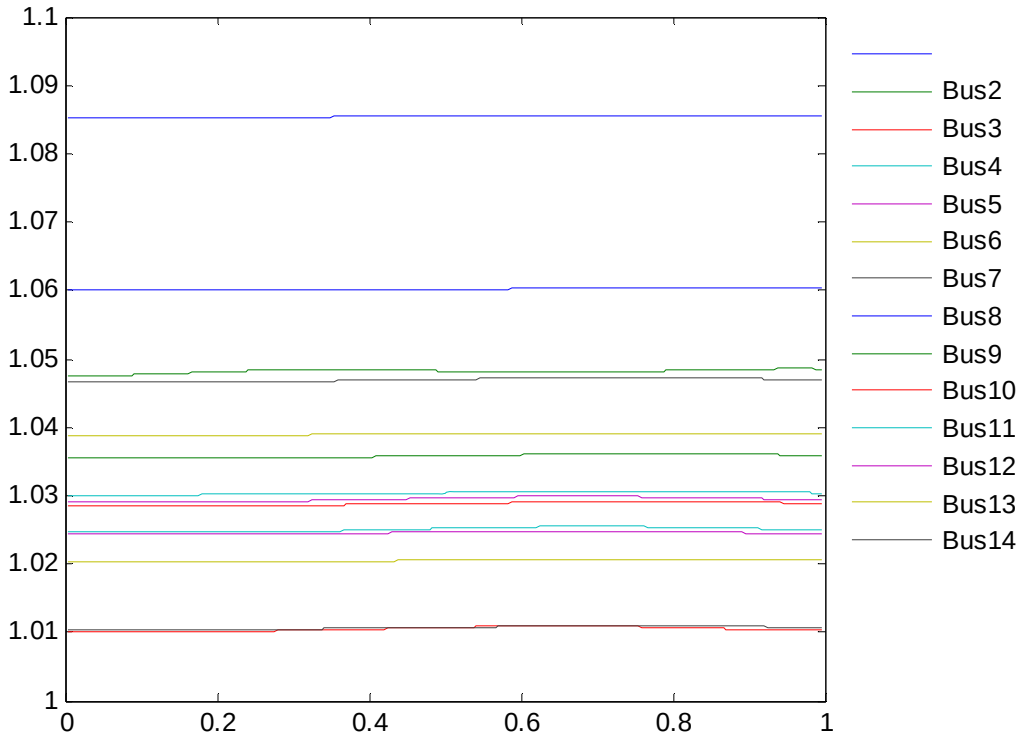

Figure 3-31: Simulating Results for Bus Voltage Magnitudes in the IEEE-14 Bus System

The response of the voltage angles throughout the system can be approximated by simplifying the circuit through a series of wye-delta and delta-wye transformations, so that the response of any bus in the system can be calculated based on the event at Bus 2. Figure 3-32 and Figure 3-33 illustrate how a wye-delta transformation can be used to reduce the complexity of the system. Even in a small system such as this, it would have to be done several more times to calculate the response at a bus that is relatively far from Bus 2. Each resulting delta configuration will contain terms that are far more complex than the terms in the previous wye configuration.

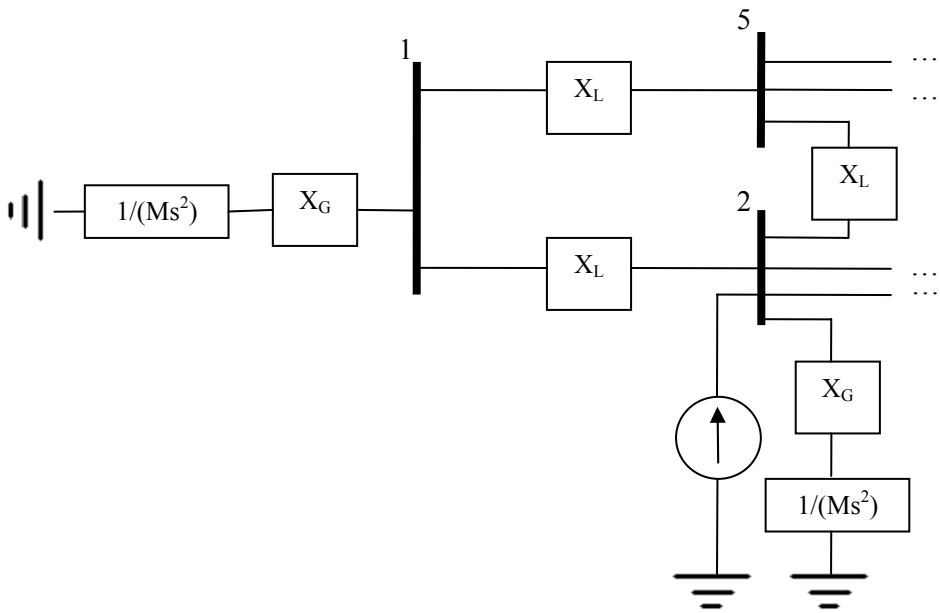

Figure 3-32: The IEEE-14 Bus System in the P-δ Domain

The machine inertia must be referred to the system base, 100MVA.

$$M_1 = \frac{2(5.148)}{2\pi 60} * \frac{615}{100} = 0.168 \text{ s}^2/\text{rad} \tag{3.72}$$

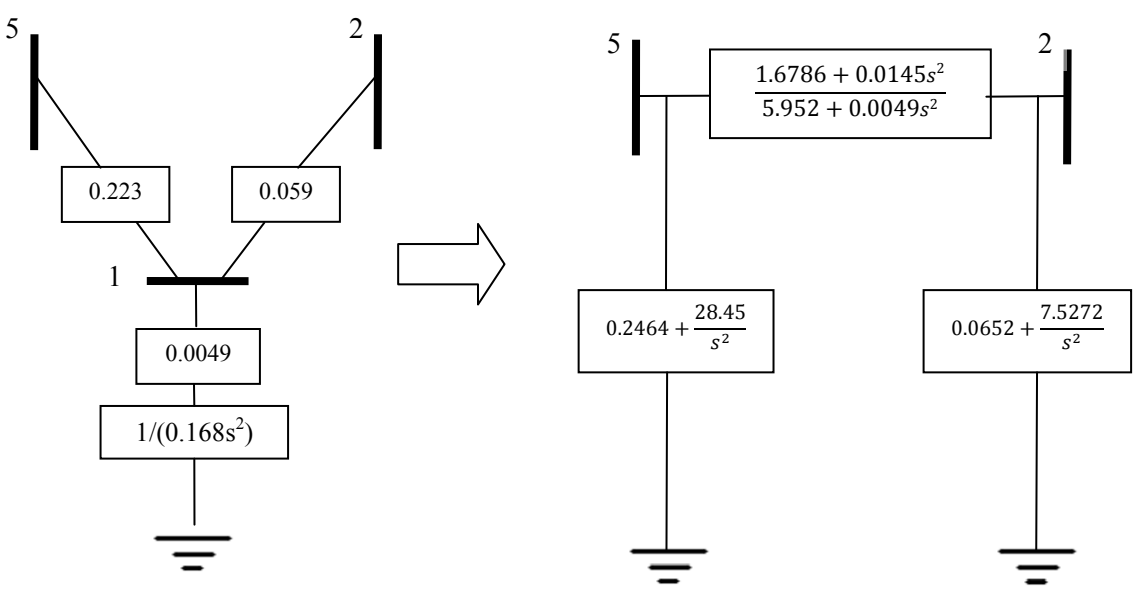

Figure 3-33: Wye-Delta Conversion

The most efficient method of solving this system in the P-δ domain is with matrix analysis. Furthermore, to reduce the computational requirements for finding the inverse of the Y matrix the size of the matrix can be significantly reduced by making reasonable simplifications. In this case, there is no inertia above buses 8 and 6 so there will be very little propagation delay there. Most of the buses can be removed with minimal impact to the accuracy of the following calculations if the transmission path between buses 6 and 9 is still preserved. The impedance of the line between Bus 6 and Bus 9 is calculated by combining the total impedances of the lines being removed. Figure 3-34 shows the simplified IEEE-14 Bus System.

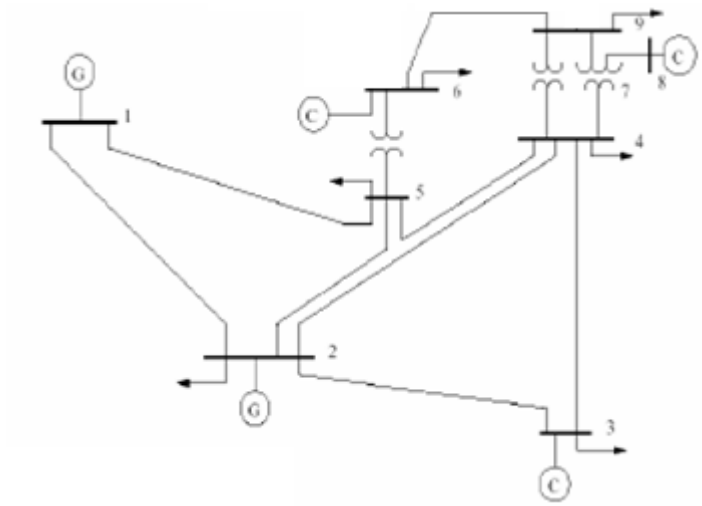

Figure 3-34: Simplifying the IEEE-14 Bus System

The matrices for the network equations are shown below:

$$\Delta P = \begin{bmatrix} 0 \\ \frac{-0.41}{s} \\ 0 \\ 0 \\ 0 \\ 0 \\ 0 \\ 0 \\ 0 \end{bmatrix}, \quad \Delta\theta = \begin{bmatrix} \Delta\theta_1 \\ \Delta\theta_2 \\ \Delta\theta_3 \\ \Delta\theta_4 \\ \Delta\theta_5 \\ \Delta\theta_6 \\ \Delta\theta_7 \\ \Delta\theta_5 \\ \Delta\theta_5 \end{bmatrix}$$

Admittances are inserted in the Y matrix without the imaginary operator "j":

$$Y = \begin{bmatrix} 21.4 + \frac{1}{0.00049 + \frac{1}{0.168s^2 + .02s}} & -16.9 & 0.00 & 0.00 & -4.48 & 0.00 & 0.00 & 0.00 & 0.00 \\ -16.9 & 33.4 + \frac{1}{0.00308 + \frac{1}{0.021s^2 + .02s}} & -5.05 & -5.67 & -5.75 & 0.00 & 0.00 & 0.00 & 0.00 \\ 0.00 & -5.05 & 10.9 + \frac{1}{0.00308 + \frac{1}{0.021s^2 + .02s}} & -5.85 & 0.00 & 0.00 & 0.00 & 0.00 & 0.00 \\ 0.00 & -5.67 & -5.85 & 41.9 & -23.8 & 0.00 & -4.78 & 0.00 & -1.80 \\ -4.48 & -5.75 & 0.00 & -23.8 & 38.0 & -3.97 & 0.00 & 0.00 & 0.00 \\ 0.00 & 0.00 & 0.00 & 0.00 & -3.97 & 7.42 + \frac{1}{0.00928 + \frac{1}{0.007s^2 + .02s}} & 0.00 & 0.00 & -3.45 \\ 0.00 & 0.00 & 0.00 & 0.00 & -4.78 & 0.00 & 0.00 & 19.6 & -5.68 \\ 0.00 & 0.00 & 0.00 & 0.00 & 0.00 & 0.00 & -5.68 & 7.42 + \frac{1}{0.00928 + \frac{1}{0.007s^2 + .02s}} & 0.00 \\ 0.00 & 0.00 & 0.00 & 0.00 & -1.80 & 0.00 & -3.45 & -9.09 & 0.00 \\ -9.09 & -14.3 & & & & & & & \end{bmatrix}$$

$$\alpha = \left(\begin{bmatrix} 1.0600 \\ 1.0450 \\ 1.0100 \\ 1.0237 \\ 1.0281 \\ 1.0386 \\ 1.0461 \\ 1.0851 \\ 1.0349 \end{bmatrix} \begin{bmatrix} 1.0600 \\ 1.0450 \\ 1.0100 \\ 1.0237 \\ 1.0281 \\ 1.0386 \\ 1.0461 \\ 1.0851 \\ 1.0349 \end{bmatrix}^T \cdot \begin{bmatrix} 1.000 & 0.996 & 0.976 & 0.984 & 0.988 & 0.969 & 0.973 & 0.973 & 0.966 \\ 0.996 & 1.000 & 0.991 & 0.996 & 0.998 & 0.987 & 0.989 & 0.989 & 0.985 \\ 0.976 & 0.991 & 1.000 & 0.999 & 0.998 & 1.000 & 1.000 & 1.000 & 0.999 \\ 0.984 & 0.996 & 0.999 & 1.000 & 1.000 & 0.998 & 0.999 & 0.999 & 0.997 \\ 0.988 & 0.998 & 0.998 & 1.000 & 1.000 & 0.996 & 0.997 & 0.997 & 0.994 \\ 0.967 & 0.986 & 1.000 & 0.998 & 0.996 & 1.000 & 1.000 & 1.000 & 1.000 \\ 0.971 & 0.989 & 1.000 & 0.999 & 0.997 & 1.000 & 1.000 & 1.000 & 1.000 \\ 0.971 & 0.989 & 1.000 & 0.999 & 0.997 & 1.000 & 1.000 & 1.000 & 1.000 \\ 0.964 & 0.984 & 0.999 & 0.997 & 0.994 & 1.000 & 1.000 & 1.000 & 1.000 \end{bmatrix} \right)$$

Note that the division in the preceding equation is element-wise and is not a matrix inversion.

$$\alpha = \begin{bmatrix} 1.124 & 1.103 & 1.045 & 1.068 & 1.077 & 1.067 & 1.079 & 1.119 & 1.060 \\ 1.103 & 1.092 & 1.046 & 1.066 & 1.072 & 1.071 & 1.081 & 1.122 & 1.065 \\ 1.045 & 1.046 & 1.020 & 1.033 & 1.036 & 1.049 & 1.057 & 1.096 & 1.044 \\ 1.068 & 1.066 & 1.033 & 1.048 & 1.053 & 1.061 & 1.070 & 1.110 & 1.056 \\ 1.077 & 1.072 & 1.036 & 1.053 & 1.057 & 1.064 & 1.072 & 1.112 & 1.058 \\ 1.065 & 1.070 & 1.049 & 1.061 & 1.064 & 1.079 & 1.087 & 1.127 & 1.075 \\ 1.077 & 1.081 & 1.057 & 1.069 & 1.071 & 1.087 & 1.094 & 1.135 & 1.083 \\ 1.117 & 1.122 & 1.096 & 1.110 & 1.112 & 1.127 & 1.135 & 1.177 & 1.123 \\ 1.058 & 1.064 & 1.044 & 1.056 & 1.058 & 1.075 & 1.083 & 1.123 & 1.071 \end{bmatrix}$$

It should be noted that most of the elements of α are meaningless and are not actually used in computing the response. The off-diagonal elements that do not correspond to an actual branch will be neglected since it will be multiplied by a zero in the Y matrix. The diagonal elements of the alpha matrix are also meaningless and unused unless the internal voltage of the machine is known and then that node should be included in the Y matrix. The *resistance to power flow* due to the generator's internal impedance is insignificant compared to the *resistance to power flow* due the generator's step-up transformer. Evaluating (3.70) in matlab and plotting the results yields the figure below. It can be seen that this is very similar to the results obtained from simulation, Figure 3-30. The results may not be exact since a simplified version of the system is being used. 5 buses have been removed and all lines are considered to be lossless.

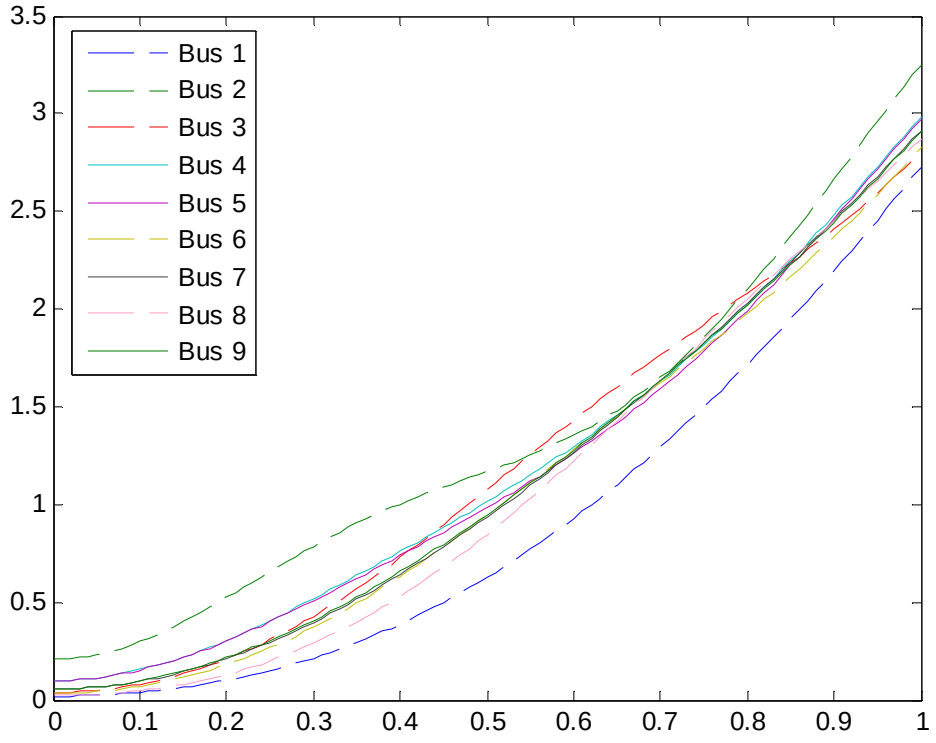

Figure 3-35: Calculation Results for Bus Angles in the IEEE-14 Bus System

Figure 3-36 shows the results when the initial conditions are ignored by setting α to a unity matrix. It can be seen that the changes in bus angles are slightly higher in this case than when alpha was properly calculated.

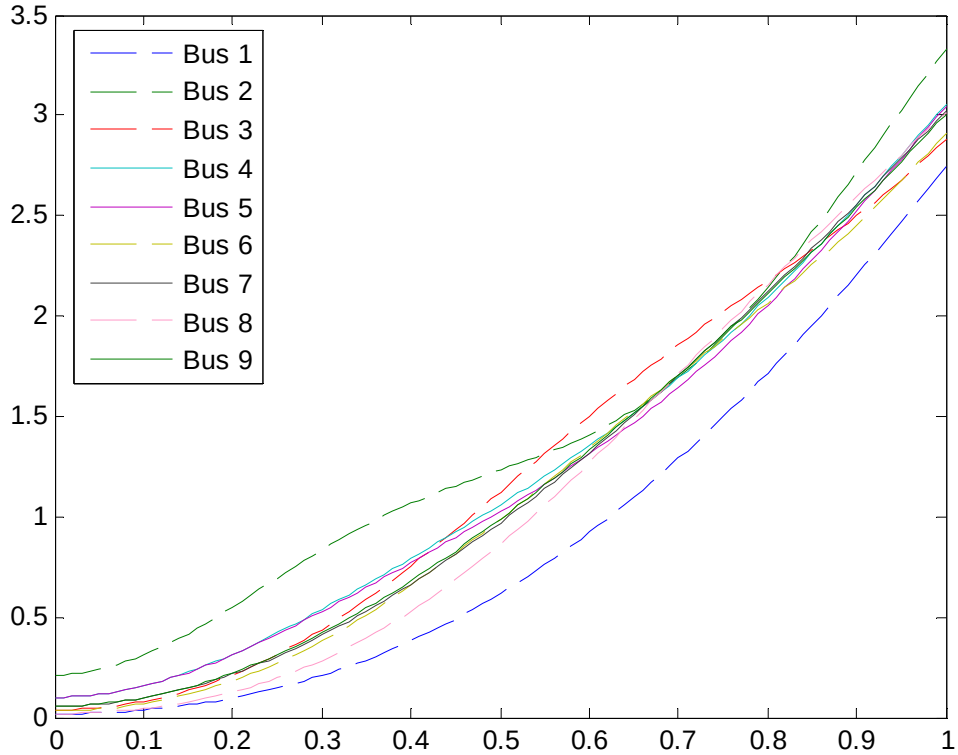

Figure 3-36: Calculation Results for Bus Angles in the IEEE-14 Bus System Ignoring Initial Conditions

The transmission network is usually operated at voltages above 1.0 pu; infact, many EHV lines are routinely operated between 1.05 pu and 1.08 pu. In normal conditions angle differences across transmission lines rarely exceed 15^0 so the cosine of their difference will be close to 1. As a result, when the voltage magnitude and initial power flow are accounted for, most of the elements of alpha will usually be slightly higher than 1 and the change in angle will be slightly lower than it would be otherwise. This change in the angle response is small enough to justify ignoring the voltage magnitude and the initial power flow for transmission networks that have

the overwhelming majority of their voltage magnitudes above 1.0 pu and small angle differences across transmission lines.

Finally, let's demonstrate how an equivalent machine representing every bus in the IEEE-14 bus system excluding Bus 2 could be created for this system. This is the type of operation that would be required if there was another system attached to Bus 2 that was of concern and the IEEE-14 Bus system was outside the study area. The diagram below illustrates how the system is being equivalenced.

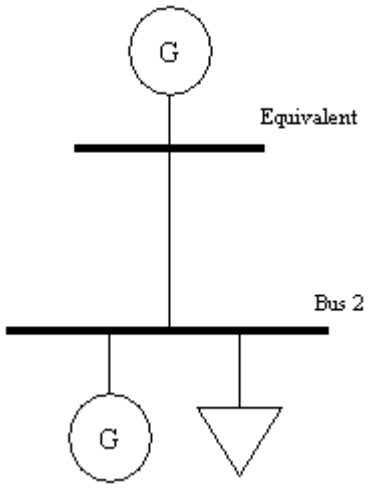

Figure 3-37: Equivalent for the IEEE-14 Bus System

The first step is to calculate the equivalent inertia of the system using (3.46). The inertia is referred to the system base of 100MVA.

$$M_{eq} = \sum_{i=1}^{N} \frac{2H_i S_i}{\omega} \tag{3.73}$$

$$= 2.2301$$

The second step is to find the center of inertia of the system using (3.49). Bus 2 will be used as a reference point and the equivalent reactance between Bus 2 and every other machine in the

system will be calculated using the technique described in section 3.4. The matlab program, calculate_coi.m is created to automate this. The net reactance between Bus 2 and the each machine in the system and the reactance between Bus 2 and the center of angle is shown below.

X_{21} = 0.0496 pu

X_{23} = 0.1106 pu

X_{26} = 0.2234 pu

X_{28} = 0.3708 pu

X_{coi} = 0.0581 pu

Note that the net reactance between Bus 2 and the machines at buses at Bus 1 and Bus 3, which are directly connected to Bus 2, are slightly less than the impedance of the line connected the buses to Bus 2. The net reactance is calculated by considering the multiple paths that exist between Bus 2 and Bus 1 and Bus 3; therefore, it is lower than if only one path existed. Based on the distance of each machine from Bus 2, as shown in Figure 3-28, it is expected that X_{21} is smallest and X_{28} is largest. The equation for the reactance between the reference bus, Bus 2, and the center of inertia, is essentially an inertia-weighted average of the reactances between each machine and the reference bus. Given that the generator at Bus 1 is more than ten times larger than each of the other machines; it will have the greatest impact on the center of inertia. The figure below compares the response of the equivalent system and the response of the system with 9 buses to a load drop at Bus 2.

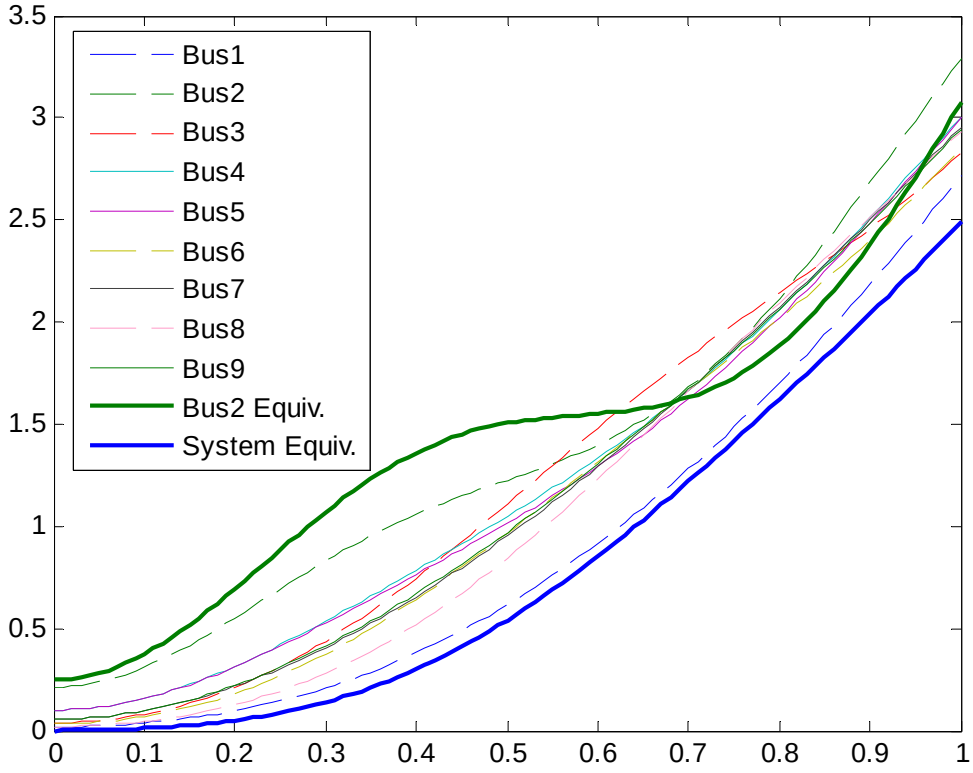

Figure 3-38: Results from the Equivalent of the IEEE-14 Bus System

The results show that the equivalent reasonably represents the buses that were removed. Similar to the previous example, the small-signal behavior of the system is not preserved, but the transient behavior and overall trends are preserved.

3.6 Non-idealized modeling

This chapter has developed the concept of power system analysis in the P-δ domain using an idealized system model. Some of the features of this system that make it idealized are that the transmission lines are lossless, there are no loads within the electrical network, line charging susceptance is neglected, and there are no governors, exciters, or stabilizers associated with any of the generators. These are all simplifications that are commonly used in power system state-

space analysis; nevertheless, this section will consider these simplifications and determine whether they are reasonable for a practical system (12). Some features, such as generator governors, can also be accommodated in the power-angle domain model, but others such as exciters and stabilizers cannot. Exciters and stabilizers do have an impact on the small-signal behavior of power systems, but they cannot be analyzed with P-δ domain analysis, state-space analysis, or the continuum model. If the effect of these control systems is to be considered, then detailed time-domain simulations may be necessary.

3.6.1 Transmission line losses

To consider the effect of transmission line losses on the electromechanical dynamics of a power system, specifically the synchronizing power and the damping power, the power flow along lossy transmission lines should be computed. The nodal equations for a power system are shown below (12).

$$[I] = [Y][E] \tag{3.74}$$

For a single transmission line the power flow becomes:

$$I_i = Y_{ii}E_i + \sum_{\substack{j=1 \\ j\neq i}}^{n} Y_{ij}E_j \tag{3.75}$$

The complex power flowing from this bus can then be computed as:

$$S_i^* = E_i^* E_i Y_{ii} + \sum_{\substack{j=1 \\ j\neq i}}^{n} Y_{ij}E_i^* E_j \tag{3.76}$$

Using trigonometry to simplify this expression, the real power flow can be found:

$$P_{ei} = Re\{S_i^*\} = E_i^2 G_{ii} + \sum_{\substack{j=1 \\ j \neq i}}^{n} E_i E_j [B_{ij} sin\delta_{ij} + G_{ij} cos\delta_{ij}] \qquad (3.77)$$

This equation represents the power flowing from the ith bus to every generator in the system. If the system has constant power loads and no shunt susceptances, then the following inequality relationships exist:

For $i \neq j$: $\qquad B_{ij} \geq 0, \quad G_{ij} \leq 0 \qquad (3.78)$

(3.78) shows that the presence of transmission losses, G_{ij}, effectively reduces the power flows in the network. To determine the effect of transmission losses on the dynamic characteristics of the system insert Equation (3.71) into the swing equation.

$$M_i \frac{d\delta_i^2}{dt^2} = P_{mi} - P_{ei} = P_{mi} - \left(E_i^2 G_{ii} + \sum_{\substack{j=1 \\ j \neq i}}^{n} E_i E_j [B_{ij} sin\delta_{ij} + G_{ij} cos\delta_{ij}] \right) \qquad (3.79)$$

Linearizing this equation around a quiescent operating point yields:

$$M_i \frac{d\Delta\delta_i^2}{dt^2} = -\sum_{\substack{j=1 \\ j \neq i}}^{n} E_i E_j \left[B_{ij} cos\delta_{ij_0} - G_{ij} sin\delta_{ij_0} \right] \Delta\delta_{ij}(t) \qquad (3.80)$$

Note that there are no additional terms first derivatives of $\Delta\delta_i$ in the equation. This indicates that there is no damping introduced in the system due to transmission losses.

In section 4.2 the synchronizing power is used in stability analysis as a measure of the system's ability to maintain synchronism following small-signal disturbances. In this section, the expressions for the synchronizing power with and without transmission losses are compared so that the effect of assuming that the transmission lines are lossless can be properly assessed. The synchronizing power coefficient is the derivative of electrical power with respect to angle at

the quiescent operating point. Given the equation for power flow in (3.80), the synchronizing power coefficient can be computed as follows:

$$P_{s_{ij}} = \left.\frac{\partial P_{e_{ij}}}{\partial \delta_{ij}}\right|_{\delta_{ij_0}} = E_i E_j [B_{ij} cos\delta_{ij_0} - G_{ij} sin\delta_{ij_0}] \tag{3.81}$$

Since $G_{ij} \leq 0$, the presence of transmission line losses actually increases the synchronizing power coefficients. In other words, higher line losses will better enable the system to maintain synchronism following a disturbance. This is counter-intuitive since higher impedances typically lead to a lower coupling between different machines or groups of machines. The X/R ratio for practical transmission lines varies from 15 to 20. In such cases it has been found that the increase in the synchronizing power coefficient is negligible (12). Since considering transmission line losses has no effect on the damping coefficients and negligible effect on the synchronizing coefficients, it is justifiable to consider lines to be purely inductive in the power-angle domain models.

3.6.2 Load modeling

The type of loads used in a power system model has a significant effect on the small-signal characteristics of the model. For models representing the bulk power system, often a single load is used to represent the entire load connected to a single transmission bus. For this simplification to be reasonable the composite load must reasonably reflect the frequency and voltage dependencies of all the individual loads that it represents. Most system operators have standard load compositions that they use for their stability studies. For example, in the WECC 20% of the load is modeled as an induction motor and of the remaining 80%, the real power is modeled as constant current and the reactive power is modeled as constant admittance. Numerous dynamic

models have been proposed to represent the voltage and frequency dependence of composite loads in more detail.

The power-angle domain model assumes constant power loads, but the frequency sensitivity of the loads can be accommodated for by specifying a non-zero damping factor in the expression for the *admittance to power flow* of the synchronous machines, $\frac{\Delta\delta}{P} = \frac{1}{Ms^2+D}$, as explained in section 3.5.1. Loads that are fed by power electronic processors generally draw a constant power regardless of changes in the system frequency and the local voltages. For both steady-state and dynamic purposes it is acceptable to consider them to be constant power loads. However, the vast majority of loads in the power system are not fed by electronic processors and their power consumption does vary as the voltage magnitude varies. As a result, constant power loads are rarely used for dynamic simulations. The power-angle domain model will not yield accurate results for an event that leads to large swings in the voltage magnitude. A fundamental assumption of P-δ domain analysis is that the change in voltage magnitude caused by the disturbance is negligible. If this is the case, then the constant admittance and constant current loads behave like constant power loads.

Other researchers have analyzed the effect of dynamic load models on the modes and the synchronizing power coefficients of the system. These calculations will not be shown here because load modeling is so detailed that it should be treated as a research topic in itself. However, it has been found that for the most common type of load model for dynamic simulations, constant admittance loads, the net effect of increasing such a load is to decrease the synchronizing power coefficient. Also, using constant admittance loads instead of constant power loads has no effect on the damping of the system (12).

3.6.3 Governor modeling

When a generator's electrical load is suddenly changed the electrical power no longer matches the mechanical power input and the mismatch in power is accommodated for by an increase or decrease in the kinetic energy stored in the rotating system, which consequently causes a change in speed and frequency. The governor is responsible for sensing this change in speed and adjusting the turbine's input valve so that the mechanical power is increased or decreased to eliminate the mismatch in power at the generator. The frequency, however, will not return to nominal unless an integrator is used to form an automatic generation control (AGC) loop. Governors are designed to permit the speed to drop as the load is increased and vice versa. The amount by which the speed is allowed to change with respect to the power mismatch is governed by the speed regulation, R. The equation below relates the governor's output signal, P_g, to its reference power, P_{ref}, and the mismatch in power, ΔP (18).

$$\Delta P_G(s) = \Delta P_{ref}(s) - \Delta P(s) \tag{3.82}$$

If the governor's speed characteristics are known this equation becomes:

$$\Delta P_G(s) = \Delta P_{ref}(s) - \frac{1}{R}\Delta\omega(s) \tag{3.83}$$

The signal, ΔP_G, causes a change in the valve position signal, ΔP_V. Assuming a linear relationship and a simple time constant, the relationship between the two signals is given below.

$$\Delta P_V(s) = \frac{1}{1+\tau_g s}\Delta P_G(s) \tag{3.84}$$

The governor response to either a change in the reference power or a change in frequency can be represented with the block diagram of Figure 3-39. Combining this block diagram with a block representing the swing equation of synchronous machine, results in the load frequency

control block diagram of Figure 3-40. This block diagram represents the simplest possible models for turbine governor's response. Detailed models will have multiple time constants.

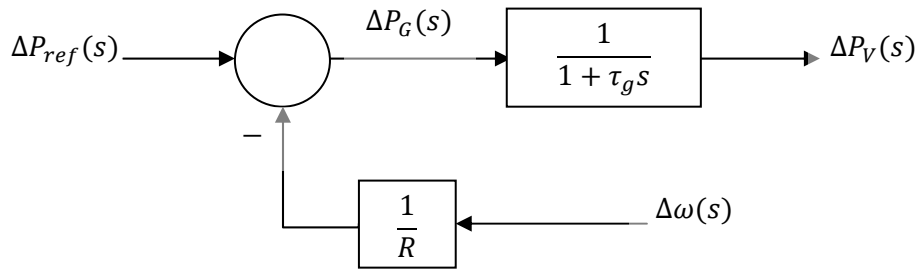

Figure 3-39: Block Diagram Representation of a Turbine Governor

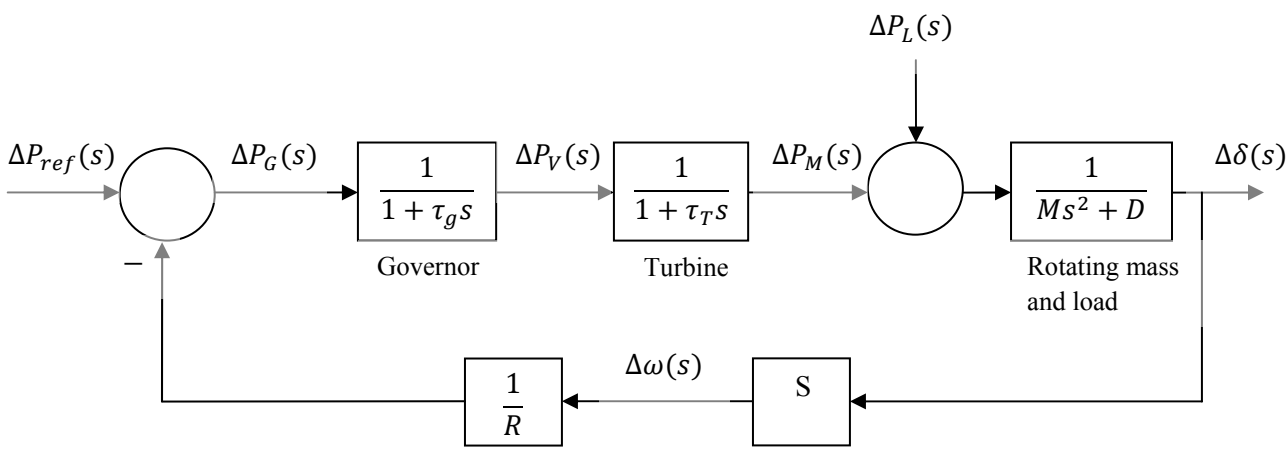

Figure 3-40: Load Frequency Control of an Isolated Power System

If it is assumed that the reference signal, P_{ref}, is unchanged, which means that the generator's output is not changed due to operator action, then the only input to the load frequency control block is ΔP_L. Block diagram reduction techniques can also be used to represent load frequency control with a single block.

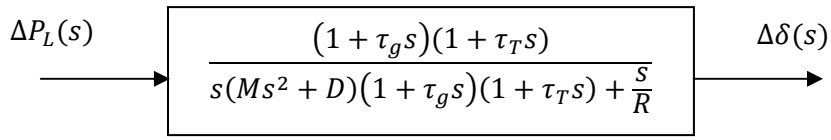

Figure 3-41: Reduced LFC Block Diagram with ΔP_L as the Input

The ratio of angle to power is the effective *admittance to power flow* of the generator, turbine, and governor model.

$$\frac{\Delta\delta(s)}{\Delta P_L(s)} = \frac{(1+\tau_g s)(1+\tau_T s)}{s(Ms^2+D)(1+\tau_g s)(1+\tau_T s)+\frac{s}{R}} \tag{3.85}$$

To account for the effects of the turbine and the governor in a power-angle domain analysis the entire term in (3.85) will have to be used. Obviously, this significantly increases the complexity of the computation. It should be noted that many of the machines in the power system do not have governors associated with them for technical and economic reasons. Additionally, the generators that do have governors are often simulated without governor and turbine models.

From the block diagrams for load frequency control we can see that the governor and turbine models have a *time constant* type response and not a *time delay* type response. With a *time constant* type response, the governors react instantly to changes in the machine's speed. A time constant of 0.5 seconds is typical for a turbine governor, so it can be assumed that a governor will take approximately 2 seconds to fully respond to a step change in speed. The change in speed will not be a step function for any practical disturbance due to the inertia of the generator, so the governor response will appear to be even slower. Because of this slow response, many engineers may not consider governors and turbines when simulating events that lead to electromechanical dynamics that are of the order of 1 hz or faster (12).

Based on the argument in the preceding paragraph, it is intuitive that the governors should both damp oscillations and increase the synchronizing power. Governors act to increase the accelerating power as the machine speed decreases and vice versa. As the governor's time constant decreases, it will have a greater effect on the damping and synchronizing power. For a large interconnection the system inertia will be quite large and the rate of change of machine speed resulting from events that cause power mismatches will be quite small. Lower rates of change of speed will lead to even slower governor and turbine responses. Therefore, for most events within large interconnections it is unlikely that the governors will have a significant impact on the short-term dynamics of the system.

Chapter 4 Contingency Screening in the Power-Angle Domain

Most modern control centers use an operator's load flow program to approve clearances and ensure that the N-1 security criterion is being met for the prevailing system conditions. An operator's load flow, or online load flow, uses the status of all transmission lines and generators, as well as the voltages and angles throughout the network to update a model of the system before performing a load flow simulation. Even though operations engineers are generally required to approve clearances before an operator executes them, this is useful to verify their findings. Due to the complexity of dynamic simulations, very few applications exist to consider the dynamics of a system when screening contingencies.

Load flow simulations do have certain limitations. In load flow analysis, the real power output of all synchronous machines is fixed and any power mismatch created by the contingency is completely picked up by the generator at the swing bus. This may reflect a change in operating conditions due to operator re-dispatch, but in the time immediately after an outage, especially an unplanned outage, the power mismatch is distributed among the different generators according to their inertia or governor droop settings. Some modern power system simulation programs now have the capability to perform inertial and governor droop load flows if sufficient information on the generators and governors is provided.

In load flow analysis, the terminal voltages of synchronous machines are also fixed until their reactive limits are exceeded. Even with excitation systems modeled, the voltage magnitude still varies following most contingencies; however, in many cases this may be small enough to be neglected and analysis in the P-δ domain does not consider it either.

Perhaps the most significant limitation of load flow analysis is that it only shows the system's transition from one state to another. The power system is subject to both steady-state and

transient stability limits (14). The transient stability limit, which is generally the lower limit, cannot be determined through load flow analysis since it depends on the dynamic characteristics of the machines and control systems in the power system. If only the steady-state limit is considered before approving clearances, some clearances may result in the system losing transient stability.

The power-angle domain model is a linearized model so it cannot be used to analyze transient stability. Instead it can be used to analyze small-signal stability and to develop metrics to determine how close the system is to transient instability. These metrics can be better developed in the power-angle domain than in load flow analysis since the P-δ domain model contains information on the generator inertias and possibly the governor and turbine parameters. In this section the modes of an 18 bus system are determined from the P-δ domain model and then metrics are developed to determine the system's ability to withstand transient events in different conditions.

4.1 Analysis of an 18 Bus System

In this section the 18 bus system of Figure 4-1 is analyzed with load flow analysis and dynamic simulations in GE-PSLF and also analyzed in the P-δ domain. This dynamics of this system are more detailed than the IEEE-14bus system. The system contains detailed generator models each with governors and exciters. At Bus 101 two generators models are used to represent a power plant with two generators in it. Purely real constant power loads are used throughout the system. Appendix III contains the load flow and dynamic data needed to simulate this system in GE-PSLF. The techniques described in this chapter are best used on systems of less than 50 buses. The methods of creating equivalents described in the previous chapter may be useful for simplifying the areas of the system that are not pertinent to the study.

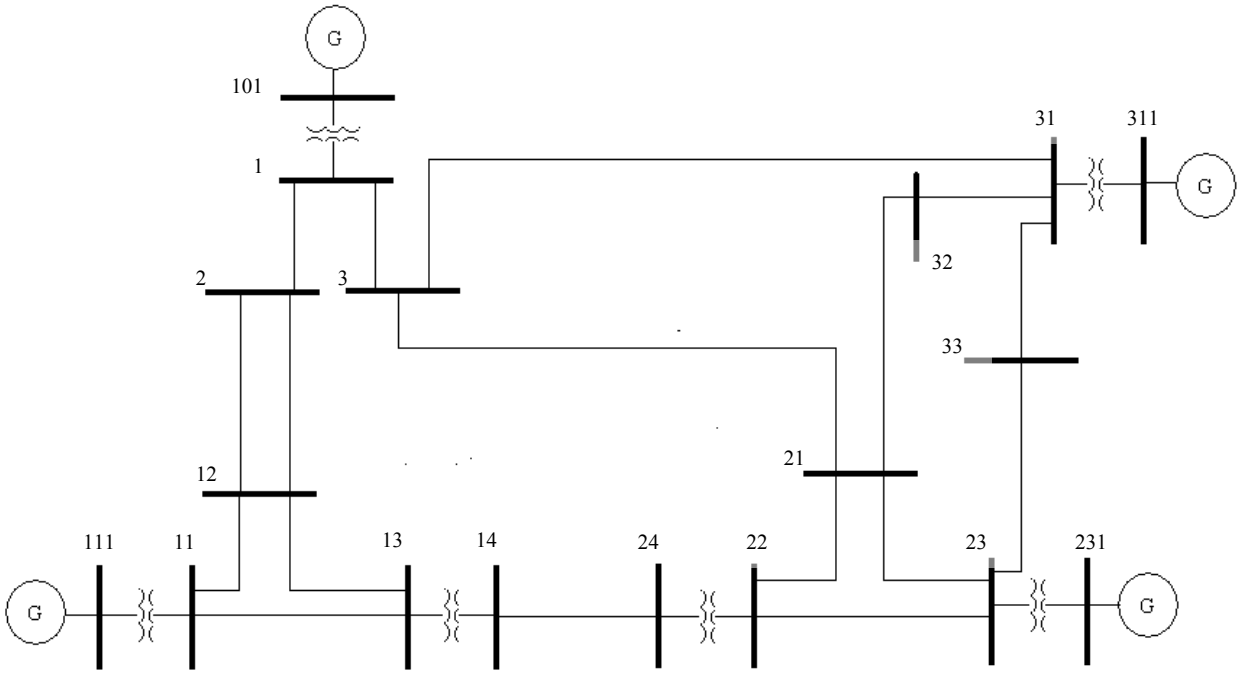

Figure 4-1: 18 Bus Power System

4.1.1 Comparison to simulation data

The system response to a load drop at Bus 23 is evaluated in dynamic simulation in PSLF and through analysis in the P-δ domain. It is important to remember that the P-δ domain model is a simplification of the detailed dynamic model so the results are expected to be similar, but not exact. Line resistances, excitation systems, stabilizers, and detailed generator models cannot be reproduced in the P-δ domain. Figure 4-2 shows the response of bus angles in PSLF following the load trip. The changes in angles are shown instead of the absolute angles. Note that all of the angles show an aperiodic drift since there is a mismatch in real power, but that the relative angle difference is small enough to be considered linear, especially for angles at either at either end of a transmission line.

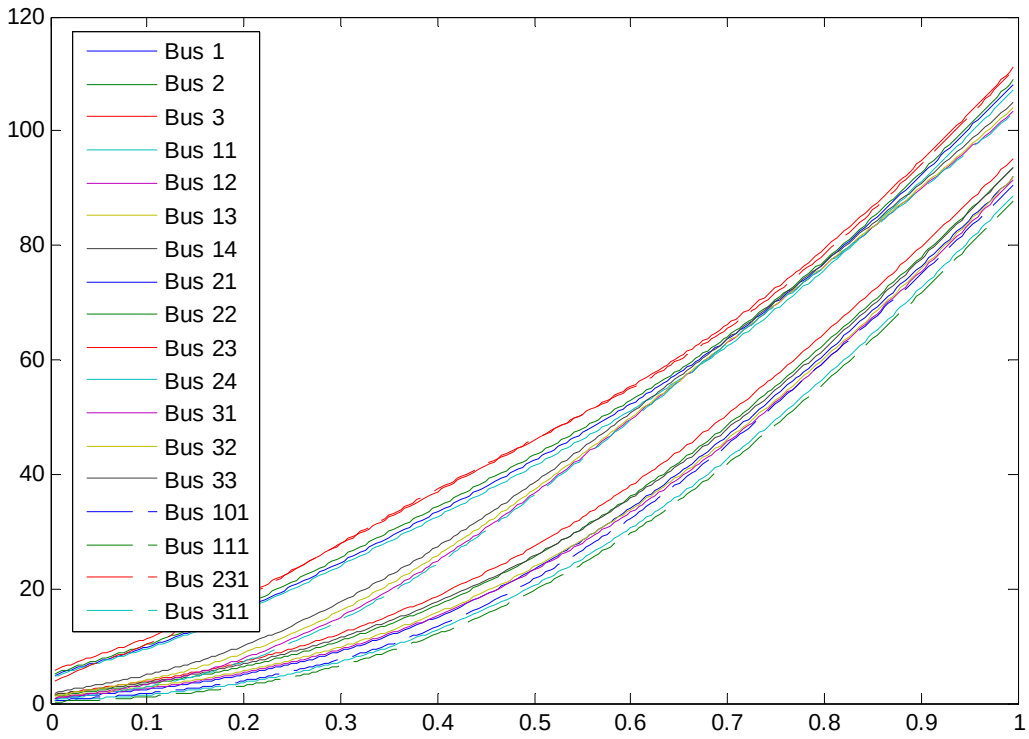

Figure 4-2: Simulated Angle Response to a Load Trip at Bus 23

In the previous sample system, the IEEE 14-bus system, classical generator models were used to represent the machines as a constant voltage source behind a transient reactance. In this example more realistic models are used that model saturation, damper windings, and both subtransient and transient direct axis short circuit time constants. The excitation systems cause the field voltage of the synchronous machines to vary, causing a larger deviation from the classical model. The damping torques within the synchronous machines are also major factors affecting the electromechanical response of the system. In the power-angle domain the damping factor, D, which represents the damping effects from the speed sensitivity of loads can be included, but not the effect of the damping windings inside machine since this also depends on electromagnetic phenomena, which cannot be modeled. The figure below shows the results of a simulation in which the excitation systems are removed, but the damper windings are still

modeled so the simulated response will still be more damped than the response calculated in the P-δ domain.

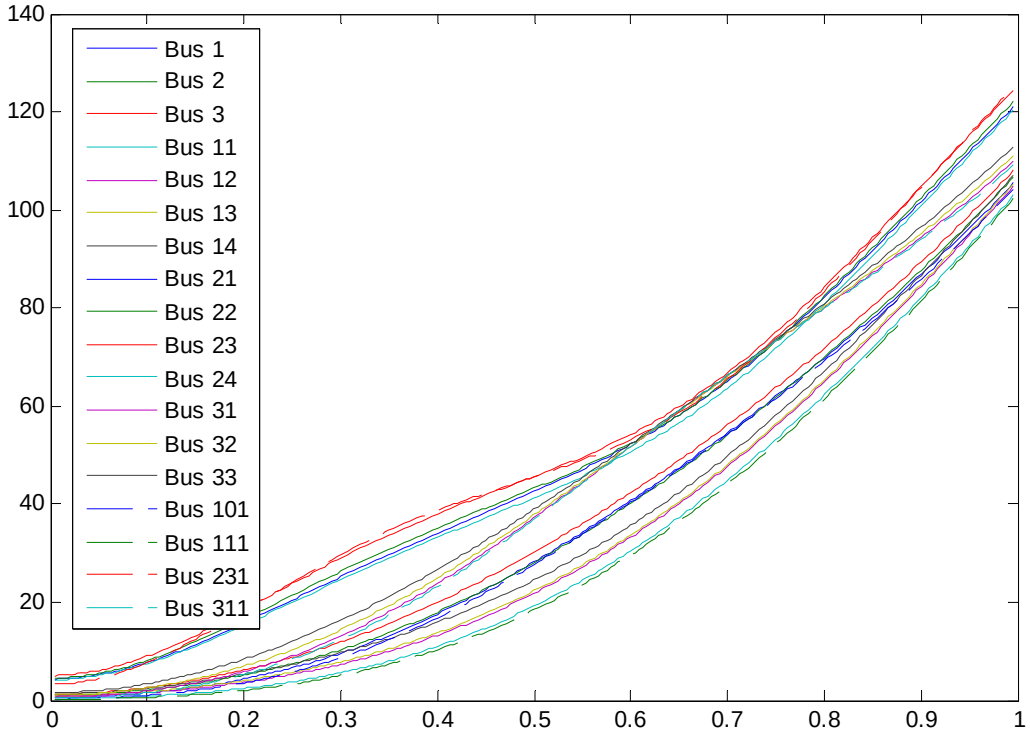

Figure 4-3: Simulated Angle Response to a Load trip at Bus 23 Neglecting the Exciters

Without the excitation systems the oscillations in bus angles have increased and the size of the changes in angle throughout the system have also increased. Another inaccuracy that cannot be avoided in the P-δ domain is the assumption that voltage magnitudes remain constant following an electromechanical disturbance. With a classical generator model this assumption may be fairly accurate, but when detailed generators models are used the voltage magnitudes may undergo significant changes, even without excitation systems included, depending on the disturbance. Figure 4-4 shows the bus voltage magnitudes following the load trip when the system is modeled without exciters.

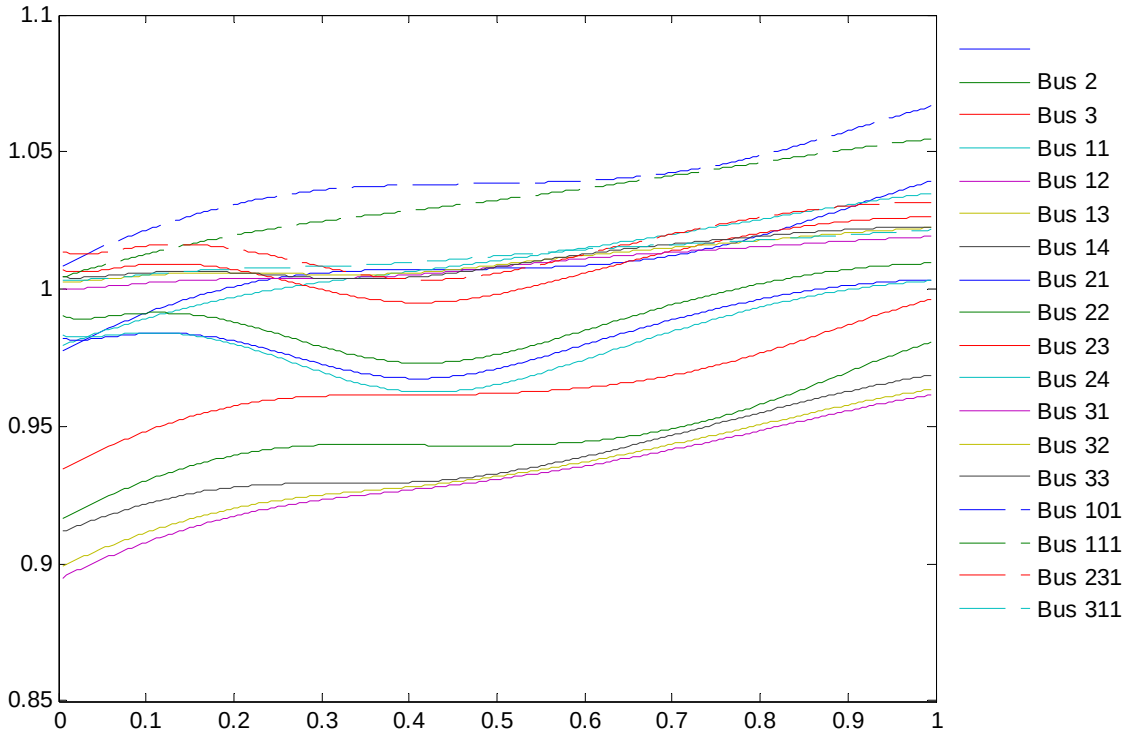

Figure 4-4: Simulated Voltage Magnitude Response to a Load Trip at Bus 23

From this figure we can see that when a purely real load is tripped there is still some variation in the voltage magnitudes throughout the system. Most voltages increase by over 5%.

Appendix IV contains the matlab code that was used to create the Y matrix from line, generator, and transformer data in tabular format. All of the reactances throughout the system are converted to the same impedance base before they are entered into the Y matrix. The load trip is modeled as a step increase in the power injection at Bus 23 equal to the size of the load being tripped. The results of this analysis are shown in the figure below.

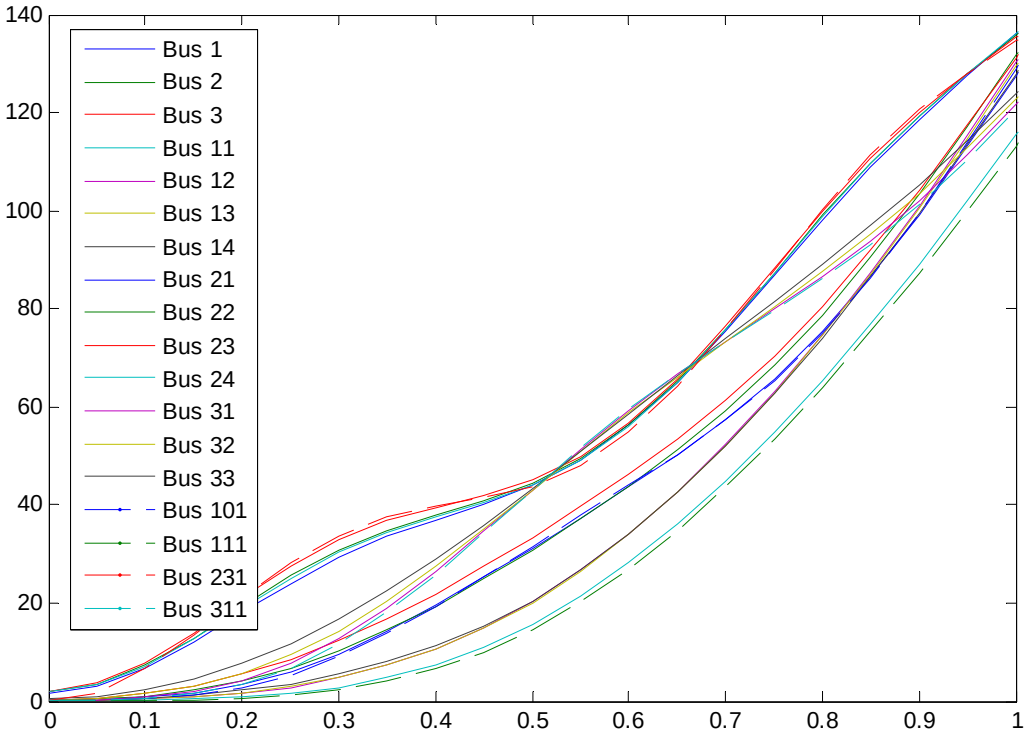

Figure 4-5: Calculated Response to a Load Trip at Bus 23

The results are far more similar to the results of the dynamic simulation when the excitation systems were neglected. It can be seen that the oscillations and overall changes in bus angles are still slightly higher than the case of the original dynamic simulation. This is partially due to the fact that the damper windings still are not accounted. Additionally, the voltage magnitudes at many buses increased by over 5% in the 1s following the event and as |V| increases, α decrease, causing Δθ to also decrease. Figure 4-6 shows the results from the analysis in the P-δ domain when the initial conditions are ignored by setting α=1.

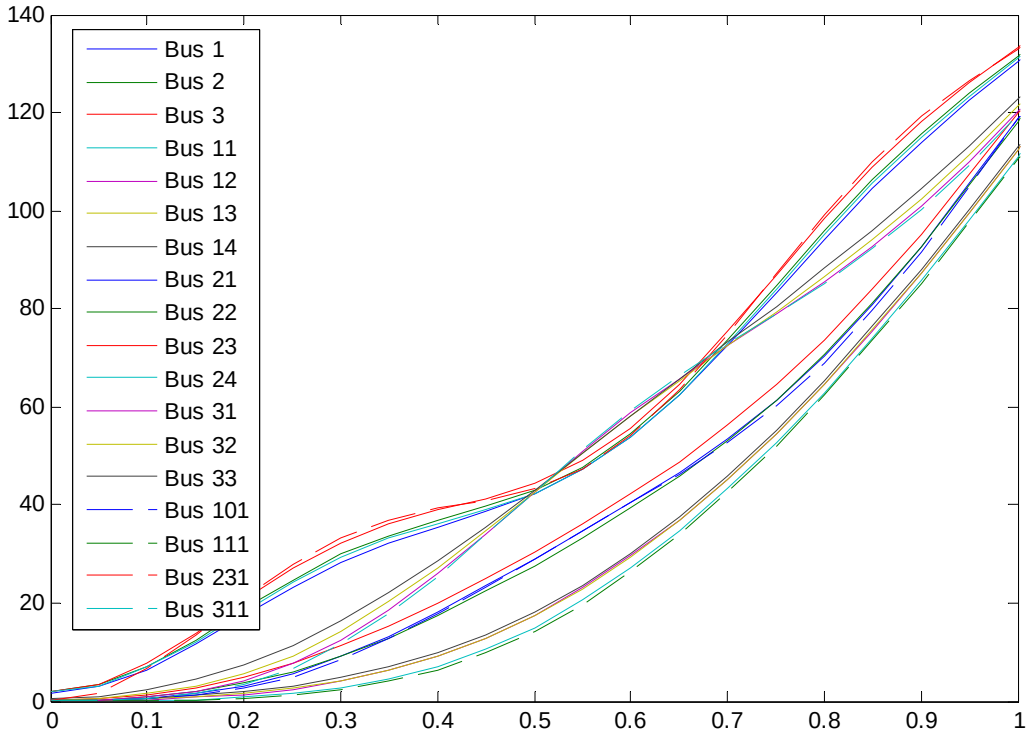

Figure 4-6: Calculated Response to a Load Trip at Bus 23 Ignoring Initial Conditions

Setting α=1 produces very similar results, but the changes in bus angles are slightly lower. For this model most of the elements of α are greater than 1 since most bus voltages are less than 1.0 pu; this is unusual for a transmission system. As a result, setting α to a unity matrix causes the changes in bus angles to be slightly lower than when α is properly calculated. It should be recognized that ignoring the initial conditions (setting α to a unity matrix) no longer gives conservative results when the majority of the bus voltages are below 1.0 pu, and a margin of error should be used.

4.1.2 Calculation of the modes

The response of a linear system can be expressed as the summation of a series of functions that all satisfy the unforced system equations (19). The form of the function is shown below:

$$e^{\alpha t}(A_i \sin(\omega t) + B_i \cos(\omega t)) \tag{4.1}$$

Each of these functions is called a characteristic mode of the system. A_i and B_i are arbitrary constants depending on the modes of the system, the initial conditions, the point at which the system response is observed and the forcing function. λ_i is an eigenvalue of the system defined by the equation below:

$$\lambda_i = \alpha_i \mp j\omega_i \tag{4.2}$$

The number of eigenvalue pairs in a system is equal to the number of differential equations required to describe the dynamic system. For a power system this is equal to N-1, where N is the number of synchronous machines in the system. The real part of the eigenvalue, α, is the damping ratio, which indicates how heavily damped the oscillation will be. If the damping is negative for all eigenvalues then the corresponding response will decay with time and the system will be stable. However, if the damping is positive for any eigenvalue then the corresponding response will grow with time and the entire system will be unstable. If α is zero the corresponding response will be undamped. The damping ratio for a typical power system is usually negative and less than 10%, which means that 10 or more full oscillations will be required before the response fully decays (12). The imaginary part of the eigenvalue, ω, is the undamped natural frequency. If the natural frequency is zero the corresponding response will be aperiodic; otherwise, it will oscillate with a frequency of ω rad/s.

Because the P-δ domain model is based on the same assumptions of state-space analysis, the modes of the system can be calculated and analyzed in a similar way. The eigenvalues of the

system are calculated by setting the determinant of the Y matrix equal to zero and solving. The results from this system are shown below:

$0.0149 \mp 4.96j$

$0.0365 \mp 9.20j$

$0.0306 \mp 10.87j$

$0.0479 \mp 235.89j$

0.0440

Based on the expression for the eigenvalues given in (4.2), the natural frequencies of the system can easily be found.

Table 4-1: Natural Frequencies of the 18 Bus System

Eigenvalue	**Natural Frequency** (hz)
0.0149±4.960j	0.789
0.0365±9.200j	1.464
0.0306±10.87j	1.730
0.0449±235.9j	37.54
0.0440	0

Since there are five generators in this system (2 at Bus 101 and 1 at Buses 111, 231 311), it is expected that there should be four pairs of eigenvalues produced by this system. The damping factor is largely dependent on the damping constant, D. Note that the damping constant was the same for all the machines in the system, yet the modes are damped to different degrees. Also, note that there is one eigenvalue pair that has a natural frequency that is substantially higher than the other three. The machine/s that this frequency is associated with can be found by removing each machine, one at a time, and recalculating the natural frequencies. Table 4-2 shows the results.

Table 4-2: Natural Frequencies Following the Removal of Machines

Machine Removed from the System	Gen 311	Gen 231	Gen 111	Bus 101 (both gens)	Bus 101 (1st gen out)	Bus 101 (2nd gen out)
Calculated Frequencies	6.6, 236, 10.08	5.2, 236, 9.3	7.4, 236, 10.8	4.9, 10.5	5.0,12.7,10.3	5.0, 13.4, 10.3

The removal of one machine removes a mode from the system and changes all of the other modes slightly. This is expected since the dynamics of each machine is a result of every other machine in the system. Generally, larger systems with higher aggregate inertias have lower oscillation frequencies; therefore, it is expected that when a generator is removed from the system the frequencies of the remaining modes should increase slightly. The results show that the high frequency component is due to the two machines at Bus 101. Since removing one of these machines removes the high frequency component, it is evident that the high frequency oscillation is caused by the interaction of the two generators at Bus 101. This is known as an intra-plant oscillation or a control oscillation. These oscillations tend to be quite localized and are damped through proper tuning of the stabilizers and exciters at the plant. For system studies, the low frequency oscillations are of primary concern since these involve two coherent areas oscillating against each other (inter-area oscillations) or a single plant or group of plants oscillating against the rest of the system (local plant oscillations). It is interesting to note that this process of associating a specific generator with a frequency signature has been used by previous researchers for generator trip identification (12). In a practical system associating a machine with a particular mode may be difficult since there will likely be thousands of modes in the measured data and many of them will be very similar.

The calculated eigenvalues of the system can be verified by computing the fast-fourier transform on the time-series data. The FFT is best calculated with a large number of periods of

the components to be analyzed. The FFT of a sample that only contains a few periods of a sinusoidal signal will appear as a sinc function. However, as the number of cycles in the sample increases to infinity the FFT approaches an impulse function. In this case a sample over 15.5 seconds was used so that it would include multiple periods of the slowest mode. The figure below shows the changes in angles over 15.5s.

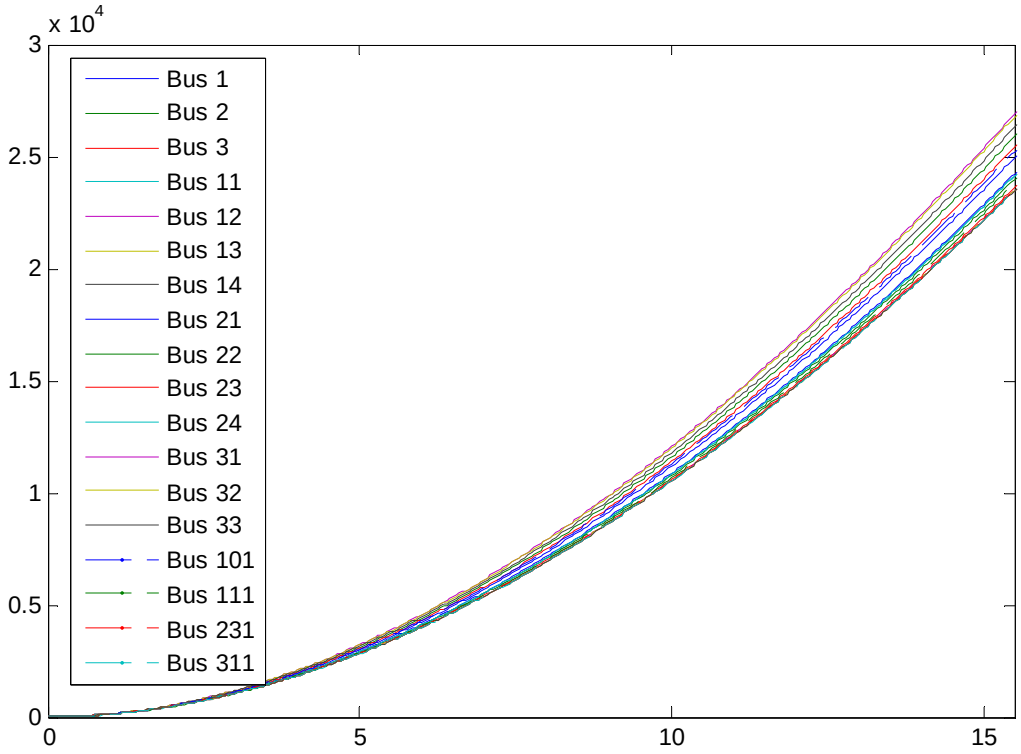

Figure 4-7: Changes in Bus Angles over 15.5s

This signal appears to have an exponential growth, and with the scale above the oscillatory components appear small compared to the aperiodic component; therefore, an FFT of this signal would show a very high component around 0 hz. The low frequency oscillations that are of principal concern will be difficult to distinguish with a very high 0 hz component. To increase the clarity of the FFT, the aperiodic component is first isolated by using a moving mean with a 1s window. The aperiodic component is then subtracted from the total response. It should be

noted that advanced filters could be designed to more adequately remove the aperiodic components, but the objective here is just to remove enough of the 0 hz component so that the other low frequency components can be properly observed. Figure 4-8 shows the de-trended bus angles.

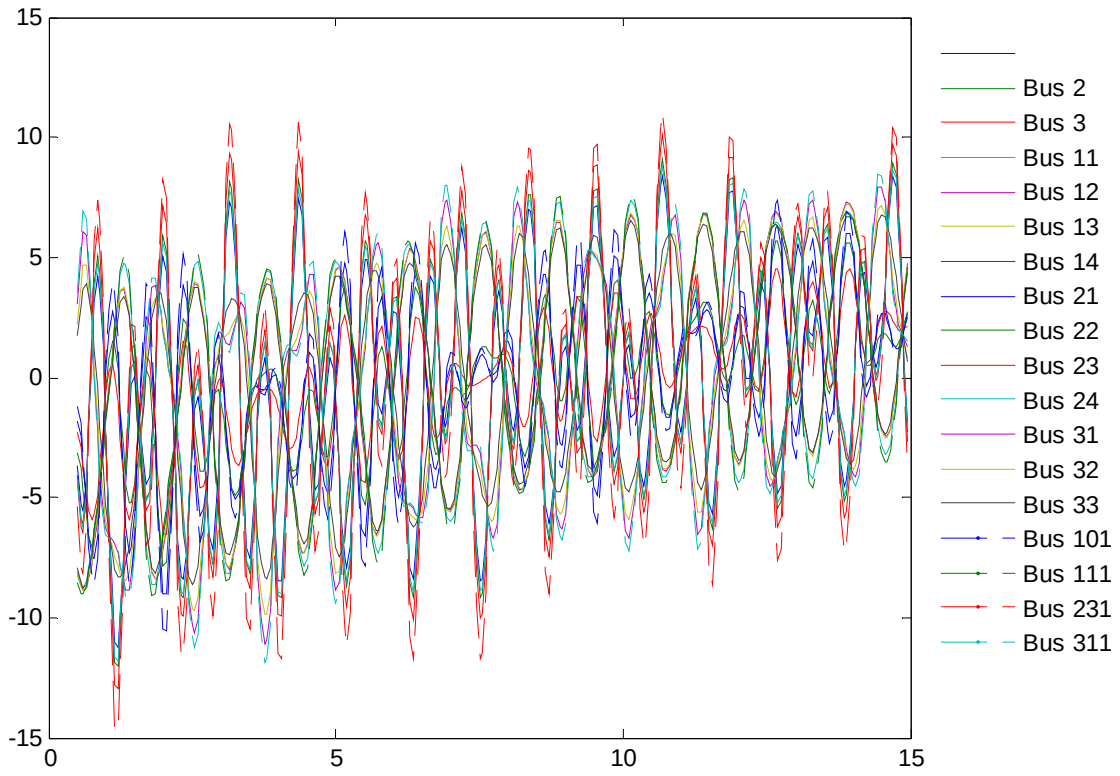

Figure 4-8: De-trended Bus Angles

The de-trended bus angle at a given time is calculated based on 0.5s of data before and after that time. Therefore, the length of the de-trended data now ranges from 0.5 – 15s instead of 0 – 15.5s. This leaves 290 points in the time-series data. A 256 point FFT is taken to observe this component. The sampling rate is 20 hz since the angle at each bus was recorded every 0.05s. It should be noted that the sampling rate should be at least double the frequency of the highest frequency component to be observed. Hence, with a sampling rate of 20 hz only frequencies less

than 10 hz can be observed. Appendix V contains the Matlab code that was used to detrend the data, compute the FFT and plot the results.

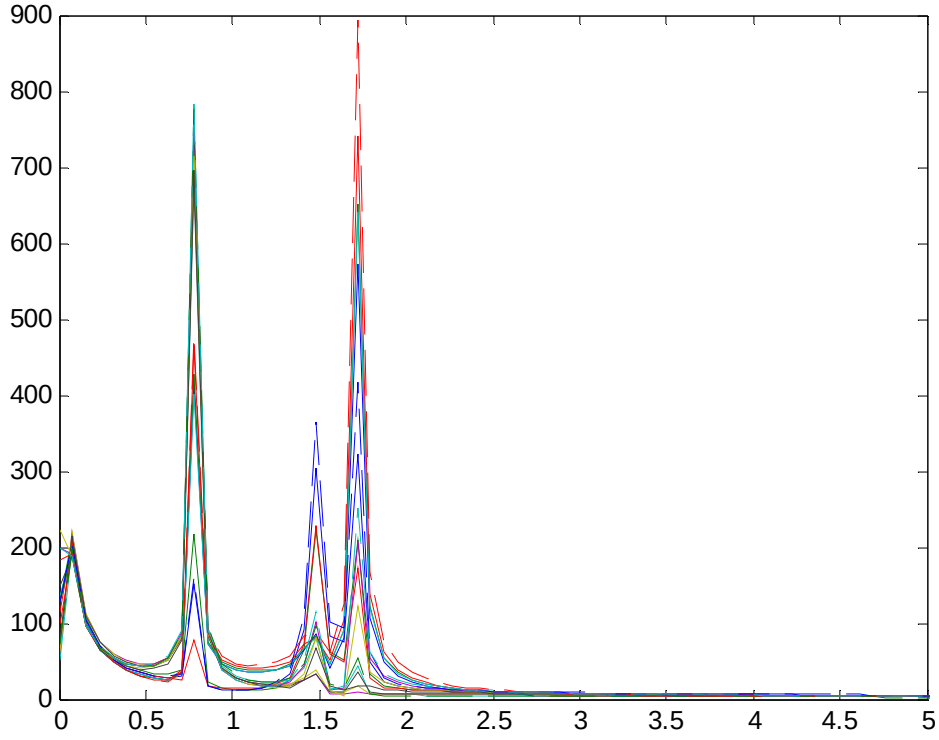

Figure 4-9: FFT of the System Response Following a Load Trip in the P-δ Domain

The FFT shows impulses at 0.781 hz, 1.48 hz, and 1.72 hz. These values closely match the results from Table 4-1. The discrepancies are less than 0.02 hz and are likely due to the inaccuracies introduced by making a frequency sweep from 0 to 10 hz with 256 points. Overall, the results found through calculations are accurate and if the matrix of admittances to power flow already exists, then the computation is simpler than using the fast Fourier transform.

For this sampling frequency the 37.54 hz component cannot be detected. For system studies and most PMU applications, the modes above 2 hz are generally ignored. In practice phasor measurement units would not accurately detect a signal with such a high frequency and at distant buses it cannot be distinguished from noise.

4.2 Stability Analysis

One of the primary advantages of analytical screening tools over load flow and dynamic simulation is that conventional simulation programs do not give a measure of how close the system is to instability. This section will describe how the synchronizing power coefficient, critical clearing time, and available acceleration or deceleration energy can be used as measures of the stability of the system.

In the power system, the change in electrical torque on the rotors of synchronous machines following a small disturbance can be resolved into two components (2).

$$\Delta T_e = T_s \Delta\delta + T_D \Delta\omega \tag{4.3}$$

$T_s\Delta\delta$ is the component that is in phase with the change in rotor angle, $\Delta\delta$. It is referred to as the synchronizing torque. $T_D\Delta\omega$ is the component that is in phase with the change in rotor speed, $\Delta\omega$. It is referred to as the damping torque. Small-signal instability arises if either torque is insufficient. A lack of synchronizing torque results in instability through an aperiodic drift in rotor angle; whereas, a lack of damping torque results in oscillatory instability. Figure 4-10 illustrates both non-oscillatory and oscillatory small-signal instability.

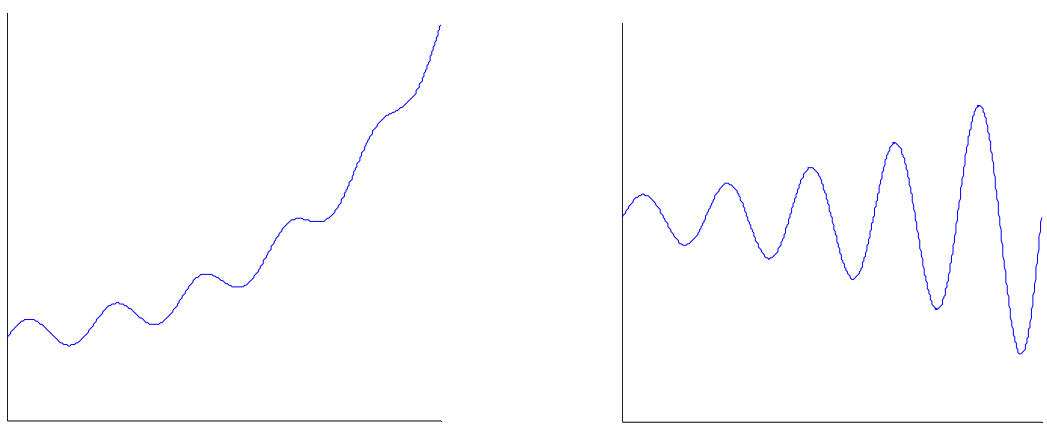

Insufficient Synchronizing Torque Insufficient Damping Torque

Figure 4-10: Small-Signal Instability

An insufficient synchronizing torque may arise for a generator or group of generators with weak links to the rest of the system; whereas, insufficient damping torques arise from poorly tuned continuously acting voltage regulators.

Equation (4.3) can be expressed in terms of the change in power instead of torque:

$$\Delta P_e = P_s \Delta\delta + D\Delta\omega \tag{4.4}$$

P_s (also S_P) is referred to as the synchronizing power coefficient. Where,

$$P_s = \left.\frac{dP}{dt}\right|_{\delta=\delta_0} = \frac{|V_1||V_2|}{x} cos\delta_0 = P_{max} cos\delta_0 \tag{4.5}$$

δ_0 is the angle at the initial operating point. The linearized swing equation of (3.10) is restated below.

$$\mathrm{M}\frac{\mathrm{d}^2\Delta\delta}{\mathrm{dt}^2} = -\frac{|\mathrm{V}_1||\mathrm{V}_2|}{\mathrm{X}}\cos\delta_0\Delta\delta \tag{4.6}$$

Substituting (4.5) and rearranging gives:

$$\frac{\mathrm{d}^2\Delta\delta}{\mathrm{dt}^2} = -\frac{\mathrm{P_s}}{\mathrm{M}}\Delta\delta \tag{4.7}$$

It is intuitive that at a stable operating point the system does not lose stability for any small perturbation in angle. Equation (4.7) shows that if $P_s > 0$, any change in angle is accompanied by a deceleration in angle that acts to return the angle to its initial operating point. In the real system, damping will reduce the oscillations and return the angle to δ_0.

A larger synchronizing coefficient leads to a larger synchronizing torque and therefore a stronger system. A negative synchronizing coefficient indicates small-signal instability, and a synchronizing coefficient of zero would indicate marginal instability. To be used as a measure of stability, the synchronizing power coefficient would have to be calculated for each machine in the system by creating an equivalent to represent every other machine in the interconnection.

This equivalent is created using the techniques developed in section 3.4. The Matlab program, stability_analysis.p in Appendix VI, performs this computation. The table below shows the synchronizing power coefficient for the 18 bus system in its original state and when components are out of service.

Table 4-3: Synchronizing Power Coefficients for the 18 Bus System

Generator Bus	No Outages	Line 3-21 Out	Line 3-21 & Line 3-31 Out
101	6.6134	3.3759	0.8967
111	4.2163	2.7525	0.9134
231	4.4344	2.1431	0.6468
311	3.9086	2.5832	0.6014

The synchronizing power coefficient indicates how strongly a machine is connected to the rest of the system as well as how stressed those connections are for the prevailing power system power flows. Generators 101 and 231 have the highest values for P_s when all lines are in service since both the North and South areas are directly connected to every other area in the system. The East and West areas only have ties to 2 other areas. Additionally, it can be seen that as lines are removed from the system the synchronizing power coefficient decreases. This is expected since as the reactance between the machines increases, P_{max} decreases and consequently, P_s must also decrease. When 2 lines are out of service the synchronizing power coefficients fall below 1 with the coefficient for the generator at Bus 311 being the lowest. This is expected since Bus 311 is now connected to the system by only one long transmission path.

The synchronizing power coefficient is useful for indicating the ability of the system to withstand small disturbances, but for transient disturbances an indicator that considers the non-linear effects of increasing angles. Calculating the critical clearing time for a bolted three phase fault and the maximum energy available for acceleration and deceleration when the power output

of the generator is changed are two indicators of transient stability. The critical clearing time for a synchronous machine is the maximum time that a bolted 3 phase fault can be applied to the terminals of the machine without the machine losing stability. Consider the power-angle curve in Figure 4-11.

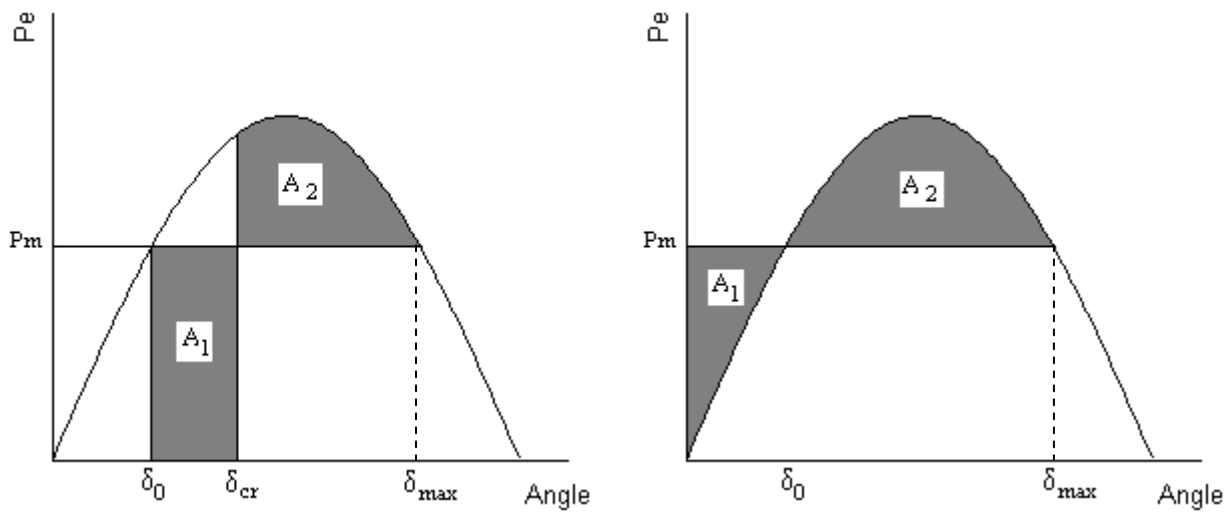

(a) Bolted 3 Phase fault (b) Load Switching

Figure 4-11: The Equal Area Criterion

This is a graphical interpretation of the energy stored in the machine's rotating mass. The x-axis shows the difference in the rotor angles of the two machines and the y-axis indicates the electrical power output from the machine at the sending end of the connecting lines. Figure 4-11(a) shows the electrical power falling to zero during the fault and then increasing to P_e when the fault is cleared at the critical clearing angle, δ_{cr}. Figure 4-11(b) shows the electrical power increasing or decreasing due to load or generator switching. The electrical power moves along the power-angle curve, but the mechanical power input remains constant. Area A_1 and A_2 are known as the accelerating and decelerating areas respectively. These areas represent the amount by which the kinetic energy of the rotor masses is increased or decreased following a

disturbance. From the swing equation we know that when the electrical power is less than the mechanical power input the rotor angles decelerate, but when the electrical power is greater than the mechanical power input the rotor angles accelerate. The equal area stability criterion states that for an angle swing to be stable the two areas must be equal (18).

$$|area\ A_1| = |area\ A_2| \tag{4.8}$$

For the case of a bolted 3 phase fault at the machine's terminals as illustrated in Figure 4-11 (a), the critical clearing time can be calculated by equating area 1 and area 2. The expressions for area 1 and 2 for this particular case are derived below.

$$area\ A_1 = \int_{\delta_0}^{\delta_{cr}} P_m\, d\delta = P_m(\delta_{cr} - \delta_0) \tag{4.9}$$

$$area\ A_2 = \int_{\delta_{cr}}^{\delta_{max}} (P_{max} \sin\delta - P_m) d\delta \tag{4.10}$$

$$= P_{max}(\cos\delta_{cr} - cos\delta_{max}) - P_m(\delta_{max} - \delta_{cr})$$

Equating the expressions for area A_1 and A_2 yields:

$$cos\delta_{cr} = \frac{P_m}{P_{max}}(\delta_{max} - \delta_0) + cos\delta_{max} \tag{4.11}$$

From the power-angle curve the following two relations can be seen:

$$\delta_{max} = \pi - \delta_0 \tag{4.12}$$

$$P_m = P_{max} sin\delta_0 \tag{4.13}$$

Substituting these two expressions into (4.11) gives an expression for the critical clearing angle:

$$\delta_{cr} = cos^{-1}[(\pi - 2\delta_0)sin\delta_0 - cos\delta_0] \tag{4.14}$$

The critical clearing angle itself gives some useful information on the stability of the machine but it cannot be used to compare the stability of different machines. The critical clearing time is

needed for this. For the fault-on period of the scenario represented by Figure 4-11 the machine's electrical power output is zero so the swing equation becomes:

$$M\frac{d\delta^2}{dt^2} = P_m \tag{4.15}$$

Rearranging this equation and integrating with respect to time gives the rate of change of the machine angle:

$$\frac{d\delta}{dt} = \frac{1}{M}P_m t \tag{4.16}$$

A further integration with time yields

$$\delta = \frac{1}{2M}P_m t^2 + \delta_0 \tag{4.17}$$

If this integration is done up to the time of fault clearing then $t=t_{cr}$:

$$\delta = \frac{1}{2M}P_m {t_{cr}}^2 + \delta_0 \tag{4.18}$$

Rearranging this equation gives:

$$t_{cr} = \sqrt{\frac{2M(\delta_{cr} - \delta_0)}{P_m}} \tag{4.19}$$

Equation (4.14) along with (4.19) is used to calculate the critical clearing time for a generator in a two machine system. It can also be used in a multi-machine system if the system is first reduced to a 2 machine equivalent. The Matlab code stability_analysis.m, which is shown in Appendix VI, is used to calculate this. The values for the N-1-1 contingency in the 18 bus system are shown below. It must be noted that the critical clearing time is a non-linear function; whereas, equivalents that are created by the techniques described in chapter 3 linearize the network around the initial operating point. This will cause inaccuracies in the results.

Table 4-4: Critical Clearing Times for the 18 Bus System

Generator Bus	No Outages	Line 3-21 Out	Line 3-21 & Line 3-31 Out
101	0.7188	0.3013	0.0428
111	0.2006	0.1092	0.0213
231	1.1404	0.4589	0.0801
311	0.2017	0.1113	0.0127

As additional lines are removed the critical clearing angle decreases, indicating that the system has less ability to withstand prolonged faults. Using the critical clearing angle as an indicator, we see the same general results as with the synchronizing power coefficient. However, if the relative effect of the disturbance on each bus in the system were being considered there would be differences. For example, the critical clearing angles for the machine at Bus 231 are larger than for the machine at Bus 101; whereas, the synchronizing power coefficient at Bus 101 is always larger than at Bus 231. These differences are expected since the indicators are measuring different forms of stability, small-signal stability and transient stability, which have different properties.

Now let's develop an indicator to determine a generator's ability to maintain stability when it experiences a sudden change in output power due to load, generator, or line tripping nearby. A disturbance that causes an increase in the generator's electrical power would cause a sharp increase in both angle and power and then the rotor angle would decrease until the decelerating energy matched the accelerating energy. Eventually the damping in the system would cause the oscillations to subside and if the disturbance was temporary, the machine will settle at its original operating point. A disturbance that causes a decrease in the generator's output has a similar response, but obviously the angle and power initially decrease. A_1 and A_2 represent the

maximum possible accelerating and decelerating energies for the machine for a given network topology and operating point.

$$area\ A_1 = \int_0^{\delta_0} (P_m - P_{max}\sin\delta)\, d\delta \tag{4.20}$$

$$= P_m\delta_0 + P_{max}cos\delta_0 + P_{max}$$

$$area\ A_2 = \int_{\delta_0}^{\delta_{max}} (P_{max}\sin\delta - P_m)\, d\delta) \tag{4.21}$$

$$= P_m(2\delta_0 - \pi) + 2P_{max}cos\delta_0$$

The smaller of these areas indicates how much energy can be suddenly introduced or removed from the machine without stability being lost. This quantity will be referred to as the machine's critical energy.

$$E_{cr} = min(area\ \ A_1, area\ \ A_2) \tag{4.22}$$

Similar to the previous indicators, the critical energy must be calculated for each machine in the system by creating an equivalent for every other machine in the interconnection. The results for the system in 3 different states are shown in Table 4-5. The critical energy is computed in units of MW rads so it is difficult to directly relate this measure to the energy that is lost or gained in an area for a given event. The critical energy of each machine shows a very similar trend to the critical clearing times. This is expected since both are measures of the system's transient stability.

Table 4-5: Critical Energies for the 18 Bus System

Generator Bus	No Outages	Line 3-21 Out	Line 3-21 & Line 3-31 Out
101	2.0981	0.3413	0.0070
111	0.4524	0.1330	0.0051
231	1.6136	0.2369	0.0071
311	0.3652	0.1105	0.0014

Chapter 5 Protection Applications

In chapter 4 several applications that may be useful in a control center were proposed. This chapter will focus on applications that can improve the performance of protections systems.

5.1 Supervision of relays during power swings

One of the main incentives of studying electromechanical traveling waves is to understand their effect on protection systems throughout the power network. Previous researchers have found that the protective devices which are significantly affected by electromechanical propagating disturbances include overcurrent relays, distance relays, out-of-step relays, loss-of-excitation relays, and underfrequency load-shedding relays (10). The phenomenon of concern is the movement of positive-sequence voltage phase angles across the network. Deviations in voltage angle cause deviations in real power throughout the network, which are known as power swings. Deviations in real power flow will also affect voltage magnitudes, but this is a second-order effect and is insignificant in most cases. The deviations in power flow will be super-imposed on the prevailing network power flows. To simulate this, a 64-node ring system with each node modeled with the continuum model, was created in matlab (4). For a step change in angle at generator 16, an electromechanical traveling wave was created, which caused deviations in current and apparent impedance throughout the system. Distance relays were modeled at each node in the system with the relay's third zone covering 150% of the adjacent line's impedance. The diagram below shows how the relay's trip characteristics were encroached upon at Bus 15 (10).

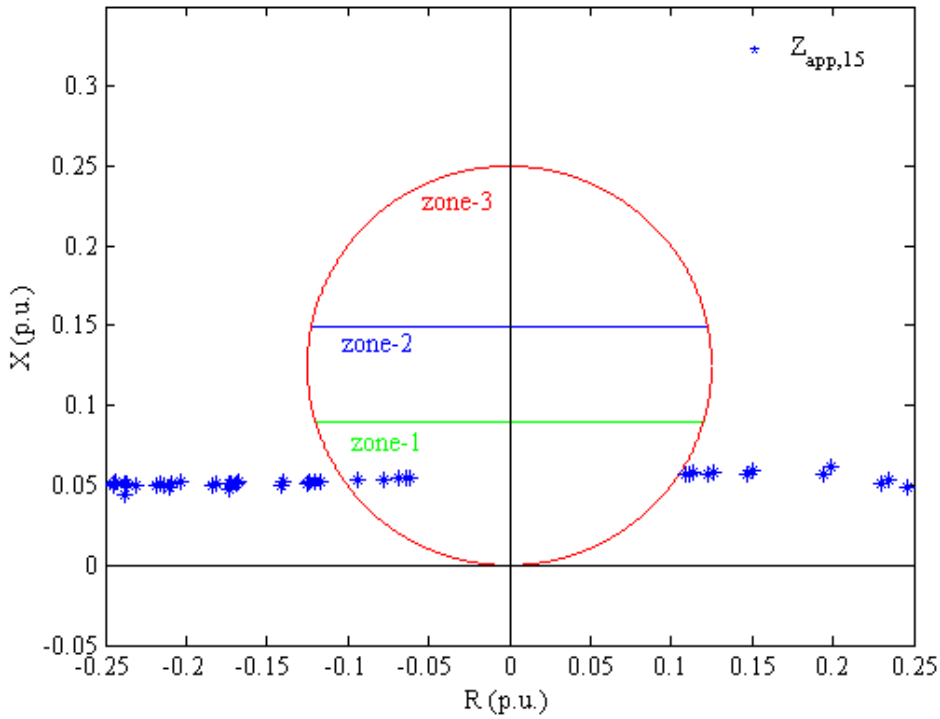

Figure 5-1: Distance Relay Encroachment with the Continuum Model (10)

Not every relay was encroached upon, but the results demonstrated how electromechanical propagating disturbances could be detrimental to distance relays. Similar tests were carried out for overcurrent, out-of-step, and underfrequency relays (10).

Another approach is to develop an alarm system utilizing phasor measurement units to safeguard against encroachment of the trip characteristics of distance relays. This alarm is intended to serve as an early warning system, not real-time control. As the apparent impedance approaches the trip characteristics of distance relays and loss-of-excitation relays due to power swings or steady-state increases in power flow, an alarm is issued to protection engineers so that they can reassess their relay settings. For a power swing the alarm is intended to warn protection engineers about future power swings that may actually cause false tripping under different loading conditions. For example, if a large generator trip caused a power swing that barely encroached upon the supervisory boundary an engineer might look at the alarm generated along

with its data and conclude that the relay's settings are secure. However, if the generator trip caused the apparent impedance to move very close to the third zone for a significant length of time then it is possible that the same contingency under peak loading conditions or in combination with a pre-disturbance outage would cause encroachment and it may be prudent to reassess the relay settings. Since protection engineers do not have the time to revisit their relay settings frequently, this alarm system will direct their attention to the relays with a high probability of false tripping. This is an important application since several large-scale blackouts, such as the 1965 North American blackout, have been initiated by misoperation of relays whose settings became outdated due to changes in load, system topology changes, or changes in generation dispatch; additionally, relay misoperation due to inappropriate relay settings has been a contributing factor in many large scale blackouts.

The alarm places a supervisory boundary around the largest zone of distance and loss-of-excitation relays and issues a warning when the apparent impedance breaches the boundary. The alarm's warning should include the time of the event, the length of time that the supervisory boundary was encroached for, a measure of how close to the third zone the apparent impedance reached, and the trajectory of the apparent impedance before and after the encroachment. A PMU at the same bus as the relay being supervised is used to measure the voltage and current that the relay sees, and transmit the data to a phasor data concentrator (PDC) in a control center. Algorithms can be loaded into the PDC to compute the apparent impedance, check for encroachment into the supervisory boundary, and send an alarm to a protection engineer if necessary. The apparent impedance could also be measured, computed, and compared to the supervisory boundary by a digital relay at the location of the encroachment if time is critical or the communication infrastructure is questionable.

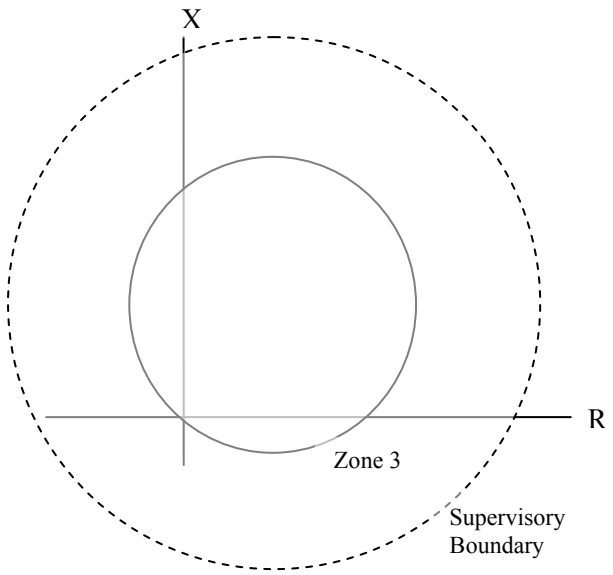

Figure 5-2: The Supervisory Boundary for the Third Zone

It should be noted that with digital relays, the supervisory boundary could be calculated on the relay and then automatic actions could be taken instead of sending an alarm. To prevent encroachment the trip region for distance and loss-of-excitation relays could be blocked, shrunk, or reshaped without significantly impacting the security of the relay. However, these devices are relatively new and most protection engineers are still reluctant to entrust such critical functions to a relatively unproven technology. Nevertheless, let's consider a complimentary system to the alarm that actually blocks relays from tripping when it is predicted that there will be encroachment due to electromechanical power swings. Consider a scenario in which electromechanical disturbance propagation that has the potential to cause encroachment into the third zone of a distance relay is propagating through the system. A supervisory system which monitors electromechanical traveling waves could be used to detect and block relays when a large traveling wave is detected(7). This system would be able to observe the wave in other locations of the system and block the relay from tripping before the traveling wave arrived. A

more sophisticated system may even be able to calculate time of arrival of the wave and the size of the swing in the R-X plane and re-adjust the trip characteristics of the relay to reduce the possibility of false tripping without impairing the relay's ability to clear faults.

5.2 Out-of-step tripping

Faults, line switching, generator trips, and large load trips cause sudden changes in the electrical power of synchronous machines and may cause power swings. These power swings start at machines closest to the location of the disturbance and propagate through the entire network. Severe disturbances can lead to a monotonic separation of the rotor angles of groups of machines and eventually a loss of synchronism between the different groups. These unstable swings are referred to as out-of-step conditions. An out-of-step condition is highly undesirable since it creates high power flows and unusual voltages throughout the network. Protection systems may not function appropriately under such abnormal conditions and generators are subjected to large cyclical torques that could cause permanent damage if they persist too long. Generally, when a system or an individual machine goes unstable it will not recover synchronism unless unusual control mechanisms are applied. Therefore it is important that an unstable swing is quickly identified and the machine or machines that are losing stability are separated from the rest of the system. If this is executed properly and the plant auxiliaries are kept energized, then the generator can be resynchronized within a fairly short amount of time. The detection of unstable swings and the subsequent separation of the unstable generator or group of generators are performed by out-of-step tripping relays (20).

Before discussing the operation of out-of-step tripping relays and how they can be improved, let's review the expressions for the power system quantities observed at the terminals of the relay. Consider a relay at Bus A in the simple 2 machine system below.

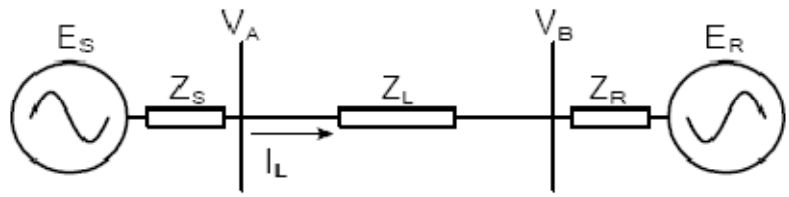

Figure 5-3: Two Machine System (21)

The expression for the current seen at the relay at Bus A is given below:

$$I_L = \frac{E_S - E_R}{Z_S + Z_L + Z_R} \tag{5.1}$$

Therefore, the apparent impedance measured at Bus A can be computed as:

$$Z_A = \frac{V_A}{I_L} = \frac{E_S - I_L * Z_S}{I_L} = \frac{E_S}{I_L} - Z_S = \frac{E_S \cdot (Z_S + Z_L + Z_R)}{E_S - E_R} - Z_S \tag{5.2}$$

If the angle on E_s leads the angle on E_R by δ and the ratio of E_s to E_R is k then we get:

$$\frac{E_S}{E_S - E_R} = \frac{k((k - cos\delta) - jsin\delta)}{(k - cos\delta)^2 + sin^2\delta} \tag{5.3}$$

If it is assumed that the machine internal voltages are equal, the preceding equation becomes:

$$\frac{E_S}{E_S - E_R} = \frac{1}{2}(1 - jcot\frac{\delta}{2}) \tag{5.4}$$

This expression can be substituted into (5.2) to give:

$$Z_A = \frac{V_A}{I_L} = \frac{(Z_S + Z_L + Z_R)}{2}(1 - jcot\frac{\delta}{2}) - Z_S \tag{5.5}$$

The geometrical interpretation of this equation is shown below.

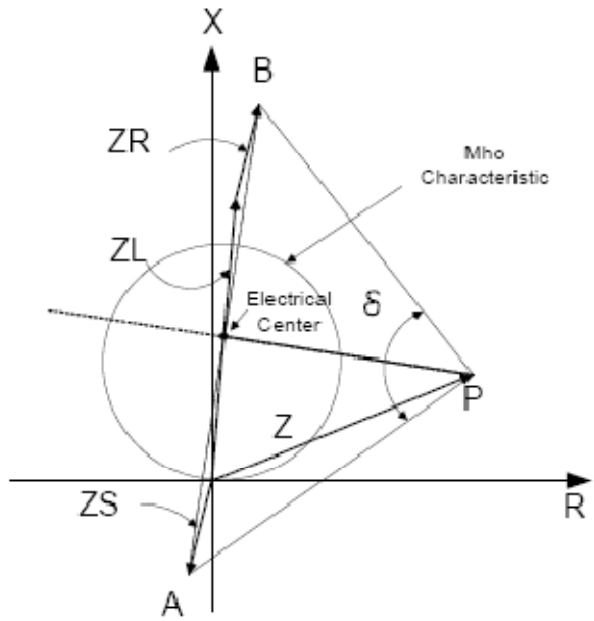

Figure 5-4: Locus of Z_A as a function of δ when k=1 (21)

Figure 5-4 shows the trajectory of the apparent impedance as seen from by the relay as a function of the angle difference between the two sources. When the magnitudes of the source voltages are equal the trajectory is a straight line. When the sources are 180^0 apart the apparent impedance is precisely at the location of the electrical center or swing center of the system. The diagram shows that if the electrical center falls on the line being protected, the impedance trajectory during a power swing will cross any relay characteristic that covers the line. Therefore, to properly separate the system during an unstable swing there must be OOS relays at the line on which the electrical center is located. There may be several electrical centers in a power system and their locations may change as the network topology and voltages magnitudes of the system changes. When the two sources are 180^0 apart the voltage magnitude at the swing center falls to zero. This fact is often used to identify the swing centers of a system through simulation.

Out-of-step tripping functions by differentiating swings from faults and also unstable swings from stable swings. Several techniques exist to do this, but it is most commonly done with the use of static boundaries or blinders and timers in an R-X plane. Figure 5-5 shows OOS relays with both concentric circles and blinders.

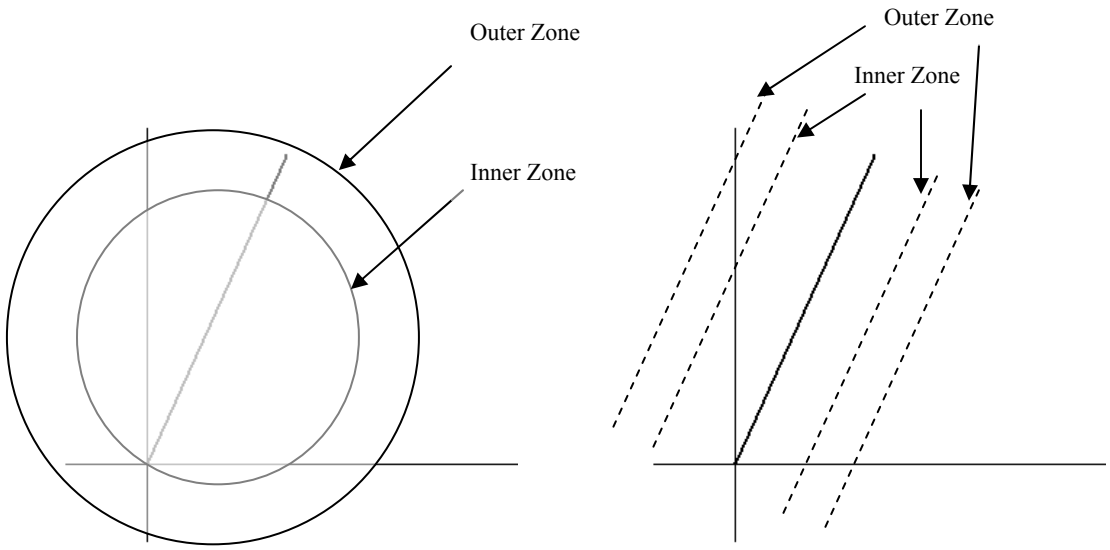

Figure 5-5: Out-of-Step Tripping Relays

The timers are used to differentiate between faults and swings. Since a fault is an electromagnetic phenomenon its trajectory will move through the inner and outer zones much faster than the trajectory of a swing. The inner zone is set so that the largest stable swing will not cross it. A large number of offline studies are required to determine the appropriate settings for the zones and timers; however, as system topology changes, generation dispatch changes, and load changes occur the settings may become obsolete and cause false trips (22). As mentioned in the previous section this problem also occurs with distance relays and loss-of-field relays, but for those relays a supervisory boundary can be implemented to trigger an alarm when encroachment

is imminent. For out-of-step relays this problem is solved by creating alarms based on known conditions for which the relay's settings are unsuitable, or by using adaptive relaying techniques.

Alarms for out-of-step relays are based on identifying conditions and contingencies that cause significant changes in the location of the swing center and hence the trajectory of the apparent impedance of an unstable swing as seen from the location of the relay. These alarms were developed and tested for out-of-step relays in the WECC system. Figure 5-6 shows the assumed characteristic of the inner zone of one of the OOS relays and the apparent impedance trajectory seen by the relay.

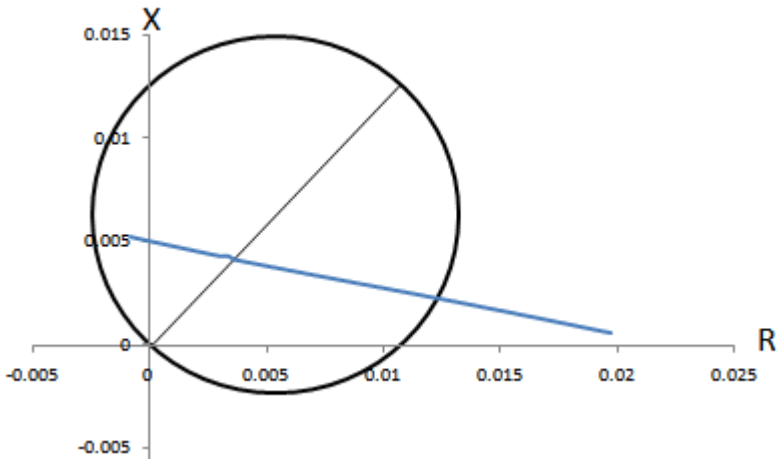

Figure 5-6: Apparent Impedance Locus for an Unstable Swing in Normal Conditions

This OOS condition was caused by a 3 phase fault on a 500kV bus followed by tripping of the entire bus within 2 cycles of the fault. The EHV buses in the WECC have either a double bus or a ring bus scheme, so for this scenario to occur in the real system one of the bus bars would have to be out-of-service prior to the fault inception so that the 500kV bus was in a single bus configuration. This may be unlikely, but most large scale power systems disturbances that are triggered by a single event occur when the system is in an unusual operating condition. Figure 5-6 shows that the apparent impedance moves directly through the trip characteristics and

crosses the line that the OOS relay is protecting. This means that the electrical center of the system lies on this line and it verifies that the OOS relay will trip correctly for this unstable swing. Observation of the voltage magnitudes during the simulation can be used to locate the electrical center/s of the system. Figure 5-7 shows the voltage magnitudes of all the EHV buses during the swing. The two buses at either end of the line that the OOS relay was located on had voltages very close to zero, which indicates that the electrical center was on the line between them. There is another bus voltage magnitude that swings close to zero so that shows that there is another electrical center in the system. Multiple swing centers are not unusual for large power systems, especially when generation and load are highly concentrated in certain areas as opposed to being more distributed.

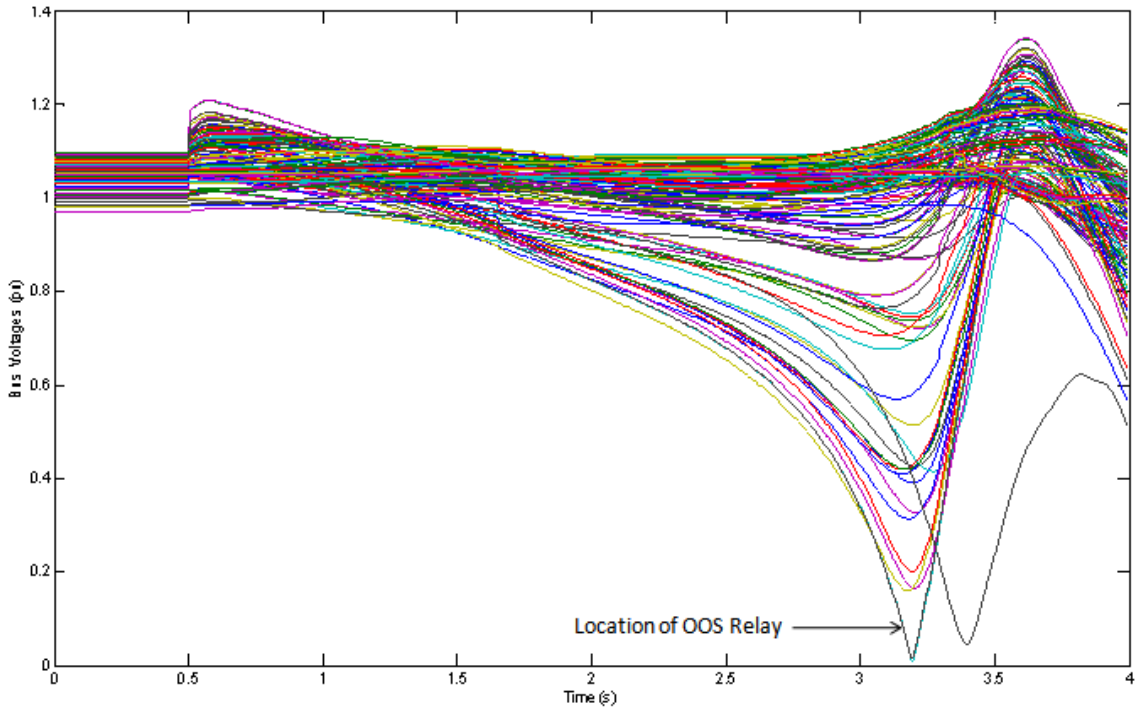

Figure 5-7: Voltage Magnitudes during OOS Condition

The same disturbance is repeated but with a major 500kV line out-of-service. The 500kV line is not connected to the same bus that the OOS relay is located at, but the outage does cause a significant reduction in power flow at the OOS relay so it is expected that the power swings should be different. The diagram below shows the locus of the apparent impedance seen by the OOS relay.

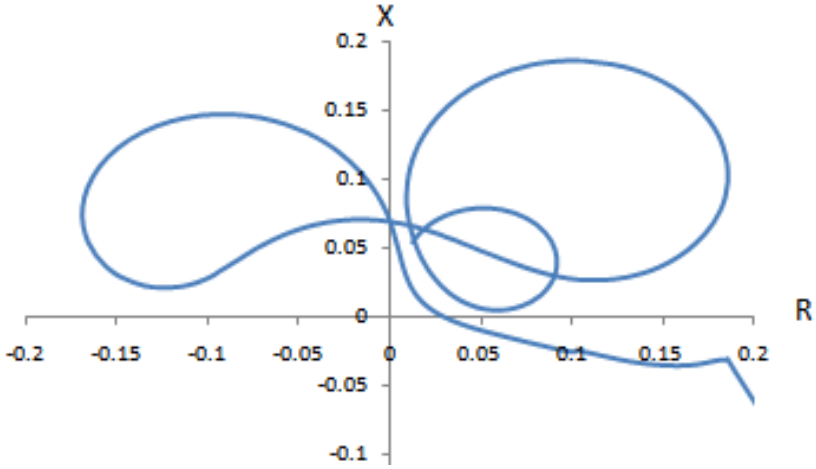

(a) Full Trajectory

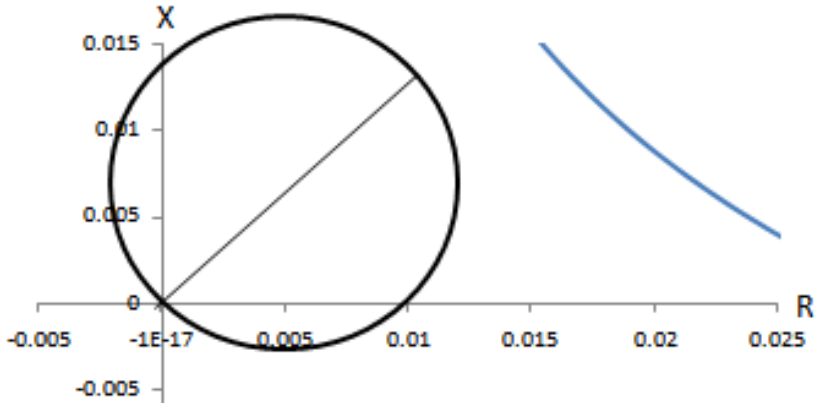

(b) Partial Trajectory Showing the OOS Relay's Trip Characteristics

Figure 5-8: Apparent Impedance Locus for an OOS Condition with a Line Out-of-Service

The figures above show the apparent impedance locus on different scales so that the entire trajectory can be observed in the first figure and the trajectory with respect to the assumed inner

boundary of an OST relay can be observed in the second figure. Figure 5-8 (a) shows that the swing is clearly unstable, yet Figure 5-8 (b) shows that the locus of the apparent impedance has changed so much that the OOS relay will fail to trip. This outage is only one of several outages that would cause this particular out-of-step relay to lose its ability to identify unstable stable swings. A list of the outages and operating conditions for which this relay will not perform correctly is generated through offline studies. Phasor measurements and SCADA can be used in real-time to detect these conditions and trigger an alarm.

Ideally, out-of-step relays should function correctly for all system conditions. However, in some cases it may be difficult to set the relays so that they perform securely and dependably for a wide range of cases. This is especially true when more serious cases such as N-1-1, N-2 and even N-3 contingencies are considered. For such cases the alarm alerts protection engineers that the OOS relay will not function properly while the system is in such a state. The protection engineer will also be provided with data from the simulation cases, an estimate of the new location of the electrical center, and recommended settings for the prevailing state.

The alternative to creating alarms to supervise OOS relays is to install adaptive relays. One of the first applications of adaptive out-of-step protection was done by Centeno and Phadke (22). Their application was based on the fact that wide area measurements of positive sequence voltage angles provide a direct path to determining system stability with real-time data. Angle swings can be observed directly and time-series extrapolation or the extended equal area criterion, if the system can be simplified to a two machine equivalent, can be used to predict the outcome of an evolving swing. Due to the slow nature of electromechanical power swings in large interconnections, it is possible to predict instability and take some form of automatic control action before the instability is fully evolved. For a completely general multi-machine

case it is difficult to assess stability by observing the angles in real-time, but with the knowledge and experience of the system gained from the current out-of-step relays, an out-of-step relay that adapts itself to changing system conditions can be designed. This system was first employed at the Florida-Georgia border. Most of Florida's load is connected to the rest of the Eastern Interconnection by long transmission lines going to the south of the state; therefore, the system can be realistically modeled as a two machine equivalent (22).

One of the first tasks in developing adaptive out-of-step relays is to create two machine model of the power system. This can be done by simulating disturbances that lead to instability and observing the coherent groups of machine angles. Several techniques exist to analytically create reduced order power systems models for stability studies; however, many of these techniques may be difficult to apply as system changes occur (23). A model of the system in the P-δ domain could be developed and used for the adaptive OOS relay. If the approximate location of the swing center is known, then the system on either side of the relay could be replaced with an equivalent machine using the techniques developed in section 3.4. Doing this will yield a value for the inertia of the two equivalent machines as well as the reactance separating them. This information along the evolving angles can be used to make a stability prediction.

5.3 Event location and identification

One of the principal applications of wide area time-synchronized measurements is for post-disturbance analysis. Post-disturbance analysis is used to identify and triangulate an event that leads to frequency or angle perturbations. This is usually a generation trip, load rejection, or a line trip. Virginia Tech's Frequency Monitoring Network (FNET) research group uses time-synchronized wide-area frequency measurements for post-disturbance analysis is real-time.

Most of their algorithms are based on the implicit assumption that the speed of electromechanical disturbance propagation is constant within an interconnection; therefore, the time delay between the occurrence of the event and the event's detection at a frequency data recorder (FDR) is directly proportional to the distance of the FDR from the location of the event (24)(25). We know from section 3.3 that this is an oversimplification. The time delay at the FDR is also a function of the event type, network topology and machine parameters. Wide-area synchronized measurements support these findings since different values for propagation speed and system inertia have been observed in different locations of the same interconnection (24). Some FNET researchers have attempted to account for the non-uniformity in the system through data analysis of previous events (26)(12). This may be an improvement on the existing techniques, but if the system conditions for which the historical data was captured are dissimilar to the current system conditions, then the results will be inaccurate. Generation trips, large load trips, and line trips each have characteristic event signatures that can be readily distinguished from each other with basic pattern recognition techniques. Therefore, the challenge usually lies in identifying the bus at which the event occurred and determining the amount of power that was tripped.

In this section a technique for locating and identifying an event that causes perturbations in angle or frequency will be developed using P-δ domain analysis. If at least one angle response is measured and the system's electromechanical properties are known and captured in a matrix of *admittances to power flow*, then this matrix can be used to calculate the change in power that is required to produce the observed response. If the event causes changes in angle that are too large for the linearized swing equation to be applicable then this technique cannot be applied. The power system is modeled as a linear system and since Y is known, if either $\Delta\delta$ or ΔP is known or

measured, the other can be readily calculated. Conceptually this can be described with the block diagrams in Figure 5-9.

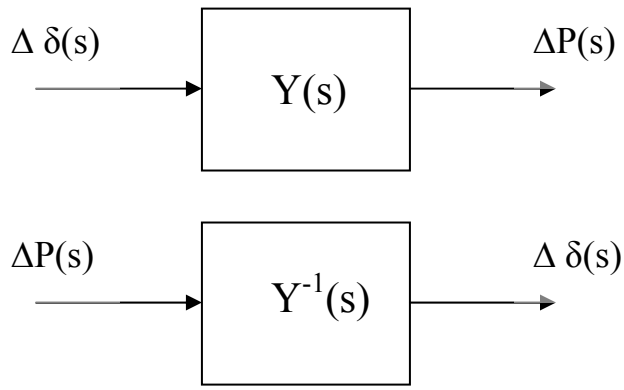

Figure 5-9: Calculating System Inputs/Outputs with the Transfer Function

This application is more complex since ΔP must be calculated from only a few measurements of Δδ instead of the entire set. The angle response of all buses corresponds to a single unique set of power injections, but the angle response of a single bus can be caused by more than one set of power injections. It will be demonstrated later in this section that the angle response of a single bus generally corresponds to very few sets of power injections if it is assumed that only one bus experiences a power injection and that the power injection is a step function. This is a reasonable assumption since large generation and load trips cause step changes in power and it is unlikely that multiple generation or load trips will occur at the same time.

Let us consider the previous example of a load trip at Bus 23 in the 18 bus system of Figure 4-1. The system diagram is shown again below for convenience. The changes in angle at Buses 1, 12, 21, 24, and 31 are recorded.

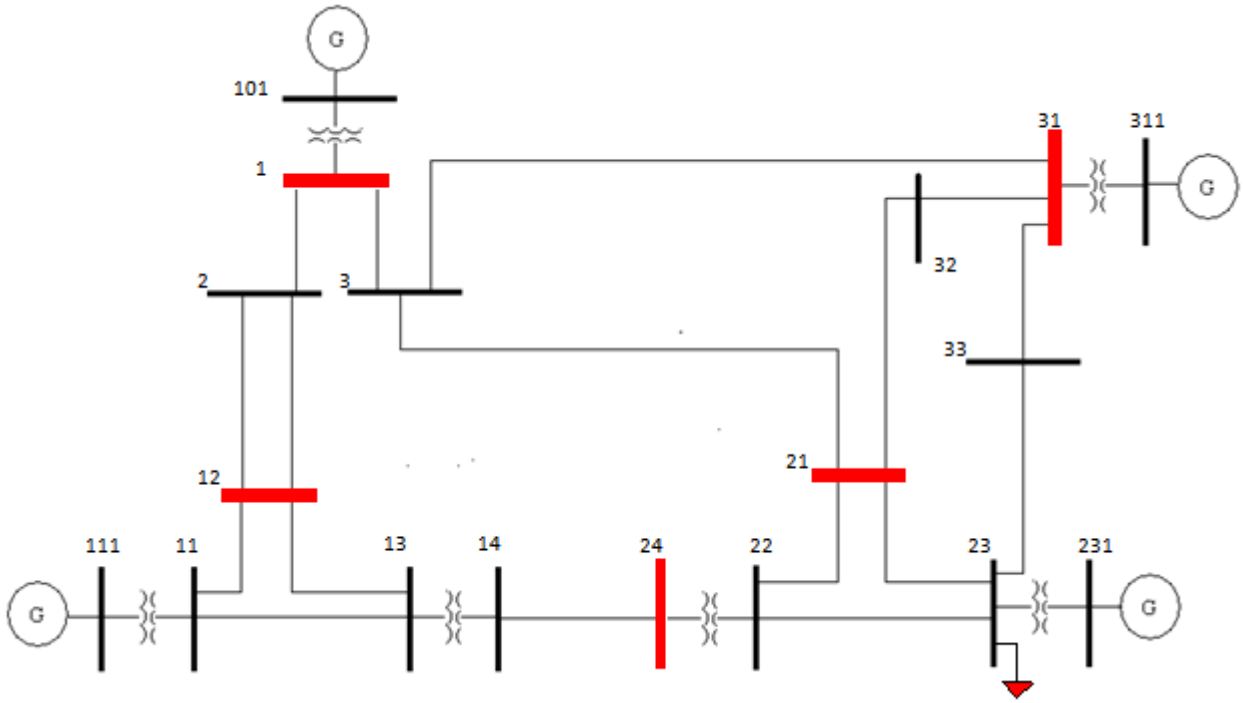

Figure 5-10: 18 Bus System with Angle Measurements

The first step is to record measurements of the angle response, $\Delta\theta(t)$, at any bus in the system excluding the buses at the swing centers. For this application the change in angle is of concern; therefore, it isn't necessary to reference the angle to any other angle in the system. The angle will have oscillations in the absence of any major event due to continuous variations in loads; additionally, there may be an angle drift if the frequency is not exactly at 60 hz. An event trigger can be used so that the event location and identification algorithm is only executed when a disturbance above a certain size occur. Event triggers for FNET applications assume that an event is characterized by a stable initial operating point, a sharp change in frequency, and a relatively stable post-disturbance operating point. The data is smoothed to remove spikes and ambient oscillations, and a moving window is used to detect an event. If the difference in pre-disturbance and post-disturbance frequency in the window exceeds a specified threshold, then an event occurred in that data window. The threshold is determined based on an estimate of the

system inertia and the minimum real power mismatch that should be detected. It is relatively easy to distinguish between generation and load trips since generation trips will cause a decrease in frequency and load trips will cause an increase. Switching events may cause either an increase or decrease in frequency, but usually the difference between the post and pre-disturbance frequencies is relatively small (27). $\Delta\theta(t)$ should contain a few periods of the angle recorded shortly after the event. It should not contain measurements before the event and it should not contain data following any subsequent events either. Angles measured at different buses do not need to be synchronized so any intelligent electronic device can be used to record the angles.

The next step is to develop an expression for $\Delta\delta(s)$ from the measured values for $\Delta\delta(t)$. It is far simpler to solve the system equations in the Laplace domain than in the time domain. The matrix pencil technique can be used to determine the eigenvalues and residuals for each frequency component in $\Delta\delta(t)$ if a sample containing a few periods of $\Delta\delta(t)$ with a sampling rate at least twice as high as the highest frequency component is recorded. In (8) Robert Gardner created a matrix pencil application to analyze frequency data recorded from FDRs in the FNET system. This application could possibly be run online. Matrix pencil outputs the eigenvalues and residuals for each sample of measured data. The tables below show the results for changes in angle measured at Buses 1, 12, 21, 24, and 31.

Table 5-1: Eigenvalues and Residuals from Matrix Pencil

(a): Eigenvalues

Bus 1	Bus 12	Bus 21	Bus 24	Bus 31
-0.0306+10.873j	-0.0366+9.200j	-0.0306+10.8729j	-0.0306+10.8729j	-0.03057+10.8729j
-0.0306-10.873j	-0.0366-9.200j	-0.0306-10.8729j	-0.0306-10.8729j	-0.03057-10.8729j
-0.0365+9.1999j	-0.0149+4.963j	-0.0366+9.1999j	-0.0366+9.1999j	-0.0365+9.1999j
-0.0365-9.1999j	-0.0149-4.9623j	-0.0366-9.1999j	-0.0366-9.1999j	-0.0365-9.1999j
-0.0149+4.962j	-0.0435+0.00j	-0.0149+4.9626j	-0.0149+4.9626j	-0.01494+4.9626j
-0.0149-4.962j	-0.0046+0.00j	-0.0149-4.9626j	-0.0149-4.9626j	-0.01494-4.9626j
-0.044+0.00j	0.0041+0.00j	-0.044+0.00j	-0.044+0.00j	-0.04405+0.00j
-0.00033+0.00j		-0.00048+0.00j	-0.000498+0.00j	-0.000179-0.00j
0.00033+0.00j		0.00048+0.00j	0.00049+0.00j	0.000178+0.00j

(b): Residuals

Bus 1	Bus 12	Bus 21	Bus 24	Bus 31
1.31-0.0092j	0.162830+0.001j	-2.456157-0.013j	-2.752676-0.014j	0.983901+0.012j
1.31+0.0092j	0.162830-0.001j	-2.456157+0.013j	-2.752676+0.014j	0.983901-0.012j
-1.227592+0.017j	3.347405+0.013j	-0.436097+0.012j	-0.410627+0.0124j	0.498616-0.0068j
-1.227592-0.017j	3.347405-0.013j	-0.436097-0.012j	-0.410627-0.0124j	0.498616+0.0068j
0.700201+0.0079j	129840.082424+0.0j	-2.277228-0.006j	-2.233454-0.0067j	-4.077384-0.01j
0.700201-0.0079j	-714272.488361-0.0j	-2.277228+0.006j	-2.233454+0.0067j	-4.077384+0.01j
123732.178910+0.0j	579356.604570-0.0j	123782.523310+0.0j	123787.641450-0.0j	123705.005775+0.0j
-8285596.935816-0.0j		-5740895.158698-0.0j	-5587441.027604+0.0j	-15340281.933247+0.0j
8151757.171462+0.0j		5607004.626188+0.0j	5453545.355163-0.0j	15206468.411122-0.0j

Note that the eigenvalues are very similar to the ones calculated in Table 4-1, but there are two additional components that correspond to the aperiodic component of the increase in bus angles. This is a rigid body mode that would not be present if referenced bus angles were used instead of absolute bus angles. This mode is the only one that has eigenvalues in the right-hand side of the real-imaginary plane. This indicates that this component will increase indefinitely unless some control, such as governor action is applied. The equations for a signal in the Laplace and time-domains from its eigenvalues and residuals are given below:

$$Y(s) = \sum_{i=1}^{n} \frac{K_i}{s-\lambda_i} \tag{5.6}$$

$$y(t) = \sum_{i=1}^{n} K_i e^{-\lambda_i t} \tag{5.7}$$

Where, n is the number of modes

K_i is the real part of the ith residual

λ_i is the ith eigenvalue

To verify (5.7) the change in angle at each of the 5 buses where the angle is recorded can be reconstructed from the eigenvalues and residuals of Table 5-1. Figure 5-11 compares the reconstructed bus angles with the original plot. The continuous lines are the original values and the dashed lines are the reconstructed values.

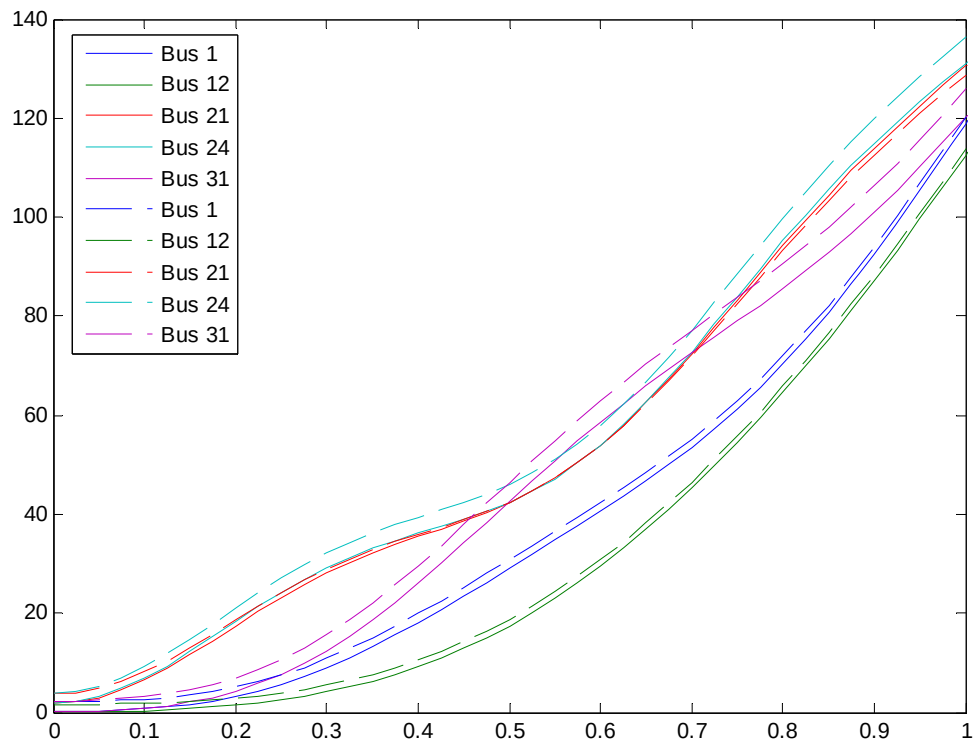

Figure 5-11: Bus Angles Constructed from Modes

The graphs show that the reconstructed bus angles are reasonably close to the original values, but due to rounding errors and errors introduced as matrix pencil filters the input data, the results aren't an exact match. In practice the errors will be even larger since there will be more noise and more modes present in the data and the computation will be more complex.

Consider the matrix equations represented in Figure 5-9:

$$[\Delta P(s)] = [Y(s)][\Delta\delta(s)] \tag{5.8}$$

$$[Y^{-1}(s)][\Delta P(s)] = [\Delta\delta(s)] \tag{5.9}$$

If it is assumed that the perturbations in angle are caused by a single step change in power at Bus j, then the matrix of power injections takes the following form:

$$\Delta P(s) = \begin{bmatrix} 0 \\ \vdots \\ 0 \\ \dfrac{\Delta P(j)}{s} \\ 0 \\ \vdots \\ 0 \end{bmatrix} = \begin{bmatrix} 0 \\ \vdots \\ 0 \\ \Delta P(j) \\ 0 \\ \vdots \\ 0 \end{bmatrix} \frac{1}{s} \tag{5.10}$$

Therefore the equations for the angle response become:

$$[Y^{-1}(s)] \begin{bmatrix} 0 \\ \vdots \\ 0 \\ \Delta P(j) \\ 0 \\ \vdots \\ 0 \end{bmatrix} \frac{1}{s} = [\Delta\delta(s)] \tag{5.11}$$

Evaluating Δδ(s) at only one location gives:

$$\Delta\delta(i,1) = \frac{{Y_{(i,j)}}^{-1}\Delta P(j,1)}{s} \tag{5.12}$$

Or

$$\Delta P(j,1) = \frac{s\Delta\delta(i,1)}{{Y_{(i,j)}}^{-1}} \tag{5.13}$$

The location of the event, Bus j, is unknown so (5.13) will have to be evaluated for every bus in the system. $\frac{\Delta P(j)}{s}$ is the power injection that is needed at Bus j to produce the change in angle, Δδ(t), at Bus i. If Bus j is the actual location of the step change in power, then ΔP(j) will be a constant equal to the amount of generation or load that was switched. For most other buses, it will be similar in size to the change in power at the actual location, but it will not be a constant. This assertion is demonstrated with the 2-machine system below:

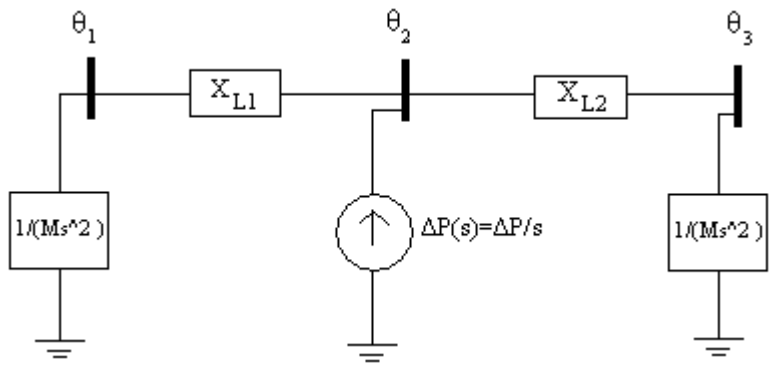

Figure 5-12: 2-Machine System for Illustrating that an Angle Response Generally Corresponds to a Unique Step Change in Power

This 2-machine system experiences a step change in power at Bus 2, where the location of Bus 2 can be varied by changing the size of the constants, X_{L1} and X_{L2}. To simplify the system the inertias of the 2 machines are equal. For a step change in power, ΔP(s), at Bus 2 the change in angle at Bus 3 can be computed with (5.14).

$$\Delta\theta_3(s) = P(s)\frac{1}{Ms^2}\frac{1 + X_{L1}Ms^2}{2 + (X_{L1} + X_{L2})Ms^2} \tag{5.14}$$

Figure 5-13 shows the location of Bus 2 for different ratios of X_{L1} and X_{L2}.

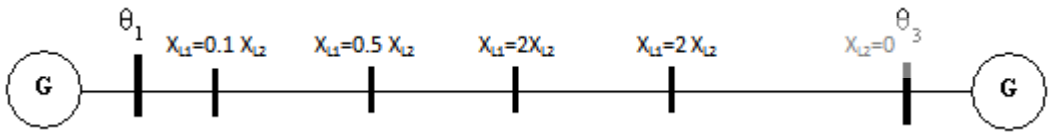

Figure 5-13: The Location of Bus 2 for different values of X_{L1} and X_{L2}

Let's compute the change in angle at Bus 3 for step changes in power at each of the locations of Bus 2 shown above.

For a change in power, P(s), when X_{L2}=0:

$$\Delta\theta_3(s) = P(s)\frac{1}{Ms^2}\frac{1 + X_{L1}Ms^2}{2 + X_{L1}Ms^2} \tag{5.15}$$

For a change in power, P(s), when X_{L1}=2 X_{L2}:

$$\Delta\theta_3(s) = P(s)\frac{1}{Ms^2}\frac{1 + X_{L1}Ms^2}{2 + 1.5X_{L1}Ms^2} \tag{5.16}$$

For a change in power, P(s), when X_{L1}= X_{L2}:

$$\Delta\theta_3(s) = P(s)\frac{1}{2Ms^2} \tag{5.17}$$

For a change in power, P(s), at when X_{L1}=0.5 X_{L2}:

$$\Delta\theta_3(s) = P(s)\frac{1}{Ms^2}\frac{1 + X_{L1}Ms^2}{2 + 3X_{L1}Ms^2} \tag{5.18}$$

For a change in power, P(s), at when X_{L1}=0.1 X_{L2}:

$$\Delta\theta_3(s) = P(s)\frac{1}{Ms^2}\frac{1 + X_{L1}Ms^2}{2 + 11X_{L1}Ms^2} \tag{5.19}$$

Next, let's compute the power injection that is needed at various locations to produce the same $\Delta\theta_3$ as a step change in power at Bus 2 when X_{L1}=2 X_{L2}.

For a step change in power, $\Delta P(s) = \frac{\Delta P}{s}$, when X_{L1} = 2X_{L2}:

$$\Delta\theta_3(s) = \frac{\Delta P}{s}\frac{1}{Ms^2}\frac{1 + X_{L1}Ms^2}{2 + 1.5X_{L1}Ms^2} \tag{5.20}$$

$$\Delta\theta_3(t) = \frac{\Delta P}{4M}\left[t^2 + 0.5X_{L1}M - 0.5X_{L1}M\cos\left(\sqrt{\frac{4}{3MX_{L1}}}t\right)\right] \tag{5.21}$$

Power needed at Bus 2 when X_{L2}=0 to produce the same response:

$$\Delta P(s) = \frac{\Delta P}{s}\left(\frac{1 + X_{L1}Ms^2}{2 + 1.5X_{L1}Ms^2}\right)\left(\frac{2 + X_{L1}Ms^2}{1 + X_{L1}Ms^2}\right) = \frac{\Delta P}{s}\frac{2 + X_{L1}Ms^2}{2 + 1.5X_{L1}Ms^2} \tag{5.22}$$

$$\Delta P(t) = \Delta P\left[1 - \frac{1}{3}\cos\left(\sqrt{\frac{4}{3MX_{L1}}}t\right)\right]u(t) \tag{5.23}$$

Power needed at Bus 2 when X_{L1}= X_{L2} to produce the same response:

$$\Delta P(s) == 2\frac{\Delta P}{s}\frac{1 + X_{L1}Ms^2}{2 + 1.5X_{L1}Ms^2} \tag{5.24}$$

$$\Delta P(t) = \Delta P\left[1 + \frac{1}{3}\cos\left(\sqrt{\frac{4}{3MX_{L1}}}t\right)\right]u(t) \tag{5.25}$$

Power needed at Bus 2 when X_{L1}= 0.5X_{L2} to produce the same response:

$$\Delta P(s) = \frac{\Delta P}{s}\left(\frac{1 + X_{L1}Ms^2}{2 + 1.5X_{L1}Ms^2}\right)\left(\frac{2 + 3X_{L1}Ms^2}{1 + X_{L1}Ms^2}\right) = \frac{\Delta P}{s}\frac{2 + 3X_{L1}Ms^2}{2 + 1.5X_{L1}Ms^2} \tag{5.26}$$

$$\Delta P(t) = \Delta P\left[1 + \cos\left(\sqrt{\frac{4}{3MX_{L1}}}t\right)\right]u(t) \tag{5.27}$$

Power needed at Bus 2 when X_{L1}= 0.1X_{L2} to produce the same response:

$$\Delta P(s) = \frac{\Delta P}{s}\left(\frac{1 + X_{L1}Ms^2}{2 + 1.5X_{L1}Ms^2}\right)\left(\frac{2 + 3X_{L1}Ms^2}{1 + X_{L1}Ms^2}\right) = \frac{\Delta P}{s}\frac{2 + 11X_{L1}Ms^2}{2 + 1.5X_{L1}Ms^2} \tag{5.28}$$

$$\Delta P(t) = \Delta P\left[1 + 6.333\cos\left(\sqrt{\frac{4}{3MX_{L1}}}t\right)\right]u(t) \tag{5.29}$$

These results show that to have the same effect as a step change in power at one location, a sinusoid in addition to a step change in power is usually required at other locations. Note that as the distance from the location of the step change increases the amplitude of the sinusoid increases.

Similar demonstrations could be used to show that there may be locations in the power system for which step changes in power at different locations produce the same angle response at another location. For example, events at equal distance away from the swing center in either direction will produce identical angle responses at the swing center. Angle measurements should never be taken near the swing center in this application. It could also be shown that for a 2-dimensional system there may be several locations that have the same equivalent *impedance to power flow* as viewed from their location. These buses are identical from an electromechanical point-of-view, so they will cause identical responses at other buses in the system. The diagram below gives an example of a 2-dimensional system for which a step change in power at three different locations, Bus 1, Bus 2, or Bus 3 would cause the same change in angle at Bus 4.

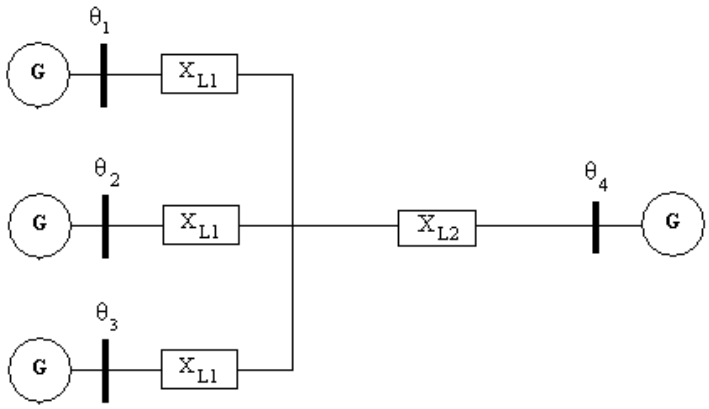

Figure 5-14: A 2-dimensional system for which the Angle Response at Bus 4 does not correspond to a unique step change in power

For Buses 1, 2, and 3 to produce the same angle response at Bus 4 the inertia of the generators attached to each bus and the electrical distance between each bus and Bus 4 must be the same. In a large interconnected system Buses 1, 2, and 3 would likely have an entire network with multiple generators connected to them, and the reactances connecting the three buses to Bus 4 would likely be a more complex network of multiple lines and machines. Hence, for a more practical system, it would be unlikely that step changes in power at Buses 1, 2, and 3 would cause identical responses at other buses electrically far away from Bus 4 even if they do produce identical responses at Bus 4. This justifies using angle measurements at multiple locations and comparing the results. Note that even if the angle at only Bus 4 was recorded, the event location algorithm would not completely fail, it would just yield 3 possible locations for the event.

So to identify the event location and the size of the power mismatch (5.13) is computed for every bus in the system and the bus at the location of the event should yield a constant value. It is unlikely that the event bus will yield a constant value since the matrix of *admittances to power flows* is not completely accurate, the angles have measurement errors, and errors are introduced while computing the Laplace transform of the angles. In practice the Y matrix may not be updated to account for the event that caused the angle perturbations, there are always significant errors associated with the measurement of dynamic variables, and Prony analysis or Matrix Pencil analysis yields will neglect many of the less significant modes while calculating the residuals and eigenvalues. Due to these errors the power injection at the location of the event will not be completely constant but it will be the closest to being constant. The location of the event can be identified by plotting the power injections of each bus and observing which one seems to be the most constant. The figure below shows the power injections that were computed using (5.13) and the angles that were measured at Bus 1.

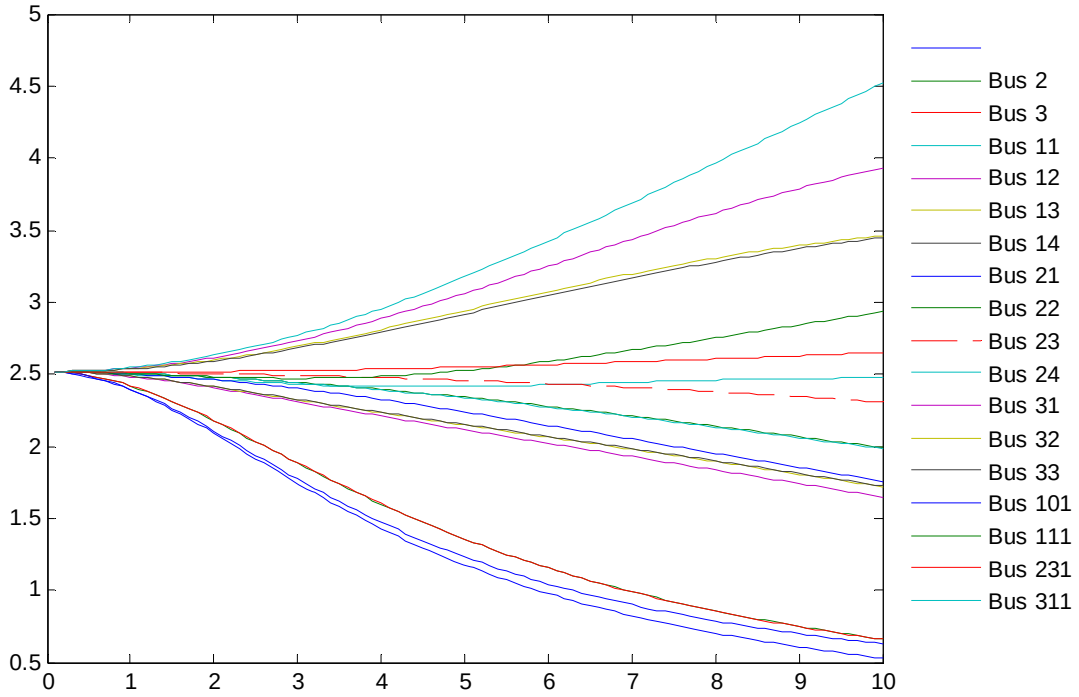

Figure 5-15: Power Injections Computed Using the PMU at Bus 1

Each curve on the graph represents the power injection in the Laplace Domain multiplied by s, which is required to produce the measured angle response at Bus 1. The graph is plotted for values of s from 0.1 to 10 since at s=0 there are discontinuities for many of the curves. Buses 23, 11, and 231 seem to show the most constant values. Note that these values are approximately 2.5 and that the actual amount of load dropped was 2.52 pu. The 3 buses that appear to be the most constant are buses 11, 23 and 231. The event occurs at Bus 23 and Bus 231 is very close to it. It is also important to observe the entire curve for the power at each bus, since some buses may appear to be constant, but might actually have a sinusoidal response. Figure 5-15 shows an example of this. With only a rudimentary observation of Figure 5-15, the power injection at Bus 11 could be mistaken as being the most constant.

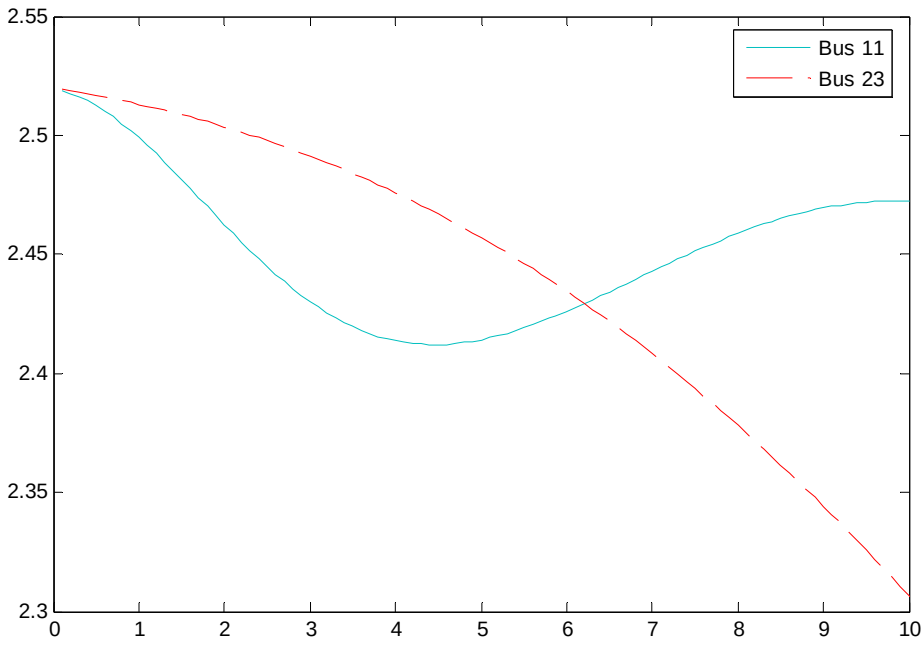

Figure 5-16: Power Injections at Bus 11 and Bus 23

This technique shows that in some situations the event can be located and identified using the change in angle at only one bus, but due to errors in the measurements, Y matrix, and the modal analysis the location of the event may be difficult to distinguish. To make this process more reliable angle measurements should be taken at multiple locations. Measurements at different buses show significantly different results for the same disturbance. The figure below shows the power injections calculated from (5.13) using angle measurements at Bus 31.

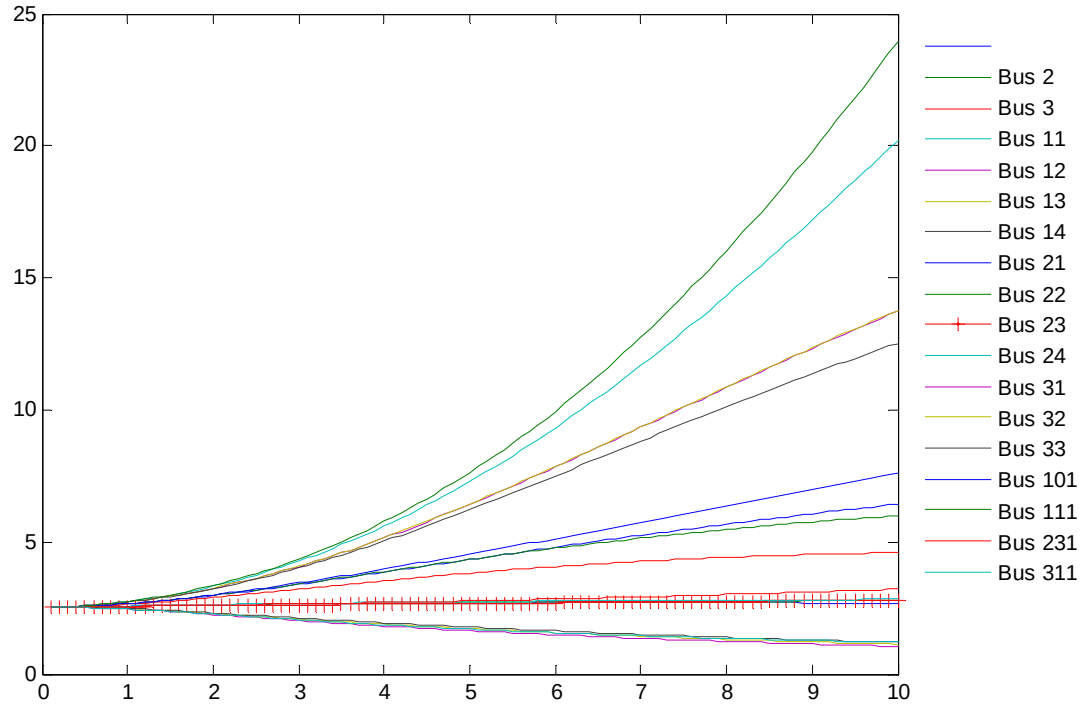

Figure 5-17: Power Injections Calculated with Measurements at Bus 31

This plot is quite different from Figure 5-15 but Bus 23, the location of the event, still appears to have a fairly constant power injection of approximately 2.5pu. The cluster of buses that is very close to Bus 23 in the diagram consists of buses that are electrically close to the Bus 23. These buses are Bus 21, 22, 24 and 231. This means that a load trip of 2.52 pu at any of these buses will produce a very similar response at Bus 31 as a load trip of 2.52pu at Bus 23. Appendix VII shows the calculated power injections from each of the 5 locations that the angle was measured at.

Graphically identifying the curve that most closely approximates a constant can be time consuming. The most constant power injection may also be identified by computing the standard deviation or the absolute change of each curve as s varies from 0.1 to 10. To consider the angle

responses from multiple locations, the median standard deviation and absolute change of each curve for each location may be computed. The table below shows the results.

Table 5-2: Absolute Change and Standard Deviation in Bus Power Injection

Bus	Mean Absolute Change	Mean Standard Deviation
1	3.289	1.067
2	3.001	0.994
3	2.133	0.717
11	10.179	3.190
12	6.905	2.237
13	6.626	2.159
14	5.469	1.814
21	0.691	0.218
22	0.692	0.215
23	0.377	0.114
24	0.840	0.263
31	2.399	0.767
32	1.581	0.524
33	1.389	0.460
101	3.999	1.267
111	12.329	3.781
231	0.278	0.086
311	2.981	0.933

Table 5-2 indicates that the event is located at Bus 231 instead of Bus 23. Bus 231 is at the low voltage side of a generator step-up transformer and Bus 23 is at the high side; therefore, the 2 buses are actually located at the same power plant. After those 2 buses the ones that yield the next lowest values are Buses 21 and 22, which are also very close Bus 23. Therefore, even if angle measurements are taken at only one location and there are inaccuracies in the measurements, it is likely that the estimated location will still be very close to the actual location.

This technique has several significant advantages over conventional event location algorithms that utilize synchronized wide-area measurements. FNET and PMU event location techniques become more accurate as the number of FDRs or PMUs that are deployed increases. Additionally, all of the angle or frequency measurements must be synchronized. This technique can produce reasonably accurate results with a very small number of unsynchronized angle measurements. Most conventional techniques do not utilize any information on the network topology or the machine parameters; instead, they implicitly assume that the system is uniformed. Event location in the power-angle domain uses the Y matrix to account for the system topology and the machine and line parameters. If the Y matrix is updated to reflect changes in the network topology, voltages, and power flows then the prevailing system conditions can be accounted for as well.

One of the major drawbacks of the P-δ domain event location algorithm is that a fairly accurate Y matrix is needed to perform the analysis. In practice the Y matrix should have only the EHV network modeled in detail and aggregate models for load and generation in the lower voltage networks should be used. It isn't necessary to model the distribution system in detail since previous research has shown that the change in angle and frequency on distribution buses closely approximates the change in angle on the transmission bus that the distribution system is attached to (28). This technique cannot be applied to a system for which the topology and machine parameters are completely unknown or when the system is severely degraded and the Y matrix is no longer accurate. As a result, PMU or SCADA measurements and signals may be needed to update the Y matrix so it matches the current system state. This algorithm utilizes the P-δ domain model so it is unsuitable for transient disturbances that are largely affected by the non-linear features of the system. It is also assumed that there are constant power loads so this

algorithm may be unsuitable for disturbances that cause significant changes in bus voltage magnitudes. Finally, this event location algorithm cannot be used when step changes in power at different buses occur at the same time or shortly after one another. This means that this algorithm cannot be used to identify line trips since that causes simultaneous step changes in power both the sending end and receiving end of the line. Additionally, major events such as prolonged faults on an EHV bus that causes multiple generators to trip immediately cannot be properly identified with this technique. It is likely that for these scenarios, there will not be any power injection curve that even closely resembles a constant.

Chapter 6 Final remarks

6.1 Conclusions

This document focused on developing the concept of electromechanical power systems analysis in the power-angle domain and proposing applications based on this technique. It is shown that electromechanical transient analysis is more complex than electromagnetic transient analysis since electromagnetic phenomena tend to be localized and the parameters of the transmission lines are continuously distributed with distance. Conventionally, time-domain simulations are used to analyze the electromechanical response of a system. The continuum model and state-space analysis are two other techniques that are useful for electromechanical analysis; however, they both have their drawbacks. The power-angle domain model is introduced as a new technique that is especially suitable for applications relating to power system electromechanical phenomena, such as developing equivalents and locating and identifying events.

Power-angle domain analysis requires that the system be operated in the linear region, all loads are assumed to be constant power loads, and the system is fairly idealized since transmission line losses, shunt capacitances, and machine controls are neglected. Because of these assumptions, power-angle domain analysis may be used to give an approximation of the system's response and detailed time-domain simulations should be used for more accurate results.

The power-angle domain model is not ideal for analyzing electromechanical traveling waves since it uses a lumped discrete model instead of a continuous model. For a practical system it may not be possible to develop a closed loop expression for the propagating disturbance since

that expression would have to include parameters from every machine in the system and the connecting lines. However, it is possible to show that the speed and size of the wave are affected by the machine inertias, line impedances, and the distance from the location of the event. Power-angle domain analysis is ideal for developing electromechanical equivalents for stability studies. Examples of equivalents in both a simple one-dimensional system and the IEEE-14 bus system showed that the overall dynamic characteristics of the system were retained with the equivalent.

P-δ domain analysis cannot be used to simulate major contingencies, but several indices can be developed to indicate how stable a system is for the prevailing conditions. The synchronizing power coefficient measures small-signal stability; whereas, the critical clearing time and the critical energy provide an indication of the margin of transient stability. These indices can be used for contingency screening. Relatively high stability indices indicate that the system will be able to maintain stability following small-signal or transient events. The last application that was proposed for the P-δ domain model was an event location and identification algorithm. This application is unlike other event location algorithms since it accounts for the network topology and the parameters of the machines and lines. Another significant advantage of this technique is that only a few unsynchronized measurements are needed. Such a technique may be useful in systems that do not have a reliable communication infrastructure or for organizations that do not have access to real-time wide area data.

This document also described alarms to supervise distance, over-excitation, and out-of-step tripping relays. This application is more practical than many of the other applications developed in this research and there is currently an ongoing project to develop and deploy these alarms in California. Unlike many real-time protection and control applications, this application does not automatically change the settings of any protection or control devices. Instead, it provides

information and recommendations on a developing problem to a protection engineer and allows him to make the final decision.

6.2 Contributions

The main contributions of this work are listed below:

- Power-angle domain model development
- Applications for the power-angle domain model
- Alarms for supervising relay trip characteristics

Power-angle domain analysis is not a completely new concept, but in this research the concept was developed in far more detail than other published documents. Much of the ideas described here were inspired by state-space analysis for power systems, but the application of circuit analysis techniques to power systems electromechanical phenomena is a new concept. The development of equivalents for stability studies, modal analysis, and stability indices using P-δ domain modeling are all new concepts as well. The event location and identification algorithm is a particularly novel idea since all previous algorithms require a large number of measurement devices to be deployed throughout the system. This algorithm is one of the first to capture the system's electromechanical behavior in a matrix and use that in event location. The alarms for relay supervision are part of a larger research project for California. Some digital relays have built in functions to perform some of these applications, but in this project PMUs are used to monitoring and supervise both digital relays and electromechanical relays. Since there are still a large number of electromechanical relays deployed in North America the alarms will provide a engineers and technicians with data that may not be available otherwise. Excluding section 3.6, which was based heavily off a similar discussion for state-space analysis, and portions of section

5.1, which was based off previous research on the continuum model, chapters 3, 4, and 5 are my contributions to this field of study.

6.3 Proposed future work

The concepts and applications developed in this research are related to wide area monitoring since they rely on detecting the prevailing system state to optimize engineering activities. The power-angle domain uses wide area phasor measurements to update a linearized model of the system, which can then be used to optimize protection and operation engineering activities. In future research this technique could be improved by modeling the system in more detail and accounting for generator control systems. It would also be very beneficial to demonstrate some of these techniques on a real system. The event location and identification technique is particularly intriguing, but it is still unknown whether it can produce accurate results in a real system with real angle measurements.

Computing the inverse of a matrix is computationally intensive, but the matrix of *admittances to power flow* will be quite sparse, so matrix sparsity techniques may be useful in simplifying the calculations. In conventional power systems network analysis the bus impedance matrix is rarely computed by inversion of the admittance matrix; instead it is built through observation of the network. It is also possible to directly modify the impedance matrix when components are added or removed (18). In future research the inverse of the admittance matrix should be computed using similar algorithms. This may enable power-angle domain analysis to be developed for larger systems.

REFERENCES

1. **J. Arrillaga, N.R Watson.** *Computer Modeling of Electrical Power Systems.* 2nd Edition. s.l. : Wiley, 2001.

2. **Kundur, Prabha.** *Power System Stability and Control.* s.l. : McGraw-Hill, 1993. 0-07-035958-X.

3. **Hathaway.** *Telefault TWS Operations Manual.* Belfast : Qualitrol Hathaway Instruments, 2004.

4. **James Thorp, Charles Seyler, Arun Phadke.** Electromechanical Wave Propagation in Large Electric Power Systems. *IEEE Transactions on Circuits and Systems.* June, 1998, Vol. 45, 6.

5. *Comanche peak unit no. 2 100% load rejection test - underfrequency and system phasors measured across TU electric system.* **Faulk, D. and Murphy, R.J.** College Station : Procedures of the Annual Conference of Protective Relay Engineers, 1994.

6. *Power System Disturbance Monitoring.* **Murphy, R.J.** Spokane : Western Protective Relay Conference, 1994.

7. **Phadke, A.G and Thorp, J.S.** *Synchronized Phasor Measurements and Their Applications.* New York : Springer, 2008.

8. **Gardner, Robert.** *A Wide-Area Perspective on Power System Operation and Dynamics.* Blacksburg, Virginia : Virginia Tech, 2008.

9. **Manu Parashar, James Thorp, Charles Seyler.** Continuum Modelling of Electromechanical Dynamics in Large-Scale Power Systems. *IEEE Transactions on Circuits and Systems.* September, 2004, Vol. 51, 9.

10. **Huang, Liling.** *Electromechanical Wave Propagation in Large Electric Power Systems.* Blacksburg : Virginia Tech, 2003.

11. **Anderson, P.M and Fouad, A.A.** *Power System Control and Stability.* Ames : Iowa State University Press, 1977.

12. **Baldwin, Mark.** *Modal Analysis Techniques in Wide-Area Frequency Monitoring Systems.* Blacksburg : Virginia Tech, 2008.

13. **Ross, S.L.** *Introduction to Ordinary Differential Equations.* New York : Wiley, 1989.

14. **Stevenson, W.D.** *Elements of Power System Analysis.* New York : McGraw-Hill, 1982.

15. **Pavella, M. and Murthy, P.G.** *Transient Stability of Power Systems.* West Sussex : John Wiley & Sons Ltd., 1994.

16. **Armando, Llamas.** *Assessment of Direct Methods in Power System Transient Stability Analysis for Online Applications.* Blacksburg : Virginia Tech, 1992.

17. **Bernabeu, Emanuel.** *Methodology for a Security/Dependability Adaptive Protection Scheme based on Data Mining.* Blacksburg : Virginia Polytechnic Institute and State University, 2009.

18. **Saadat, Hadi.** *Power System Analysis.* s.l. : McGraw-Hill, 2002. ISBN.

19. **Graham, Rogers.** Demystifying Power System Oscillations. *IEEE Computer Applications in Power.* June, 1996.

20. **Horowitz, Stanley H. and Phadke, G. Arun.** *Power System Relaying.* Bladock : Research Studies Press, 1995.

21. **D6, IEEE PSRC WG.** *Power Swing and Out-of-Step Considerations on Transmission Lines.* s.l. : IEEE Power Engineering Society, 2005.

22. **Centeno, Virgilio Antonio.** *Adaptive Out-of-Step Relaying with Phasor Measurement.* Blacksburg : Virginia Tech, 1995.

23. **Anderson, Sharon Lee.** *Reduced Order Power System Models for Transient Stability Studies.* Blacksburg : Virginia Tech, 1993.

24. *Study of Global Frequency Dynamic Behavior of Large Power Systems.* **Tsai, S., et al.** s.l. : IEEE PSCE, 2004.

25. *Non-parametric Power System Event Location Using Wide-Area Measurements.* **Gardner, R.M, et al.** Atlanta : IEEE PSCE, 2006.

26. *Generator Trip Identification Using Wide-Area Measurements and Historical Data Analysis.* **Bank, J.N, et al.** Atlanta : IEEE PSCE, 2006.

27. *Visualization and Classification of Power System Frequency Data Streams.* **Bank, Jason, Omitaomu, Olufemi and Liu, Yilu.** San Jose : IEEE International Conference on Data Mining, 2009.

28. *Estimating the Speed of Frequency Disturbance Propagation Through Transmission and Distribution Systems.* **Arana, AJ, et al.** Atlanta : IEEE PSCE, 2006.

APPENDIX I: The center of inertia and equivalent inertia

```
%Code to calculate the center of inertia;
%Node switching and reduction to calculate the distance of every machine in the system to be
%equivalenced to a node on the border of the system.

load Ybus                       %Node 1 should be outside the area to be equivalenced
load H;                         %Column array with machine inertias
a=length(Y);
ref=2;                          %Set the reference bus
Jx=0;                           %Initialize the variable representing inertia * reactance

%Set the reference node as bus 1
i=1;                             %Switch with node 1

%Node switching
x=1;                            %counter for rows
y=1;                            %counter for columns
Ynew=Y;
for x=1:1:a
        for y=1:1:a
                if ((x==i) & (y==i))                    %if i'm on a diagonal
                        Ynew(x,y)=Y(ref,ref);
                 elseif ((x==ref) & (y==ref))           %if i'm on a diagonal
                        Ynew(x,y)=Y(i,i);
                 elseif ((x==i) & (y==ref))
                        Ynew(x,y)=Y(ref,i);
                elseif ((x==ref) & (y==i))
                        Ynew(x,y)=Y(i,ref);
                elseif (x==i)
                        Ynew(x,y)=Y(ref,y);
                elseif (x==ref)
                        Ynew(x,y)=Y(i,y) ;
                elseif (y==i)
                        Ynew(x,y)=Y(x,ref);
                elseif (y==ref)
                        Ynew(x,y)=Y(x,i);
                end
        end
        Hnew(i)   = H(ref);                             %Switch the inertias
        Hnew(ref) = H(i);                               %Switch the inertias
end


%Find the distance between node 1 and each machine
i=2;                                                    %Always switch with node 2
for j=2:1:a                                             %Switch each node one at a time
        if (j>2)                                        %Avoid trying to switch node 2 with itself
                %Node switching
```

```
            x=1;                                    %counter for rows
            y=1;                                    %counter for columns
            Ynew=Y;
            for x=1:1:a
                for y=1:1:a
                    if ((x==i) & (y==i))            %if i'm on a diagonal
                        Ynew(x,y)=Y(j,j);
                    elseif ((x==j) & (y==j))        %if i'm on a diagonal
                        Ynew(x,y)=Y(i,i);
                    elseif ((x==i) & (y==j))
                        Ynew(x,y)=Y(j,i);
                    elseif ((x==j) & (y==i))
                        Ynew(x,y)=Y(i,j);
                    elseif (x==i)
                        Ynew(x,y)=Y(j,y);
                    elseif (x==j)
                        Ynew(x,y)=Y(i,y) ;
                    elseif (y==i)
                        Ynew(x,y)=Y(x,j);
                    elseif (y==j)
                        Ynew(x,y)=Y(x,i);
                    end
                end
            end
        end

        %Node reduction
        K=Ynew(1:2,1:2);
        L=Ynew(1:2,3:b);
        M=Ynew(3:b,3:b);
        Yred=K-L*inv(M)*L'

        %Calculation of the center of inertia
        Jx = Jx + 1/Yred(1,:2)*H(j);     %Find the sum of all Jx's divided by the sum of all M
end

%Distance from node 1 to the center of inertia
dist=Jx/sum(H)                           %Reactance between the referenc bus and center of inertia

clear D K L M a b i j x y s Ynew Yred
```

APPENDIX II: The IEEE-14 Bus system and matlab code to simulate a load trip

Bus Data

Bus No.	P Generated (pu)	Q Generated (pu)	P Load (pu)	Q Load (pu)	Bus Type	Q Generated Max (pu)	Q Generated Min (pu)
1	2.32	0	0	0	2	10	-10
2	0.4	-0.424	0.217	0.127	1	0.5	-0.4
3	0	0	0.942	0.19	2	0.4	0
4	0	0	0.478	0	3	0	0
5	0	0	0.076	0.016	3	0	0
6	0	0	0.112	0.075	2	0.24	-0.06
7	0	0	0	0	3	0	0
8	0	0	0	0	2	0.24	-0.06
9	0	0	0.295	0.166	3	0	0
10	0	0	0.09	0.058	3	0	0
11	0	0	0.035	0.018	3	0	0
12	0	0	0.061	0.016	3	0	0
13	0	0	0.135	0.058	3	0	0
14	0	0	0.149	0.05	3	0	0

Branch Data

From Bus	To Bus	Resistance (pu)	Reactance(pu)	Line Charging (pu)	Tap Ratio
1	2	0.01938	0.05917	0.0528	1
1	5	0.05403	0.22304	0.0492	1
2	3	0.04699	0.19797	0.0438	1
2	4	0.05811	0.17632	0.0374	1
2	5	0.05695	0.17388	0.034	1
3	4	0.06701	0.17103	0.0346	1
4	5	0.01335	0.04211	0.0128	1
4	7	0	0.20912	0	0.978
4	9	0	0.55618	0	0.969
5	6	0	0.25202	0	0.932
6	11	0.09498	0.1989	0	1
6	12	0.12291	0.25581	0	1
6	13	0.06615	0.13027	0	1

7	8	0	0.17615	0	1
7	9	0	0.11001	0	1
9	10	0.03181	0.0845	0	1
9	14	0.12711	0.27038	0	1
10	11	0.08205	0.19207	0	1
12	13	0.22092	0.19988	0	1
13	14	0.17093	0.34802	0	1

Generator Data

Generator Bus no.	1	2	3	4	5
MVA	615	60	60	25	25
xl (pu)	0.2396	0	0	0.134	0.134
ra (pu)	0	0.0031	0.0031	0.0014	0.0041
xd (pu)	0.8979	1.05	1.05	1.25	1.25
x′d (pu)	0.2995	0.185	0.185	0.232	0.232
x″d (pu)	0.23	0.13	0.13	0.12	0.12
T′do	7.4	6.1	6.1	4.75	4.75
T″do	0.03	0.04	0.04	0.06	0.06
xq (pu)	0.646	0.98	0.98	1.22	1.22
x'q (pu)	0.646	0.36	0.36	0.715	0.715
x''q (pu)	0.4	0.13	0.13	0.12	0.12
T′qo	0	0.3	0.3	1.5	1.5
T″qo	0.033	0.099	0.099	0.21	0.21
H	5.148	6.54	6.54	5.06	5.06
D	2	2	2	2	2

simulate_loadtrip_ieee14.m

```
%Code to simulate load switching at Bus 2 in the IEEE-14 bus system
%The size of each machine is increased by a factor of 10.
%M=2H/w, where H is refered to the system base.
%H_new=H_old*Smachine/100, D=0.02pu;
%Xg is refered to the system base. X_new=X_old*100/Smachine;

syms s;
%Load trip of 21.7 MW at Bus 2
P=[0;0.217/s;0;0;0;0;0;0;0];
%Input the Y matrix
Y=[21.38+1/(0.0049+1/(1.6796*s^2+2/377*s)),-16.9,0,0,-4.48,0,0,0,0; -16.9,
33.37+1/(0.0308+1/(0.208*s^2+2/377*s)),-5.05,-5.67,-5.75,0,0,0,0; 0, -5.05,
10.9+1/(0.0308+1/(0.208*s^2+2/377*s)),-5.85,0,0,0,0,0; 0,-5.67,-5.85,41.9,-23.8,0,-4.78,0,-1.8;-4.48,-
5.75,0,-23.8,38,-3.97,0,0,0;0,0,0,0,-3.97,7.42+1/(0.0928+1/(0.067*s^2+2/377*s)),0,0,-3.45;0,0,0,-
```

```
4.78,0,0,19.55,-5.68,-9.09;0,0,0,0,0,0,-5.68,5.68+1/(0.0928+1/(0.067*s^2+2/377*s)),0;0,0,0,-1.8,0,-3.45,-
9.09,0,14.3];
%initial voltage magnitudes
V=[1.06;1.045;1.01;1.0237;1.0281;1.0386;1.0461;1.0851;1.0349];
%Initial voltage angles
Initial_Angles=[0;-4.97;-12.68;-10.38;-8.76;-14.62;-13.66;-13.66;-15.36;];

%Account for the initial conditions
angles=zeros(9);
for x=1:1:9
        for y=1:1:9
                angles(x,y)=cosd(Initial_Angles(x)-Initial_Angles(y));
        end
end
alpha=V*V'.*angles;                             %Compute alpha
Ylines=Y-diag(diag(Y));                         %Remove the diagonal elements from Y
Ygen=diag(Y)+sum(Ylines,2);                     %Find generator admittances to power flow
Ynew=alpha .* Ylines;                           %Multiply line impedances to power flow by alpha
Ynew=Ynew + diag(Ygen) - diag(sum(Ynew,2));     %Fill in the diagonals
theta=inv(Ynew)*P;
thetat=ilaplace(theta);

%Plot results
angle=[];
time=[];
syms t;
for i=0:0.01:1
        a=double(subs(thetat,t,i)) * 180/pi;    %Convert from radians to degrees and add initial angle
        angle=[angle real(a)];
        time=[time; double(i)];
end
plot(time,angle)
```

APPENDIX III: The PSLF 18 bus system

Load flow data in *.cmf format

Bus data

1	NORTH-01	230	1	1	0	0.9667	-8.12	0	0	0	0	230	1	0	0	0	0	0	1
2	NORTH-02	230	1	1	0	0.9043	-21.85	334.93	0	0	0	230	1	0	0	0	0	0	2
3	NORTH-03	230	1	1	0	0.9214	-20.36	272.96	0	0	0	230	1	0	0	0	0	0	3
11	WEST--01	230	2	1	0	0.9736	-16.52	0	0	0	0	230	1	0	0	0	0	0	4
12	WEST--02	230	2	1	0	0.8858	-32.43	547.56	0	0	0	230	1	0	0	0	0	0	5
13	WEST--03	230	2	1	0	0.89	-32.39	543.53	0	0	0	230	1	0	0	0	0	0	6
14	WEST--04	500	2	1	0	0.9031	-31.58	0	0	0	0	500	1	0	0	0	0	0	7
21	SOUTH-01	230	3	2	0	0.9699	-26.17	261.58	0	0	0	230	1	0	0	0	0	0	8
22	SOUTH-02	230	3	2	0	0.9777	-24.36	0	0	0	0	230	1	0	0	0	0	0	9
23	SOUTH-03	230	3	2	0	0.9923	-21.82	252.49	0	0	0	230	1	0	0	0	0	0	10
24	SOUTH-04	500	3	2	0	0.9724	-25.13	0	0	0	0	500	1	0	0	0	0	0	11
31	EAST--01	230	4	2	0	0.9966	-23.2	1005.15	0	0	0	230	1	0	0	0	0	0	12
32	EAST--02	230	4	2	0	0.9974	-23.56	0	0	0	0	230	1	0	0	0	0	0	13
33	EAST--03	230	4	2	0	0.9981	-22.94	0	0	0	0	230	1	0	0	0	0	0	14
101	NORTH-G1	16	1	1	3	1	0	0	0	819.5	257.84	16	1	999	-999	0	0	0	15
111	WEST--G1	16	2	1	2	1	-11.61	0	0	1000	359.88	16	1	500	-500	0	0	0	16
231	SOUTH-G1	16	3	2	2	1	-17.01	0	0	500	67.18	16	1	250	-250	0	0	0	17
311	EAST--G1	16	4	2	2	1	-18.4	0	0	1000	82.51	16	1	500	-500	0	0	0	18

Branch data

1	2	1	1	1	0	0.01	0.05	0	600	0	0	0	0	0	0	0	0	0	0	0	1
1	3	1	1	1	0	0.01	0.05	0	600	0	0	0	0	0	0	0	0	0	0	0	2
2	3	1	1	1	0	0.01	0.05	0	600	0	0	0	0	0	0	0	0	0	0	0	3
2	12	1	1	1	0	0.02	0.2	0	600	0	0	0	0	0	0	0	0	0	0	0	4
2	13	1	1	1	0	0.03	0.3	0	600	0	0	0	0	0	0	0	0	0	0	0	5
3	21	1	1	1	0	0.02	0.2	0	600	0	0	0	0	0	0	0	0	0	0	0	6
3	31	1	1	1	0	0.05	0.5	0	600	0	0	0	0	0	0	0	0	0	0	0	7
11	12	2	1	1	0	0.01	0.05	0	600	0	0	0	0	0	0	0	0	0	0	0	8
11	13	2	1	1	0	0.01	0.05	0	600	0	0	0	0	0	0	0	0	0	0	0	9
12	13	2	1	1	0	0.01	0.05	0	600	0	0	0	0	0	0	0	0	0	0	0	10
14	24	2	1	1	0	0.06	0.4	0	2000	0	0	0	0	0	0	0	0	0	0	0	11
21	22	3	2	1	0	0.01	0.05	0	600	0	0	0	0	0	0	0	0	0	0	0	12
21	23	3	2	1	0	0.01	0.05	0	600	0	0	0	0	0	0	0	0	0	0	0	13
21	32	3	2	1	0	0.04	0.4	0	600	0	0	0	0	0	0	0	0	0	0	0	14
22	23	3	2	1	0	0.01	0.05	0	600	0	0	0	0	0	0	0	0	0	0	0	15

23	33	3	2	1	0	0.02	0.2	0	600	0	0	0	0	0	0	0	0	0	0	0	16
31	32	4	2	1	0	0.01	0.05	0	600	0	0	0	0	0	0	0	0	0	0	0	17
31	33	4	2	1	0	0.01	0.05	0	600	0	0	0	0	0	0	0	0	0	0	0	18
1	101	1	1	1	1	0	0.016667	0	600	0	0	0	0	1	0	1	2	0	0.51	1.5	19
11	111	2	1	1	1	0	0.008333	0	1200	0	0	0	0	1	0	1	2	0	0.51	1.5	20
13	14	2	1	1	1	0.01	0.05	0	100	0	0	0	0	1	0	1	2	0	0.51	1.5	21
22	24	3	2	1	1	0.01	0.05	0	100	0	0	0	0	1	0	1	2	0	0.51	1.5	22
23	231	3	2	1	1	0	0.016667	0	600	0	0	0	0	1	0	1	2	0	0.51	1.5	23
31	311	4	2	1	1	0	0.008333	0	1200	0	0	0	0	1	0	1	2	0	0.51	1.5	24

Dynamic data in *.dyd format

```
#   area 1 [AREA 1                    ]
models
gencc      101 "NORTH-G1"  16.00 "h1" : #9 mva=318.0000  99999.0000 99999.0000 99999.0000 99999.0000 /
 3.5000 2.0000 0.6000 0.6000 0.2000 0.2000 0.1600 0.1600 0.0000 /
 0.0001 0.0010 0.0000 -0.0500 0.0000 0.4000 0.5300 0.5000
gencc      101 "NORTH-G1"  16.00 "h2" : #9 mva=282.0000  99999.0000 99999.0000 99999.0000 99999.0000 /
 3.5000 2.0000 0.6000 0.6000 0.2000 0.2000 0.1600 0.1600 0.0000 /
 0.0001 0.0010 0.0000 -0.0500 0.0000 0.4000 0.4700 0.5000
exdc1      101 "NORTH-G1"  16.00 "h1" : #9 0.0  40.0000 0.100000 0.0 0.0 0.0 0.0 0.0 0.500000 0.050000 /
 1.000000 0.0   2.2000 0.100000   3.5000 0.400000
exdc1      101 "NORTH-G1"  16.00 "h2" : #9 0.0  40.0000 0.100000 0.0 0.0 0.0 0.0 0.0 0.500000 0.050000 /
 1.000000 0.0   2.2000 0.100000   3.5000 0.400000
ieeeg1     101 "NORTH-G1"  16.00 "h1"      101 "NORTH-G1"  16.00 "h2"  1 : #9 mwcap=600.0000  20.0000 0.500000 0.0
0.200000 0.060000 -0.500000 1.000000 0.0 0.400000 0.300000 /
 0.0   7.5000 0.230000 0.0 0.600000 0.0 0.470000 0.0 0.0 0.0 /
 0.0 0.0 0.0 0.0 0.0 0.0 0.0 0.0 0.0 0.0 /
 0.0 0.0 0.0 0.0 0.0
vmetr        3 "NORTH-03" 230.00 "1 " : #9 0.0
#   area 2 [AREA 2                    ]
models
genrou     111 "WEST--G1"  16.00 "1 " : #9 mva=1200.0000 0.0000 0.0000 0.0000 0.0000 /
 3.5000 2.0000 0.2000 0.2000 0.2000 0.2000 0.2000 /
 0.0000 0.0300 0.2900 0.0000 0.0000 0.0000 0.0000
exac1      111 "WEST--G1"  16.00 "1 " : #9 0.050000 1.000000 1.000000  40.0000 0.100000   5.0000  -5.0000 0.500000
0.200000 1.000000 /
 0.100000 0.600000 1.000000 1.000000 0.030000   2.0000 0.300000   5.0000  -5.0000
gast       111 "WEST--G1"  16.00 "1 " : #9 mwcap=1200.0000 0.050000 0.500000 0.500000   3.0000   1.5000   3.0000   1.1000
0.0 0.0 0.0 /
  99.0000  99.0000  99.0000  99.0000 0.0 1.000000 0.0 0.0 0.0 0.0 /
 0.0 0.0 0.0 0.0 0.0 0.0 0.0 0.0 0.0 0.0 /
 0.0 0.0 0.0 0.0
```

```
#   area 3 [AREA 3                    ]
models
gensal     231 "SOUTH-G1"  16.00 "1 " : #9 mva=600.0000  0.0000 0.0000 0.0000 /
 2.8000 2.0000 0.2000 0.2000 0.2000 0.2000 /
 0.0000 0.0300 0.3000 0.0050 0.0000 0.0000
exac1      231 "SOUTH-G1"  16.00 "1 " : #9 0.050000 1.000000 1.000000  40.0000 0.100000   5.0000  -5.0000 0.500000
0.200000 1.000000 /
 0.100000 0.600000 1.000000 1.000000 0.030000   2.0000 0.300000   5.0000  -5.0000
hygov      231 "SOUTH-G1"  16.00 "1 " : #9 mwcap=600.0000 0.050000 0.500000  10.0000 0.050000 0.500000 0.200000
1.000000 0.0   2.5000   1.2500 /
 0.500000 0.080000 0.0 0.0 0.0 0.0 0.0 0.0 0.0 0.0 /
 0.0 0.0 0.0 0.0 0.0 0.0 0.0 0.0 0.0 0.0 /
 1.000000 0.0 0.0 0.0 0.0 0.0 0.0 0.0  99.0000
vmetr       21 "SOUTH-01" 230.00 "1 " : #9 0.0
vmetr       24 "SOUTH-04" 500.00 "1 " : #9 0.0
fmetr       24 "SOUTH-04" 500.00 "1 " : #9 0.0
fmetr       24 "SOUTH-04" 500.00 "1 " : #9 0.050000
#   area 4 [AREA 4                    ]
models
gensal     311 "EAST--G1"  16.00 "1 " : #9 mva=1200.0000 0.0000 0.0000 0.0000 /
 2.8000 2.0000 0.2000 0.2000 0.2000 0.2000 /
 0.0000 0.0300 0.3000 0.0050 0.0000 0.0000
exac1      311 "EAST--G1"  16.00 "1 " : #9 0.050000 1.000000 1.000000  40.0000 0.100000   5.0000  -5.0000 0.500000 0.200000
1.000000 /
 0.100000 0.600000 1.000000 1.000000 0.030000   2.0000 0.300000   5.0000  -5.0000
hygov      311 "EAST--G1"  16.00 "1 " : #9 mwcap=1200.0000 0.050000 0.500000  10.0000 0.050000 0.500000 0.200000
1.000000 0.0   2.5000   1.2500 /
 0.500000 0.080000 0.0 0.0 0.0 0.0 0.0 0.0 0.0 0.0 /
 0.0 0.0 0.0 0.0 0.0 0.0 0.0 0.0 0.0 0.0 /
 1.000000 0.0 0.0 0.0 0.0 0.0 0.0 0.0  99.0000
vmetr       33 "EAST--03" 230.00 "1 " : #9 0.0
```

APPENDIX IV: Matlab code to build the Y matrix and simulate a load trip

Required Microsoft Excel Data

Buses =

1	-8.12	0.9667
2	-21.85	0.9043
3	-20.36	0.9214
11	-16.52	0.9736
12	-32.43	0.8858
13	-32.39	0.89
14	-31.58	0.9031
21	-26.17	0.9699
22	-24.36	0.9777
23	-21.82	0.9923
24	-25.13	0.9724
31	-23.2	0.9966
32	-23.56	0.9974
33	-22.94	0.9981
101	0	1
111	-11.61	1
231	-17.01	1
311	-18.4	1

Lines =

1	2	230	0.05
1	3	230	0.05
2	3	230	0.05
2	12	230	0.2
2	13	230	0.3
3	21	230	0.2
3	31	230	0.5
11	12	230	0.05
11	13	230	0.05
12	13	230	0.05
14	24	500	0.4
21	22	230	0.05
21	23	230	0.05
21	32	230	0.4
22	23	230	0.05

23	33	230	0.2
31	32	230	0.05
31	33	230	0.05

Gens =

101	318	3.5	0.0053	318	16	0.2
101	282	3.5	0.0053	282	16	0.2
111	1200	3.5	0.0053	1200	16	0.2
231	600	2.8	0.0053	600	16	0.2
311	1200	2.8	0.0053	1200	16	0.2

Tfxs =

1	101	600	230	0.1
11	111	1200	230	0.1
13	14	100	230	0.05
22	24	100	230	0.05
23	231	600	230	0.1
31	311	1200	230	0.1

<u>BuildY.m</u>

```
%Matlab code to build the matrix of admittances to power flows

%Load Microsoft excel files containing bus, line, generator, and transformer data
buses = xlsread('buses.xls');
lines = xlsread('lines.xls');
gens = xlsread('gens.xls');
tfxs = xlsread('tfxs.xls');

syms s t;                          %Initialize the laplacian operator

%Mapping of bus numbers to their internal number
for i=1:1:size(buses,1)
        for j=1:1:size(lines,1)          %Replace bus numbers in lines
                if (lines(j,1)==buses(i))
                        lines(j,1)=i;
                end
                if (lines(j,2)==buses(i))
                        lines(j,2)=i;
                end
        end
        for j=1:1:size(tfxs,1)           %Replace bus numbers in tfxs
                 if (tfxs(j,1)==buses(i))
```

```
                        tfxs(j,1)=i;
                end
                if (tfxs(j,2)==buses(i))
                        tfxs(j,2)=i;
                end
        end
        for j=1:1:size(gens,1)          %Replace bus numbers in gens
                if (gens(j,1)==buses(i))
                        gens(j,1)=i;
                end
        end
end

%Put line admittances into the Y matrix on a 230kV, 100MVA base
Y=zeros(size(buses,1));
for i=1:1:size(lines,1)
        Y(lines(i,1),lines(i,2))=Y(lines(i,1),lines(i,2))+1/(lines(i,4)*lines(i,3)^2/230^2);
end

%Put transformer admittances into the Y matrix on a 230kV, 100MVA base
%Xtrans(pu) = Xtrans(pu_old) * V^2/S * 100/230^2
for i=1:1:size(tfxs,1)
        Y(tfxs(i,1),tfxs(i,2))=Y(tfxs(i,1),tfxs(i,2))+1/(tfxs(i,5)*tfxs(i,4)^2/tfxs(i,3)*100/230^2);
end
Y = (Y + Y')*-1;                        %Get the symmetrical matrix
Y=sym(Y);                               %Must be a sym object

for i=1:1:length(Y)
   temp(i)=-sum(Y(i,:));                %Get negative of all branch admittances
end

%Put generator inertias and admittances into the Y matrix on a 100MVA base
%M= 2*H*S/(2*pi*f)/100*s^2 + D*s
%Xgen(pu) = Xgen(pu) * V^2/S * 100/230^2
for i=1:1:size(gens,1)
        M=2*gens(i,2)*gens(i,3)/(2*pi*60)/100*s^2 + gens(i,4)*s;
        %Add generator admittances to generator inertia (admittances in series)
        xg = gens(i,7)*gens(i,6)^2/gens(i,2)*100/230^2;
        igen=gens(i,1);                 %Get bus internal number for each generator
        %Add generator inertia to the diagonal of the Y matrix
        Y(igen,igen)=Y(igen,igen)+1/(1/M+xg);
end

for i=1:1:length(Y)
        Y(i,i)=Y(i,i)+temp(i);          %Add the negative of the branch admittances
end
```

simulate_load_trip.m

```
%Matlab code to simulate a load trip in the power-angle domain
%Also compute the modes of the system

%Input Microsoft Excel files with line, bus, generator, and transformer data
lines = xlsread('lines.xls');
gens = xlsread('gens.xls');
tfxs = xlsread('tfxs.xls');
buses = xlsread('buses.xls');

%%%%%%%%%%%%%%%% Initialize %%%%%%%%%%%%%%%%
Event_bus = 23;                     %External number of bus with fault, gen trip, or load trip
mag=2.52;                           %Size of load trip
P=sym(zeros(length(buses),1));      %Initially fill with zeros, must be a sym object
syms s;                             %Initialize the laplacian operator
load Ymatrix;                       %In practice this will not be computed often

%Account for the initial conditions
angles=zeros(length(Y));
for x=1:1:length(Y)
        for y=1:1:length(Y)
                angles(x,y)=cosd(buses(x,2)-buses(y,2));
        end
end
alpha=buses(:,3)*buses(:,3)'.*angles;
alpha=1./alpha;
Ytemp=Y - diag(diag(Y));            %Remove the diagonal elements of Y
sum_branches=-diag(sum(Ytemp));     %Find the sum of the branch admittances at each bus
Ytemp=Y - sum_branches;             %Diagonals modified to show only machine admittances
Ytemp= alpha .* Ytemp;              %Multiply branch and machine admittances by alpha
machines = diag(diag(Ytemp));       %Store the machine admittances
Ytemp=Ytemp - machines;             %Remove the machine admittances
sum_branches=-diag(sum(Ytemp));     %Find the sum of the branch admittances at each bus
Ytemp=Ytemp + sum_branches;         %Add in the sum of the branch admittances
Y= Ytemp + machines;

%Get modes
D=det(Y);                           %Compute the determinant
modes=solve(D,s);                   %Set the determinant equal to zero and solve
modes=double(modes)

%Simulate load trip at bus i (i is the internal number of the generator)
i = find(buses(:,1)==Event_bus);    %Get internal bus number for event
P(i)= mag/s;                        %Step change in power at Bus i

%Determine the angles
if (Plot_angles==1)
        delta=inv(Y)*P;             %Compute the angles
        deltat=ilaplace(delta);     %Take the inverse Laplace Transform
        syms t;
```

```
        angle=[];
        time=[];
        for i=0:0.025:1
                %Convert from radians to degrees and add initial angle
                a=double(subs(deltat,t,i)) * 180/pi;
                angle=[angle real(a)];                  %Build the delta(t) matrix
                time=[time; double(i)];                 %Build the time matrix
        end
        plot(time,angle)

        %Create a legend with the bus external numbers, ensure that each string has the same length
        L=[];
        for i=1:1:length(buses)
                temp = int2str(buses(i));
                if (length(temp) < 2)
                        L=[L; 'Bus ' temp '    '];
                elseif (length(temp) < 3)
                        L=[L; 'Bus ' temp '   '];
                elseif (length(temp) < 4)
                        L=[L; 'Bus ' temp '  '];
                elseif (length(temp) < 5)
                        L=[L; 'Bus ' temp ' '];
                else
                        L=[L; 'Bus ' temp];
                end
        end
        legend(L)
        legend('off')
        xlabel('Time (s)')
        ylabel('Bus Angles (deg)')
end
clear M i j D s t a mag delta L temp igen Ptrip            %Clean up workspace
```

APPENDIX V: De-trending the data and computing the FFT

Fastfft.m

```
%Remove the aperiodic components of a signal using a moving average and compute the FFT

load resultsmatrixpencil          %Load results from matrix pencil

x=angle';                         %Signal to be smoothed
tstep=time(2);                    %Record the time step
window = .1;                      %Actual window size = window+tstep
samp = window/tstep;              %Should be an even number number

%Calculate the moving median for all bus angles
for bus=1:1:size(x,2)
        for i=samp/2+1:1:length(x)-samp/2
                xnew(i,bus) = sum(x(i-samp/2:i + samp/2,bus))/(samp+1);
        end
end

%Remove the extraneous data
xnew(1:samp/2,:)=[];              %Remove the zero padding
x(1:samp/2,:)=[];                 %remove the first half window
time(1:samp/2)=[];

x(length(x)-samp/2+1:length(x),:)=[];                    %Remove the last half window
time(length(time)-samp/2+1:length(time))=[];

%Remove any remaining offsets
xdetrended=x-xnew;                %Remove the trend
temp=median(xdetrended);
for i=1:1:length(xdetrended)
        xdetrended(i,:)=xdetrended(i,:) - temp;
end

%Plot results
plot(time,xdetrended)
xlabel('Time (s)')
ylabel('Detrended Bus Angles (deg.)')
legend('Bus 1','Bus 11','Bus 14','Bus 21','Bus 31');
legend('off')
clear angle i samp tstep window x xnew temp;          %Clear unneeded variables

%Compute the FFT
N=512;
fs=40;                            %Sampling frequency used to produce data
x=xdetrended;
X=fft(x,N);
Px=X.*conj(X)/N;
```

```
f=(0:N/2)*fs/N;
plot(f,abs(X(1:N/2+1,:)));
legend('Bus 1','Bus 11','Bus 14','Bus 21','Bus 31');
legend('off')
xlabel('Frequency (hz)')
ylabel('Magnitude of the FFT (256 point, 14.5s sample)')
```

APPENDIX VI: Computing indices for stability analysis

stability_analysis.m

```
%Compute the synchronizing power coefficient, critical clearing time, and critical energy
%To do this, first calculating the center of inertia in the 18 Bus System
%The 18 bus system is used

syms s
load Ymatrix;
load lines;                     %List of lines, with the bus #s matching the rows & columns of Ymatrix
buses = xlsread('buses56.xls');     %Input Bus Data
gen_output = [8.273; 10; 5; 10];    %Line 5 & 6 out

%Trip line 5
a=lines(5+1,1);
b=lines(5+1,2);
Y(a,a)=Y(a,a)+Y(a,b);
Y(b,b)=Y(b,b)+Y(a,b);
Y(a,b)=0;
Y(b,a)=0;
%Trip line 6
a=lines(6+1,1);
b=lines(6+1,2);
Y(a,a)=Y(a,a)+Y(a,b);
Y(b,b)=Y(b,b)+Y(a,b);
Y(a,b)=0;
Y(b,a)=0;

%Account for the initial conditions
angles=zeros(length(Y));
for x=1:1:length(Y)                         %Account for angle differences
    for y=1:1:length(Y)
        angles(x,y)=cosd(buses(x,2)-buses(y,2));
    end
end
alpha=buses(:,3)*buses(:,3)'.*angles;       %Account for voltage magnitude
alpha=1./alpha;

%The generator inertias and reactances should be removed from the Y matrix.
Ytemp = Y - diag(diag(Y));                  %Remove the diagonal elements of Y
sum_branches = -diag(sum(Ytemp));           %Find the sum of the branch admittances at each bus
Ytemp = Ytemp + sum_branches;               %Diagonals modified to show only branch admittances
machines = diag(Y) - diag(Ytemp);           %Store the machine admittances
Ytemp = alpha .* (Ytemp - sum_branches);    %Consider initial conditions
Y = double(Ytemp -diag(sum(Ytemp)));

%Remove non-generator buses
Gen_buses=[];
```

```
j=1;                                        %Counter for Gen_buses
for i=1:1:length(machines)
        if (machines(i)~=0)
                Gen_buses(j)=i;
                j=j+1;
        end
end
machines=machines(Gen_buses);               %Consider only the generator buses
machines = 1./machines;                     %machines= Xg +1/(Ms^2)
xg = double(subs(machines,s,Inf));          %Remove the generator inertia
Mi = 1./(machines - xg);                    %Remove the generator reactance
Mi = double(subs(machines,s,1));            %Remove the Laplacian operator

for bus=1:1:length(Gen_buses)
        %Node Switching: set the reference node as bus 1
        ref=Gen_buses(bus);                 %Reference bus (each machine bus)
        x=1;                                %counter for rows
        y=1;                                %counter for columns
        Ynew=Y;
        For x=1:1:length(Y)
                for y=1:1:length(Y)
                        if ((x==1) & (y==1))            %if its on a diagonal
                                Ynew(x,y)=Y(ref,ref);
                        elseif ((x==ref) & (y==ref))    %if its on a diagonal
                                Ynew(x,y)=Y(1,1);
                        elseif ((x==1) & (y==ref))
                                Ynew(x,y)=Y(ref,1);
                        elseif ((x==ref) & (y==1))
                                Ynew(x,y)=Y(1,ref);
                        elseif (x==1)
                                Ynew(x,y)=Y(ref,y);
                        elseif (x==ref)
                                Ynew(x,y)=Y(1,y) ;
                        elseif (y==1)
                                Ynew(x,y)=Y(x,ref);
                        elseif (y==ref)
                                Ynew(x,y)=Y(x,1);
                        end
                end
        end
        %Update the matrices
        Y=Ynew;
        Gen_buses_tmp=Gen_buses;
        Mi_tmp=Mi;
        xg_tmp=xg;
        Gen_buses_1=find(Gen_buses==1);
        Gen_buses_ref=find(Gen_buses==ref);

        %If node 1 and ref have machines switch the machine properties
        if ((length(Gen_buses_1) > 0) & (length(Gen_buses_ref) > 0))
                Gen_buses_tmp(Gen_buses_1)=ref;
```

```
            Gen_buses_tmp(Gen_buses_ref)=[];
            Mi_tmp(Gen_buses_ref)=[];
           xg_tmp(Gen_buses_ref)=[];
end

%If node 1 but not ref has machines
 if ((length(Gen_buses_1)>0) & (length(Gen_buses_ref)==0))
           Gen_buses_tmp(Gen_buses_1)=ref;
end

%If ref but not node 1 has machines
if ((length(Gen_buses_1)> 0) & (length(Gen_buses_ref)==0))
           Gen_buses_tmp(Gen_buses_ref)=[];
           Mi_tmp(Gen_buses_ref)=[];
           xg_tmp(Gen_buses_ref)=[];
end
Gen_buses=Gen_buses_tmp;
Mi=Mi_tmp;
xg=xg_tmp;

%Find the distance between node 1 and each machine
i=2;                                %Always switch with node 2
count=0;                            %Count the number of times through the loop
Jx=0;                               %Initialize the variable representing inertia reactance
for x=1:1:length(Gen_buses)         %Switch each node that has a machine one at a time
           count=count+1;
           j=Gen_buses(count);      %Identify the node to be switched
           if (j>2)                 %Avoid trying to switch node 2 with itself
                      %Node switching
                      x=1;                %counter for rows
                      y=1;                %counter for columns
                      Ynew=Y;
                      for x=1:1:length(Y)
                                 for y=1:1:length(Y)
                                            if ((x==i) & (y==i))            %if its on a diagonal
                                                       Ynew(x,y)=Y(j,j);
                                            elseif ((x==j) & (y==j))        %if its on a diagonal
                                                       Ynew(x,y)=Y(i,i);
                                            elseif ((x==i) & (y==j))
                                                       Ynew(x,y)=Y(j,i);
                                            elseif ((x==j) & (y==i))
                                                       Ynew(x,y)=Y(i,j);
                                            elseif (x==i)
                                                       Ynew(x,y)=Y(j,y);
                                            elseif (x==j)
                                                       Ynew(x,y)=Y(i,y) ;
                                            elseif (y==i)
                                                       Ynew(x,y)=Y(x,j);
                                            elseif (y==j)
                                                       Ynew(x,y)=Y(x,i);
                                            end
```

```
                    end
                end
            end
            %Node reduction
            K=Ynew(1:2,1:2);
            L=Ynew(1:2,3:length(Y));
            M=Ynew(3:length(Y),3:length(Y));
            Yred=K-L*inv(M)*L';
            %Calculation of the center of inertia
            1/Yred(1,2);
            bus;
            %Find the sum of all Jx's divided by the sum of all M;
            Jx = Jx + (xg(count)-1/Yred(1,2))*Mi(count);
        end

        %Calculate the synchronizing power coefficient
        dist=Jx/sum(Mi);                        %dist between the reference bus and center of inertia
        Ps(bus)=1/dist;                         %Ps between the reference bus and center of inertia
        bus_num(bus)=buses(Gen_buses(bus),1);   %Get the bus external number
        delta = atan(gen_output(bus)/Ps(bus));  %Angle between gen and equivalent

        %Calculate the critical clearing time
        delta_cr = acos((pi-2*delta)*sin(delta) - cos(delta));
        t_cr(bus) = sqrt(2*Mi(bus)*(delta_cr - delta)/gen_output(bus));

        %Calculate the critical energy
        Pmax(bus) = sqrt(gen_output(bus)^2+ Ps(bus)^2);
        dec_energy(bus) = 2*Ps(bus) - gen_output(bus)*(pi - 2*delta);
        acc_energy(bus) = Ps(bus) - Pmax(bus) + gen_output(bus)*delta;
    critical_energy(bus) = min(dec_energy(bus),acc_energy(bus));
end
results = [bus_num' Mi Ps' critical_energy' t_cr']
```

APPENDIX VII: Event location and identification algorithm and results

event_location.m

```
%Algorithm to estimate the location of a disturbance based using analysis
%in the power-angle domain

syms s;                                 %Initialize the Laplacian operator

load Rresidual.dat;                     %Textfile with residuals from matrix pencil
load Reig.dat;                          %Textfile with real part of eigenvalues
load Ieig.dat;                          %Textfile with imaginary part of eigenvalues
load ave;                               %Median of signal
load initial;                           %Initial value of signal not needed if changes in angle are used
eigenvalues = Reig + j* Ieig;
residual=Rresidual;

%Find delta(s)
for i=1:1:size(residual,2)
        j=1;
        while ((j <= size(residual,1)) & (residual(j,i) ~= 0))
                if (j==1)
                        delta1(i,1)=residual(j,i)/(s - eigenvalues(j,i));
                else
                        delta1(i,1)=delta1(i) + residual(j,i)/(s - eigenvalues(j,i));
                end
                j=j+1;
        end
end
delta1 = delta1 - initial'/s;           %Not needed if changes in angle are used
load invYmatrixD;                       %Load the inverse Y matrix
pmu = [1;5;8;11;12];                    %Buses with PMUs at them
S = 0.1:0.1:10;                         %Variable to plot power injection against

%Create a legend with the bus external numbers, ensure that each string has the same length
L=[];
buses = xlsread('buses.xls');           %Load excel file with bus data
for i=1:1:length(buses)
        temp = int2str(buses(i));
        if (length(temp) < 2)
                L=[L; 'Bus ' temp '    '];
        elseif (length(temp) < 3)
                L=[L; 'Bus ' temp '   '];
        elseif (length(temp) < 4)
                L=[L; 'Bus ' temp '  '];
        elseif (length(temp) < 5)
                L=[L; 'Bus ' temp ' '];
        else
                L=[L; 'Bus ' temp];
```

```
        end
end
for x=1:1:length(pmu)                          %Scroll through all PMU buses
        i=pmu(x);                              %no. for PMU bus
        for y=1:1:length(iY)                   %Scroll through all buses
                temp=s*delta1(x)/iY(i,y);
                P(y,:)=double(subs(temp,s,S))*pi/180;          %Variable to plot in the s domain
                Abs_change(y,x)=P(y,length(P))-P(y,1);         %Compute absolute change
                Std_dev(y,x)=std(P(y,:));                      %Compute standard deviation
        end
end
Abs_change = mean(abs(Abs_change),2)                           %Print the mean change
Std_dev = mean(Std_dev,2)
clear Ieig L Reig Rresidual S ave buses delta1 eigenvalues i iY initial j residual s temp x y pmu
```

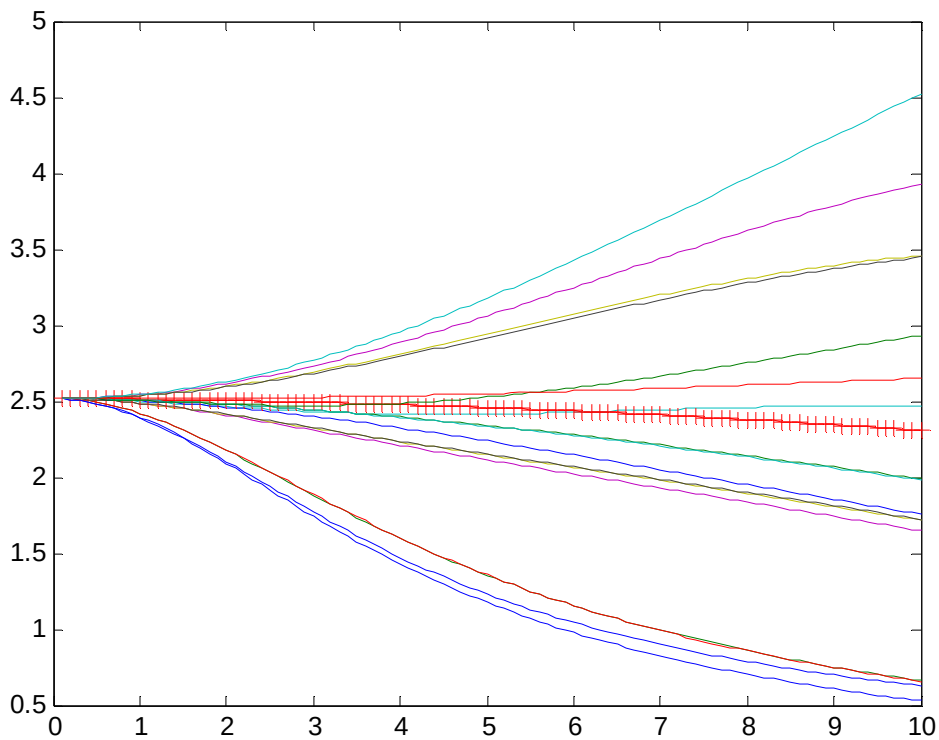

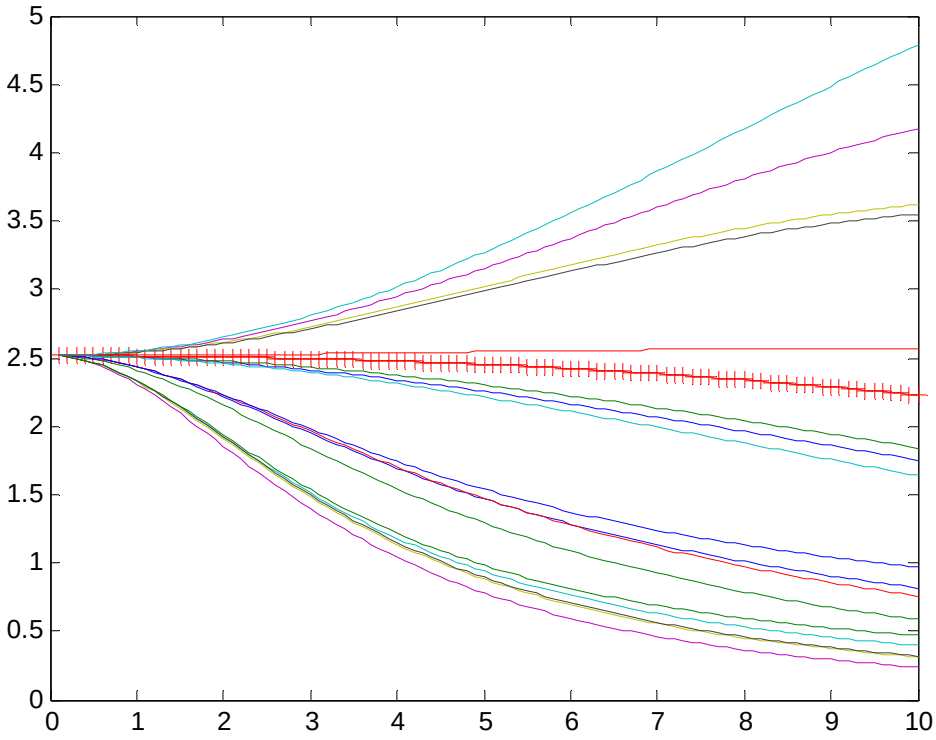
5
4.5
4
3.5
3
2.5
2
1.5
1
0.5
0
0
1
2
3
4
5
6
7
8
9
10

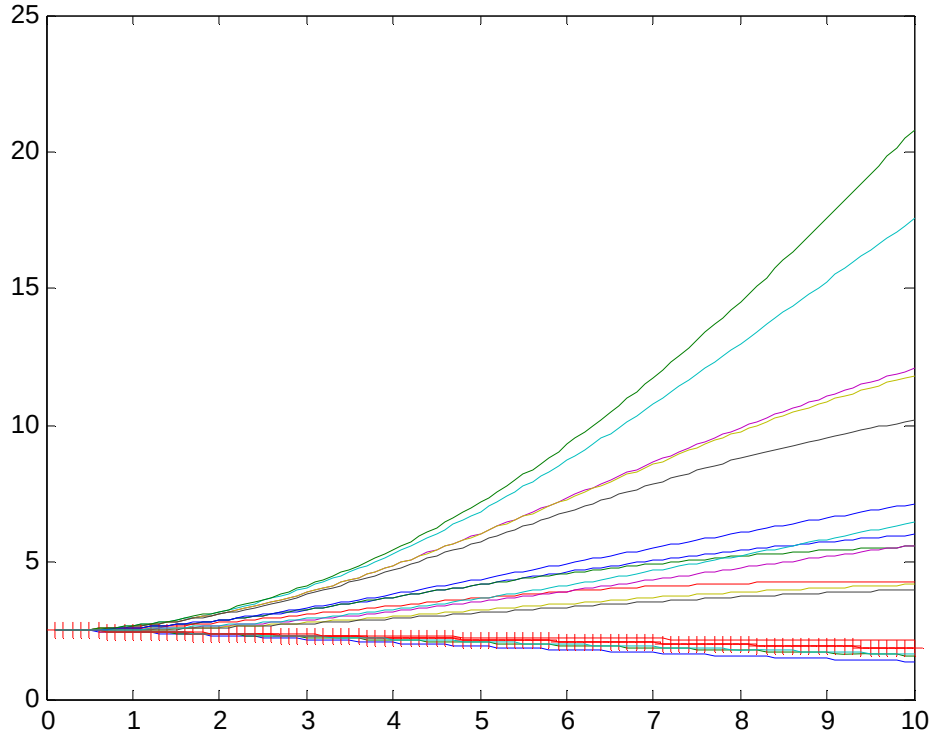
25
20
15
10
5
0
0
1
2
3
4
5
6
7
8
9
10

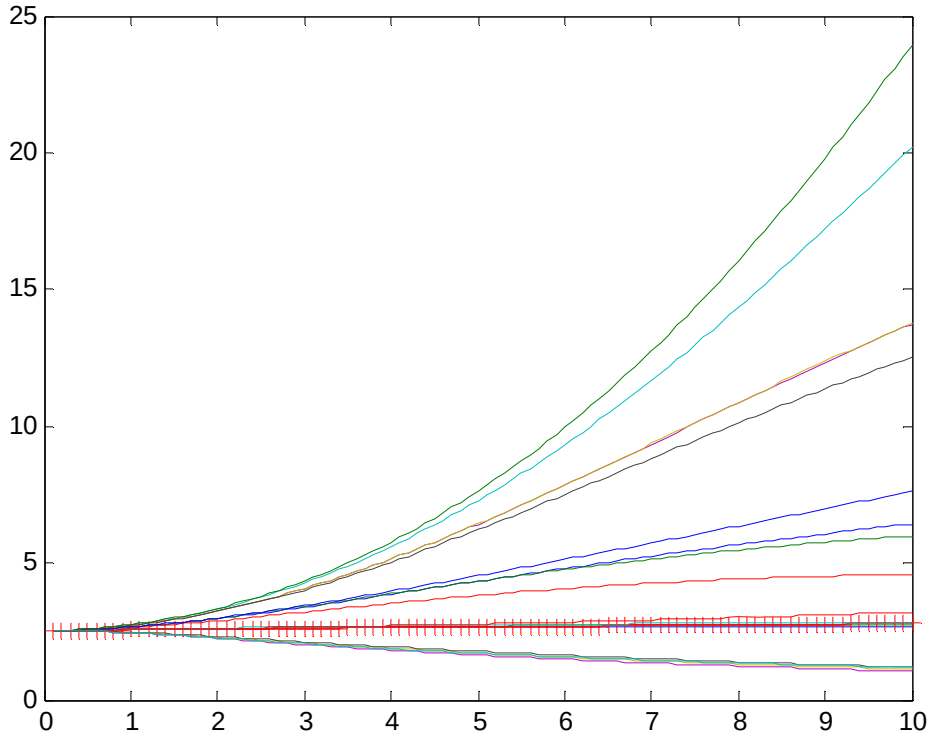
25
20
15
10
5
0
0
1
2
3
4
5
6
7
8
9
10

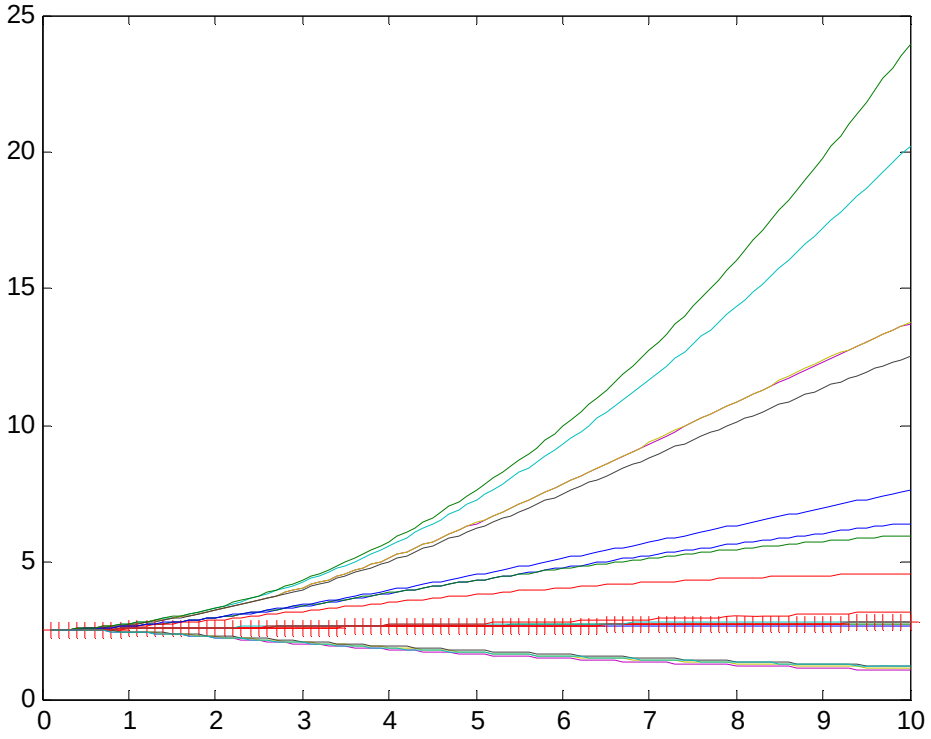
25
20
15
10
5
0
0
1
2
3
4
5
6
7
8
9
10